


8-2012

New Insights into Disinfection Byproduct Formation and Control: Assessing Dissolved Organic Matter Diffusivity and Chemical Functionality

Ashley Pifer

University of Arkansas, Fayetteville

Follow this and additional works at: <http://scholarworks.uark.edu/etd>

 Part of the [Civil Engineering Commons](#), and the [Environmental Engineering Commons](#)

Recommended Citation

Pifer, Ashley, "New Insights into Disinfection Byproduct Formation and Control: Assessing Dissolved Organic Matter Diffusivity and Chemical Functionality" (2012). *Theses and Dissertations*. 498.
<http://scholarworks.uark.edu/etd/498>

This Dissertation is brought to you for free and open access by ScholarWorks@UARK. It has been accepted for inclusion in Theses and Dissertations by an authorized administrator of ScholarWorks@UARK. For more information, please contact scholar@uark.edu, ccmiddle@uark.edu.

NEW INSIGHTS INTO DISINFECTION BYPRODUCT FORMATION AND CONTROL:
ASSESSING DISSOLVED ORGANIC MATTER DIFFUSIVITY AND CHEMICAL
FUNCTIONALITY

NEW INSIGHTS INTO DISINFECTION BYPRODUCT FORMATION AND CONTROL:
ASSESSING DISSOLVED ORGANIC MATTER DIFFUSIVITY AND CHEMICAL
FUNCTIONALITY

A dissertation submitted in partial fulfillment
of the requirements for the degree of
Doctor of Philosophy in Civil Engineering

By

Ashley Dale Pifer
University of Arkansas
Bachelor of Science in Civil Engineering, 2009

August 2012
University of Arkansas

ABSTRACT

Methods were developed for application of asymmetric flow field-flow fractionation (AF4) and fluorescence parallel factor (PARAFAC) analysis to raw and treated samples from drinking water sources to improve characterizations of dissolved organic matter (DOM) and discover DOM properties correlated to disinfection byproduct (DBP) formation potential (FP). Raw water samples were collected from a reservoir, adjusted to pH 6, 7, and 8 and subjected to (1) jar tests using aluminum sulfate (alum) and (2) treatment with magnetic ion exchange (MIEX[®]) resin. Both treatments were followed by DBPFP tests at pH 7. AF4 was used to size DOM in raw and alum treated samples at pH 6 and 8. AF4 fractograms showed that DOM removal was more effective at pH 6 than at pH 8, and preferential removal of larger-sized DOM occurred at pH 6 but not at pH 8.

A fluorescence-PARAFAC model was constructed using excitation-emission matrices (EEMs) from all samples. A strong linear correlation ($r^2 = 0.87$) between chloroform FP and a humic-like PARAFAC component (C1) was developed. This correlation was a significant improvement over the correlation ($r^2 = 0.03$) between chloroform FP and specific ultraviolet absorbance at 254 nm (SUVA₂₅₄), a DBPFP surrogate commonly used in drinking water treatment plants to optimize DOM removal processes. This indicated that chloroform FP-C1 correlations were not treatment-specific.

Alum coagulation at pH 6, 7, and 8 and DBPFP tests at pH 7 were performed on a set of raw waters from eleven drinking water treatment plants from across the United States. AF4 was used to size DOM before and after alum coagulation, and showed similar results to the earlier study, i.e., increased removal at pH 6 compared to pH 8. A fluorescence-PARAFAC model was constructed and total trihalomethane (TTHM) FP was strongly correlated ($r^2 = 0.91$) to C1 for

eight water sources. TTHMFP-SUVA₂₅₄ correlations for ten locations were weak ($r^2 = 0.15$), which indicated that C1 was an improved DBPFP surrogate relative to SUVA₂₅₄ and could be used as a surrogate to select and optimize DBP precursor removal processes.

This dissertation is approved for recommendation
to the Graduate Council.

Dissertation Director:

Dr. Julian L. Fairey

Dissertation Committee:

Dr. Jamie A. Hestekin

Dr. David M. Miller

Dr. Rodney D. Williams

DISSERTATION DUPLICATION RELEASE

I hereby authorize the University of Arkansas Libraries to duplicate this dissertation when needed for research and/or scholarship.

Agreed

Ashley Pifer

Refused

Ashley Pifer

ACKNOWLEDGMENTS

I would like to thank my family and friends for the encouragement, support, and comic relief. I would like to thank my advisor and committee members for their guidance. I am grateful to the University of Arkansas for the Distinguished Academic Fellowship.

TABLE OF CONTENTS

Chapter 1: Introduction	1
Problem Statement	2
Objectives and Approach	3
Document Organization	5
References	5
Chapter 2: Coupling Asymmetric Flow-Field Flow Fractionation and Fluorescence Parallel Factor Analysis Reveals Stratification of Dissolved Organic Matter in a Drinking Water Reservoir	8
1. Introduction	10
2. Materials and Methods	14
2.1. Site Description	14
2.2. Sample Handling and Collection	15
2.3. Water Quality Tests	15
2.4. Asymmetric Flow-Field Flow Fractionation	17
2.5. Fluorescence	19
3. Calculation	22
4. Results and Discussion	23
4.1. Water Quality Parameters	23
4.2. AF4-Fractograms	24
4.3. Fluorescence-PARAFAC Analyses	27
5. Conclusions	29
6. References	39

Appendix 1 Supporting Material for “Coupling Asymmetric Flow-Field Flow Fractionation and Fluorescence Parallel Factor Analysis Reveals Stratification of Dissolved Organic Matter in a Drinking Water Reservoir”	44
Chapter 3 Improving on SUVA ₂₅₄ Using Fluorescence-PARAFAC Analysis and Asymmetric Flow-Field Flow Fractionation for Assessing Disinfection Byproduct Formation and Control	53
1. Introduction and Motivation	55
2. Materials and Methods.....	59
2.1. Site description	59
2.2. Sample collection and handling.....	59
2.3. Water Quality Tests	59
2.4. Jar Tests	60
2.5. Disinfection byproducts.....	61
2.6. Asymmetric flow-field flow fractionation.....	62
2.7. Fluorescence-PARAFAC analysis.....	62
3. Results and Discussion	63
3.1. Raw Water Parameters.....	63
3.2. AF4-UV ₂₅₄ Fractograms	63
3.3. Fluorescence-PARAFAC Analysis.....	65
3.4. Disinfection Byproducts	66
3.5. Correlations between DBP formation and DOM properties.....	68
4. Conclusions.....	69
5. References.....	78

Appendix 2 Supplementary Data for Improving on SUVA₂₅₄ Using Fluorescence-PARAFAC

Analysis and Asymmetric Flow-Field Flow Fractionation for Assessing Disinfection

Byproduct Formation and Control	81
1. Materials and Methods.....	82
1.1. Sample collection and handling	82
1.2. Water Quality Tests.	82
1.3. Fluorescence-PARAFAC analysis.....	82
2. Results and Discussion	83
2.1. Raw Water Parameters.....	83
2.2. References.....	90

Chapter 4 Tracking Disinfection Byproduct Precursor Removal by Magnetic Ion Exchange Resin and Alum Coagulation Using Fluorescence-PARAFAC.....91

1. Introduction and Motivation	93
2. Materials and Methods.....	97
2.1. Sampling Locations	97
2.2. Water Quality Tests	97
2.3. MIEX [®] Experiments	98
2.4. Disinfection Byproduct Formation Potential Tests	98
2.5. Fluorescence-PARAFAC Analysis.....	99
3. Results and Discussion	100
3.1. Raw Water Parameters.....	100
3.2. Fluorescence-PARAFAC Analysis.....	100
3.3. Specific Ultraviolet Absorbance.....	103

3.4. Disinfection Byproduct Formation Potential.....	103
3.5. Correlations Between DBPs and DBP-Precursor Properties.....	104
4. Conclusions.....	105
5. References.....	114
 Chapter 5 Assessing Fluorescence-PARAFAC as a Disinfection Byproduct Formation Potential	
Surrogate in Drinking Water Sources from Diverse Watersheds	117
1. Introduction.....	118
2. Experimental.....	120
2.1. Sample collection and handling.....	120
2.2. Glassware and reagents.....	121
2.3. Water quality tests.	122
2.4. Jar tests.....	122
2.5. Disinfection byproducts.....	122
2.6. Asymmetric flow-field flow fractionation.....	123
2.7. Fluorescence-PARAFAC analysis.....	123
3. Results and Discussion	124
3.1. Raw water parameters.....	124
3.2. Size characterization of chromophoric dissolved organic matter.....	125
3.3. Fluorescence-PARAFAC Analysis.....	126
3.4. Disinfection Byproducts.	128
3.5. Correlations between TTHMFP and DOM properties.	129
4. Associated Content	131
5. Author Information.....	131

6. References.....	140
Appendix 3 Supporting Information for Assessing Fluorescence-PARAFAC for Prediction of Disinfection Byproduct Formation Potential in Drinking Water from Diverse Watersheds.	143
Chapter 6: Conclusion.....	150
1. Summary.....	151
1.1. Objective 1 – Development of AF4 and fluorescence-PARAFAC methods	152
1.2. Objective 2 – Impact of treatment on DOM properties	152
1.3. Objective 3 – DBPFP-PARAFAC correlations for alum-treated waters.....	154
1.4. Objective 4 – Validation of DBPFP-PARAFAC correlations for two DOM removal processes	154
1.5. Objective 5 – Validation of DBPFP-PARAFAC correlations for eleven source waters	154
2. Significance and future work.....	155

LIST OF PAPERS

CHAPTER 2

Pifer, A. D., Miskin, D. R., Cousins, S. L. and Fairey, J. L., 2011. Coupling asymmetric flow-field flow fractionation and fluorescence parallel factor analysis reveals stratification of dissolved organic matter in a drinking water reservoir. *Journal of Chromatography A* 1218 (27), 4167-4178.

CHAPTER 3

Pifer, A. D. and Fairey, J. L., 2012. Improving on SUVA₂₅₄ using fluorescence-PARAFAC analysis and asymmetric flow-field flow fractionation for assessing disinfection byproduct formation and control. *Water Research* 46 (9), 2927-2936.

CHAPTER 4

Pifer, A. D., Cousins, S. L. and Fairey, J. L., submitted. Tracking disinfection byproduct precursor removal by magnetic ion exchange resin and alum coagulation using fluorescence-PARAFAC, University of Arkansas.

CHAPTER 5

Pifer, A. D. and Fairey, J. L., submitted. Assessing fluorescence-PARAFAC as a disinfection byproduct formation potential surrogate in drinking water sources from diverse watersheds, University of Arkansas.

CHAPTER 1

Introduction

1. PROBLEM STATEMENT

Disinfection of drinking water has been crucial in the protection of public health since the early twentieth century, but is not without challenges. In the 1970s, Rook reported the formation of haloforms following chlorination of natural waters (Rook 1976; 1977) from reactions with dissolved organic matter (DOM), which is ubiquitous in surface- and ground waters.

Trihalomethanes (THMs) are the most abundant group of DBPs formed during chlorination, and have been linked to increased health risks (Cantor et al. 1998; Nieuwenhuijsen et al. 2000). The sum of the four THMs were regulated in drinking water under the United States Environmental Protection Agency's (USEPA) Stage 1 Disinfectants/Disinfection Byproducts (D/DBP) rule; THM regulations became more stringent in the promulgation of the Stage 2 D/DBP rule.

Drinking water treatment plant (DWTP) managers can draw from a two-pronged approach to decrease formation of THMs and achieve regulatory compliance: (1) alter the disinfectant and/or (2) remove more DOM (e.g., by processes such as enhanced coagulation, ion exchange). A 1997 survey of 100 DWTPs showed that 20 exceeded the USEPA's maximum contaminant level (MCL) for total THMs of 80 $\mu\text{g/L}$ (Arora et al. 1997). This is due in part to the complexity and variability of DBP precursors within the DOM pool and the limited metrics (e.g. specific ultraviolet absorbance at 254 nm (SUVA_{254}) and total organic carbon (TOC)) that are used to design DBP precursor removal processes. Development of highly effective DOM removal strategies would be aided by improved DOM characterization methods and an increase in understanding of DOM properties before and after treatment.

DOM has been physically and chemically characterized by a variety of techniques (Kitis et al. 2002; Yohannes et al. 2005; Cawley et al. 2009; Worms et al. 2010) which have led to valuable insights into DBP formation (Kim and Yu 2005; Yang et al. 2008; Chu et al. 2010).

However, many techniques require large sample volumes, pre-concentration, and perturbations in acid/base chemistry, which can make characterizations of samples treated at the laboratory scale difficult and can even introduce artifacts (Gadmar et al. 2005). Symmetrical flow field-flow fractionation (FIFFF) and asymmetrical FIFFF (AF4) have been used to separate and size DOM in natural water samples (Floge and Wells 2007; Alasonati et al. 2010) without need for pre-concentration, interaction with a stationary phase, or perturbations of solution chemistry. Although these relatively recent techniques have many advantages (Schimpf and Wahlund 1997; Yohannes et al. 2005), FIFFF and AF4 are not yet commonly applied to drinking water treatment studies.

Fluorescence spectroscopy is becoming a common tool for chemical DOM characterizations (Coble et al. 1990; Coble 1996; Hall et al. 2005; Korshin et al. 2007) and has been applied to DBP studies (Roccaro et al. 2009). The use of parallel factor analysis (PARAFAC), a statistical algorithm used to decompose fluorescence excitation emission matrices into fluorophores (called components) (Andersen and Bro 2003), has simplified identification of relationships between DBPFP and components. Strong DBPFP-PARAFAC correlations have been reported within a DWTP (Johnstone et al. 2009), but these correlations have not been verified for different treatment processes or a wide range of source waters.

Although fluorescence-PARAFAC measures bulk DOM properties, it has the potential to be a useful DBPFP surrogate for DWTPs.

2. OBJECTIVES AND APPROACH

The overall objective of this work was to relate physicochemical DOM characteristics to DBP formation and control, which could help DWTPs curb DBPs. The characterization techniques used in this work were chosen such that sample preparation and perturbation were

minimized to better represent DOM behavior within DWTPs. Throughout this work, continuous DOM size distributions were obtained using AF4 coupled with absorbance at 254 nm (UV_{254}). AF4- UV_{254} data in the form of fractograms allowed assessment of spatial and temporal DOM variability and visualization of preferential removal of specific DOM sizes by DOM removal processes. Fluorescence-PARAFAC analysis data were used to identify correlations between chemical DOM characteristics and DBP formation before and after simulated drinking water treatment processes, and the broad applicability of these correlations was investigated. Specific objectives were to:

(1) Develop detailed methods for AF4- UV_{254} and fluorescence-PARAFAC for analysis of DOM in natural water samples.

(2) Investigate the impacts of DOM removal processes on physicochemical DOM properties.

(3) Develop correlations between formation potential (FP) of individual DBPs and fluorescence-PARAFAC components using samples collected from the four drinking water treatment plants on Beaver Lake before and after alum coagulation.

(4) Investigate the applicability of DBPFP-PARAFAC correlations to waters treated with magnetic ion exchange (MIEX) resin.

(5) Assess the broad applicability of DBPFP-PARAFAC correlations using raw water samples collected from drinking water treatment plants across the United States.

The correlations discovered in this work could be used by drinking water treatment plants to not only predict DBP formation, but also to select and optimize DOM removal strategies with greater success than is possible using traditional bulk metrics such as $SUVA_{254}$.

3. DOCUMENT ORGANIZATION

This dissertation comprises two published and two submitted journal articles which build on each other to address the specific research objectives. Chapter 1 contains the problem statement, general research objectives, and approaches used for this work. Chapter 2 is a published article and its supplementary data (Appendix 1) regarding objective (1). Chapter 3 is a published article and its supplementary data (Appendix 2) which address objectives (2) and (3). Chapter 4 is a submitted paper on objectives (2) and (4). Chapter 5 is a submitted paper and its supplementary data (Appendix 3) which focus on objectives (2) and (5). Chapter 6 contains overall conclusions, contributions to the field of drinking water treatment, and recommendations for future studies.

4. REFERENCES

- Alasonati, E., Slaveykova, V. I., Gallard, H., Croue, J. P. and Benedetti, M. F., 2010. Characterization of the colloidal organic matter from the Amazonian basin by asymmetrical flow field-flow fractionation and size exclusion chromatography. *Water Research* 44 (1), 223-231.
- Andersen, C. M. and Bro, R., 2003. Practical aspects of PARAFAC modeling of fluorescence excitation-emission data. *Journal of Chemometrics* 17 (4), 200-215.
- Arora, H., LeChevallier, M. W. and Dixon, K. L., 1997. DBP occurrence survey. *Journal American Water Works Association* 89 (6), 60-68.
- Cantor, K. P., Lynch, C. F., Hildesheim, M. E., Dosemeci, M., Lubin, J., Alavanja, M. and Craun, G., 1998. Drinking water source and chlorination byproducts I. Risk of bladder cancer. *Epidemiology* 9 (1), 21-28.
- Cawley, K. M., Hakala, J. A. and Chin, Y. P., 2009. Evaluating the triplet state photoreactivity of dissolved organic matter isolated by chromatography and ultrafiltration using an alkylphenol probe molecule. *Limnology and Oceanography-Methods* 7, 391-398.
- Chu, W.-H., Gao, N.-Y., Deng, Y. and Krasner, S. W., 2010. Precursors of Dichloroacetamide, an Emerging Nitrogenous DBP Formed during Chlorination or Chloramination. *Environmental Science & Technology* 44 (10), 3908-3912.
- Coble, P. G., 1996. Characterization of marine and terrestrial DOM in seawater using excitation emission matrix spectroscopy. *Marine Chemistry* 51 (4), 325-346.

- Coble, P. G., Green, S. A., Blough, N. V. and Gagosian, R. B., 1990. Characterization of dissolved organic matter in the Black Sea by fluorescence spectroscopy. *Nature* 348 (6300), 432-435.
- Floge, S. A. and Wells, M. L., 2007. Variation in colloidal chromophoric dissolved organic matter in the Damariscotta Estuary, Maine. *Limnology and Oceanography* 52 (1), 32-45.
- Gadmar, T. C., Vogt, R. D. and Evje, L., 2005. Artifacts in XAD-8 NOM fractionation. *International Journal of Environmental Analytical Chemistry* 85 (6), 365-376.
- Hall, G. J., Clow, K. E. and Kenny, J. E., 2005. Estuarial Fingerprinting through Multidimensional Fluorescence and Multivariate Analysis. *Environmental Science & Technology* 39 (19), 7560-7567.
- Johnstone, D. W., Sanchez, N. P. and Miller, C. M., 2009. Parallel Factor Analysis of Excitation-Emission Matrices to Assess Drinking Water Disinfection Byproduct Formation During a Peak Formation Period. *Environmental Engineering Science* 26 (10), 1551-1559.
- Kim, H. C. and Yu, M. J., 2005. Characterization of natural organic matter in conventional water treatment processes for selection of treatment processes focused on DBPs control. *Water Research* 39 (19), 4779-4789.
- Kitis, M., Karanfil, T., Wigton, A. and Kilduff, J. E., 2002. Probing reactivity of dissolved organic matter for disinfection by-product formation using XAD-8 resin adsorption and ultrafiltration fractionation. *Water Research* 36 (15), 3834-3848.
- Korshin, G. V., Benjamin, M. M., Chang, H. S. and Gallard, H., 2007. Examination of NOM chlorination reactions by conventional and stop-flow differential absorbance spectroscopy. *Environmental Science & Technology* 41 (8), 2776-2781.
- Nieuwenhuijsen, M. J., Toledano, M. B., Eaton, N. E., Fawell, J. and Elliott, P., 2000. Chlorination disinfection byproducts in water and their association with adverse reproductive outcomes: a review. *Occupational and Environmental Medicine* 57 (2), 73-85.
- Roccaro, P., Vagliasindi, F. G. A. and Korshin, G. V., 2009. Changes in NOM Fluorescence Caused by Chlorination and their Associations with Disinfection by-Products Formation. *Environmental Science & Technology* 43 (3), 724-729.
- Rook, J. J., 1976. Haloforms in drinking water. *Journal American Water Works Association* 68 (3), 168-172.
- Rook, J. J., 1977. Chlorination reactions of fulvic acids in natural waters. *Environmental Science & Technology* 11 (5), 478-482.
- Schimpf, M. E. and Wahlund, K. G., 1997. Asymmetrical flow field-flow fractionation as a method to study the behavior of humic acids in solution. *Journal of Microcolumn Separations* 9 (7), 535-543.

- Worms, I. A. M., Al-Gorani Szigeti, Z., Dubascoux, S., Lespes, G., Traber, J., Sigg, L. and Slaveykova, V. I., 2010. Colloidal organic matter from wastewater treatment plant effluents: Characterization and role in metal distribution. *Water Research* 44 (1), 340-350.
- Yang, X., Shang, C., Lee, W., Westerhoff, P. and Fan, C., 2008. Correlations between organic matter properties and DBP formation during chloramination. *Water Research* 42 (8-9), 2329-2339.
- Yohannes, G., Wiedmer, S. K., Jussila, M. and Riekkola, M. L., 2005. Fractionation of Humic Substances by Asymmetrical Flow Field-Flow Fractionation. *Chromatographia* 61 (7), 359-364.

CHAPTER 2

**Coupling Asymmetric Flow-Field Flow Fractionation and Fluorescence Parallel Factor
Analysis Reveals Stratification of Dissolved Organic Matter in a Drinking Water Reservoir**

ABSTRACT

Using asymmetrical flow field-flow fractionation (AF4) and fluorescence parallel factor analysis (PARAFAC), we showed physicochemical properties of chromophoric dissolved organic matter (CDOM) in the Beaver Lake Reservoir (Lowell, AR) were stratified by depth. Sampling was performed at a drinking water intake structure from May-July, 2010 at three depths (3-, 10-, and 18-m) below the water surface. AF4-fractograms showed that the CDOM had diffusion coefficient peak maximums between $3.5\text{-}2.8 \times 10^{-6} \text{ cm}^2 \text{ s}^{-1}$, which corresponded to a molecular weight range of 680-1,950 Da and a size of 1.6-2.5 nm. Fluorescence excitation-emission matrices of whole water samples and AF4-generated fractions were decomposed with a PARAFAC model into five principal components. For the whole water samples, the average total maximum fluorescence was highest for the 10-m depth samples and lowest (about 40% less) for 18-m depth samples. While humic-like fluorophores comprised the majority of the total fluorescence at each depth, a protein-like fluorophore was in the least abundance at the 10-m depth, indicating stratification of both total fluorescence and the type of fluorophores. The results present a powerful approach to investigate CDOM properties and can be extended to investigate CDOM reactivity, with particular applications in areas such as disinfection byproduct formation and control and evaluating changes in drinking water source quality driven by climate change.

KEYWORDS

Diffusion coefficient, polystyrene sulfonate salt, PARAFAC, dissolved organic matter stratification, disinfection byproduct precursors

1. INTRODUCTION

In aqueous systems, the term dissolved organic matter (DOM) is used to refer to mixtures of molecules comprised mainly of organic carbon, present in ground and surface waters at low milligram as carbon per liter (mg C L^{-1}) levels. DOM controls geochemical processes, affecting transport, speciation, and bioavailability of trace elements (Santschi et al. 2002), serves as a carbon substrate for the growth of biofilms in water distribution systems (LeChevallier et al. 1996), and reacts with drinking water disinfectants to form disinfection byproducts, DBPs (Rook 1977). The formation of DBPs in treated drinking waters is a public health issue, as many DBPs are regulated because they are suspected human carcinogens. Aquatic DOM is derived from terrestrial and aquatic sources, and can undergo biotic (e.g., microbial) and abiotic (e.g., photolysis) transformations, and, as such, exists as a dynamic carbon pool, the properties of which can vary temporally and spatially (Huguet et al. 2009). Because of its importance in aquatic systems, detailed DOM characterization techniques are needed to understand its fate in the environment and to develop strategies to minimize its deleterious effects in engineered treatment processes.

Because of the physical and chemical diversity that exists within the aquatic DOM pool, researchers have attempted to isolate various DOM fractions of like size and/or similar chemical composition. Commonly used physicochemical separations include resin adsorption techniques (Kitis et al. 2002; Chu et al. 2010), liquid chromatography (Worms et al. 2010), alum coagulation and activated carbon adsorption (Kitis 2001), ultrafiltration (Kitis et al. 2002; Cawley et al. 2009), and flow field-flow fractionation (FIFFF) (Yohannes et al. 2005; Baalousha and Lead 2007; Floge and Wells 2007; Dubascoux et al. 2008). Once a given DOM fraction has been separated, various analytical techniques are often applied with improved resolution, such as

ultraviolet (UV) spectroscopy (Alasonati et al. 2010; Stolpe et al. 2010; Worms et al. 2010), measurement of dissolved organic carbon (DOC) (Reszat and Hendry 2005), inductively coupled plasma mass spectrometry (ICP-MS) (Krachler et al. 2010; Worms et al. 2010), and fluorescence spectroscopy (Boehme and Wells 2006; Yang et al. 2008). A well known yet often overlooked aspect of UV and fluorescence spectroscopy, is that these techniques are only sensitive to the chromophoric DOM (CDOM) – the fraction of the DOM pool that absorbs light or imparts color to natural waters.

Using DOM isolated and concentrated by resin adsorption techniques, Cabaniss et al. (2000) showed that DOM size affects proton and metals binding, partitioning of organic contaminants, and coagulation and adsorption processes. Other researchers found that the low molecular weight DOM fraction (<10 kDa) was the principal component of the total DOM pool (Krachler et al. 2010), and that hydrophilic DOM fractions were linked with formation of nitrogenous DBPs (Chu et al. 2010). Despite these potentially valuable insights, previous DOM characterization methods have serious drawbacks. For example, resin adsorption techniques often require DOM pre-concentration (Yang et al. 2008), perturbations in acid/base chemistry, and employ interactions with a stationary resin phase, all of which can introduce artifacts that bias the DOM sample in varying and often unknown ways (Gadmar et al. 2005). Similarly, contact with a stationary phase is a concern in liquid chromatography separations. While DOM isolation by alum coagulation does not require acid/base perturbations, this technique suffers from inadequate separation of hydrophilic elements (Kitis 2001). Likewise, ultrafiltration (UF) does not perturb solution chemistry, but the resultant DOM separations often overlap with one another despite distinct membrane cutoffs (Assemi et al. 2004), and further, UF-separated DOM size distributions are erroneously discontinuous in nature (Stolpe et al. 2010). Coupling these

various separation methods with ICP-MS, UV spectroscopy, DOC measurements, or combinations thereof (e.g. specific UV absorbance, SUVA), can yield interesting insights, however, it is generally unknown how the results from studies with DOM isolates relate to their unperturbed natural source waters.

Symmetrical FIFFF and asymmetrical FIFFF (AF4) have been used to separate and characterize DOM in natural water samples (Floge and Wells 2007; Alasonati et al. 2010) without need for DOM pre-concentration, interaction with a stationary phase, or perturbations of solution chemistry. Both FIFFF techniques provide physical separation of DOM in a ribbon-like channel, but differ in the nature of the applied flow field. The reader is directed to discussions in Ref. (Schimpf et al. 2000) for an in-depth comparison of the two FIFFF techniques. AF4 is a newer technology and has several practical advantages over its symmetric counterpart, namely simpler channel construction and a transparent front plate in which the focusing band position can be visualized (when a colored dye is injected) and measured precisely (Wahlund and Giddings 1987). AF4 separates colloids, macromolecules, and particles from 1-nm to 100- μm in size on the basis of diffusivity (Giddings 1993). Reported sample injection sizes vary from 5- μL to 250-mL (Baalousha et al. 2005; Yohannes et al. 2005; Prestel et al. 2006; Alasonati et al. 2010), depending on the intended application. In FIFFF, shear forces that drive the sample separation within the channel are low (Yohannes et al. 2005), which prevents breakup of DOM aggregates and, as such, FIFFF data can be used to determine the hydrodynamic diameter distribution of DOM mixtures (Schimpf and Wahlund 1997). While FIFFF has some drawbacks (e.g., the inability to precisely determine DOM molecular weight due to the difficulty in finding appropriate standards), these are relatively minor when weighed against the many benefits over traditional DOM separation techniques.

To elucidate important physicochemical properties, FIFFF is often coupled with various analytical detectors. For instance, Fløge and Wells (2007) coupled FIFFF with UV₂₅₄ to study the rapid cycling of marine colloids in coastal waters; similarly, Alasonati et al. (2010) reported substantial spatial variability of DOM in Amazonian basin waters with the aid of a multi-angle light scattering detector. However, fluorescence spectroscopy is arguably the most useful and widely applied detector for DOM studies. Fluorescence measurements consist of two spectra – excitation and emission – that are plotted against one another to yield an excitation-emission matrix (or EEM). Fluorescence EEMs have been used in a variety of applications. For example, Coble (1996) showed that marine and terrestrial DOM had distinct fluorescence signatures and identified EEM regions with humic-like and protein-like fluorophores. Similarly, Hall and Kenny (2007) showed fluorophores can be used to identify the origin of a water sample in their study of ballast waters from shipping vessels. Other researchers have analyzed changes in fluorescence EEMs upon oxidation with drinking water disinfectants. For instance, Johnstone et al. (2009) correlated changes in fluorescence EEMs with formation of specific DBPs. Recently, fluorescence has been coupled with FIFFF. Notably, Stolpe et al. (2010) used FIFFF and fluorescence to characterize colloidal DOM mass transport of trace elements. Additionally, Boehme and Wells (2006) showed that the protein-like EEM signature of estuarine DOM samples was associated with the smallest (1-5 kDa) DOM size fraction. However, interpretation of fluorescence data presents analytical challenges due to the presence of water scattering regions, quenching, and instrument noise (Andersen and Bro 2003). Fluorophores have often been identified by ad-hoc “peak picking” methods (eg., (Coble et al. 1990)) and calculation of various fluorescence indexes (e.g., (Korshin et al. 2007)), but these techniques have proved to have serious limitations (Johnstone et al. 2009). To help address these concerns, parallel factor

analysis (PARAFAC), a statistical algorithm, has been developed and successfully used to decompose an array of at least 30 fluorescence EEMs (Andersen and Bro 2003; Hall and Kenny 2007; Hua et al. 2010) into several (generally less than 10) principal components. The reader is referred to the seminal work of Bro's group (e.g., (Andersen and Bro 2003; Stedmon and Bro 2008)) for detailed descriptions of PARAFAC theory and its applications to DOM analyses.

Here, AF4 was coupled with fluorescence PARAFAC analyses to elucidate physicochemical properties of CDOM in unperturbed freshwaters, sampled weekly at three depths from a drinking water treatment plant reservoir in Lowell, AR, between May-July, 2010. AF4-UV₂₅₄ was used to determine the diffusion coefficient, molecular weight, and size distributions of CDOM and separate it into three distinct fractions. Fluorescence EEMs were measured for whole water samples and AF4-generated fractions, which were decomposed with the PARAFAC model into five principal components. This novel coupling of AF4-UV₂₅₄ and fluorescence PARAFAC analyses revealed that CDOM properties in the reservoir were stratified by depth which may have implications on strategies that drinking water treatment plants use to help limit the formation of DBPs.

2. MATERIALS AND METHODS

2.1. Site Description

Water samples were collected from the Beaver Lake Reservoir, which is located on the White River in northwest Arkansas and serves as the main drinking water source for the more than 300,000 customers of the Beaver Water District (BWD). The reservoir has a surface area of 103-km², an average depth of 18-m, and an average hydraulic retention time of 1.5-years (Sen et al. 2007). The hydraulic catchment area encompasses 310,000-ha of mostly forest and agricultural lands with primary inflows from the White River, Richland Creek, War Eagle Creek,

and Brush Creek. The BWD's intake structure (the sampling site) is located in a transitional zone of the reservoir, where conditions vary from mesotrophic to eutrophic. However, with increased urbanization and poultry production in the area, conditions may become increasingly eutrophic. Increases in nutrient loadings have stimulated growth of aquatic plant life, and hence have the potential to drive changes in the concentration and reactivity of the DOM in the reservoir.

2.2. Sample Handling and Collection

Beaver Lake water (BLW) samples were collected weekly over eight weeks from May to July, 2010 at the BWD's intake structure. Sampling was performed with a 6-L Van Dorn bottle (Wildco, Model 1960-H65, Yulee, FL) tethered to a 30-m rope for collection of water at three depths (3-, 10-, 18-m) below the water surface. Samples were transferred to pre-rinsed (Milli-Q water) 9-L HDPE carboys, capped, transported to the Water Research Laboratory at the University of Arkansas, and stored in the dark at 4°C until use. Prior to AF4 and fluorescence analyses, each water sample was filtered through a 1 micron nominal pore size glass fiber filter (GFF), which was pre-combusted (at 400°C for 30 min) and pre-rinsed with 1-L of Milli-Q water. The sample filtrate was stored in the dark at 4°C in 250-mL amber glass bottles capped with PTFE-lined lids. Prior to all analyses, samples were warmed to room temperature.

Glassware was soaked in a solution of tap water and Alconox detergent, scrubbed thoroughly, rinsed with copious amounts of Milli-Q water, and baked in a muffle furnace at 400°C for 30 min. Volumetric flasks and plastic-ware were prepared similarly, but instead of baking, were dried at room temperature and 40°C, respectively.

2.3. Water Quality Tests

All water for aqueous phase preparations was made using a Millipore Integral 3 (Billerica, MA) Milli-Q water system (18.2 MΩ-cm) and ACS-grade chemical reagents. The pH

of the sample waters was measured using an Orion 8272 pH electrode (Thermo Orion, Waltham, MA) calibrated with pH standards of 4, 7, and 10 and connected to an Accumet XL60 dual channel pH/Ion/Conductivity meter. Alkalinity was measured following Standard Methods 2320B (Eaton et al. 2005), in which waters were titrated to pH 4.5 with 0.1 N HCl. Turbidity was measured using a HF Scientific DRT-100 turbidimeter (Fort Myers, FL), which was calibrated (0.5-50 NTU) with standards made by dilutions of a 4,000 mg L⁻¹ stock formazin suspension (Ricca Chemical Company, Arlington, TX). Conductivity was measured with an Accumet four-cell conductivity probe. UV₂₅₄ was measured on a Shimadzu UV-Vis 2450 (Kyoto, Japan) spectrophotometer using a 1-cm path length low volume quartz cell. Samples for UV analyses were filtered with pre-combusted and pre-rinsed GFFs. Following the same filtration protocol, dissolved organic carbon (DOC) was measured in triplicate with a Shimadzu TOC-V_{CSH} TOC analyzer (Kyoto, Japan) equipped with an auto-sampler and TOC-Control V acquisition software. Specific ultraviolet absorbance (SUVA) was calculated by dividing the UV₂₅₄ by the product of the DOC and UV cell path length.

Total ammonia (the sum of NH₃ and NH₄⁺) was measured using an ammonia electrode (Thermo Orion 9512, Waltham, MA) connected to the Accumet XL60 meter. To calibrate the ammonia probe, a 1000 mg L⁻¹-N stock ammonium chloride solution was prepared following Standard Methods 4500-NH₃ D and diluted to make standards between 0.03 and 10 mg L⁻¹-N (R² = 1, n = 19). Nitrate was measured on filtered water samples using Hach HR NitraVer 5 (Hach Company, Loveland, CO) powder pillows with the spectrophotometer at 392 nm. Nitrate standards were prepared following Standard Methods 4500-NO₃⁻ C using 10 mg L⁻¹ KNO₃ solution (JT Baker, Phillipsburg, NJ). Similarly, nitrite was measured on filtered water samples using Hach LR Nitrite powder pillows at 548 nm. Nitrite standards were prepared following

Standard Methods 4500 NO₂-B using NaNO₂ (MP Biomedicals Inc., Solon, OH). Lastly, iron was determined as total iron using Hach FerroVer Iron reagent and measured at 540 nm. Iron standards were made with FeCl₃·6H₂O at Fe³⁺ concentrations between 0.2- and 3.5-mg Fe L⁻¹.

2.4. Asymmetric Flow-Field Flow Fractionation

An AF2000-MT asymmetrical flow field-flow fractionation (AF4) system from Postnova Analytics (Salt Lake City, UT) was used to characterize the physicochemical properties of the BLW CDOM. The AF4 system consisted of four pumps, a separation channel, 1.0- to 1.5-m of black PEEK tubing (to generate adequate system pressure, 5-18 bar), an inline UV detector and fraction collector, and an offline fluorescence excitation-emission detector. The pumps were used to introduce carrier fluid (referred to herein as “eluent”) and the sample to the separation channel and create the flow-field for macromolecular separation. The AF4 pumps were controlled by Postnova Software (AF2000 Control v.1.1.0.25) and the detectors and fraction collector were controlled by Agilent Chemstation for LC Systems (rev. B.04.01 SP1). The eluent consisted of 1-mM NaCl in Milli-Q water, and was chosen to match the conductivity of the BLW samples (~160 μS cm⁻¹). The eluent was passed through an inline vacuum degasser (PN7520) before being pumped through the system to prevent formation of bubbles within the system. Two HPLC pumps (PN1130) provided independent control of the tip and focus flow rates. A syringe pump was used for the cross-flow, which drew the non-macromolecular fluid through the channel membrane to the waste and controlled the magnitude of the applied flow-field. Another syringe pump, the slot pump (PN1610), was used during elution to concentrate the sample passing through the UV detector (Prestel et al. 2006) and fraction collector.

The separation channel is the heart of the AF4 system, a schematic of which is shown in Figure SM1. The tip-to-tip channel length was 27.4 cm, with an effective channel length (L_{eff}),

the distance from the focusing band to the channel outlet, of 24.5 cm. The channel breadth geometry tapered symmetrically from a maximum of 2.0 cm (b_0) to 0.7 cm (b_L) at the outlet. The nominal Mylar spacer thickness was 500 μm , but the actual channel thickness was 410 μm , which was calculated using the AF4-elution time ($t_r = 15$ min) of the bovine serum albumin monomer in 100 mM NaCl and Eqn (1) with a diffusion coefficient of $6.7 \times 10^{-7} \text{ cm}^2 \text{ s}^{-1}$ (Chatterjee 1964). Polyethersulfone (PES) channel membranes with a 300-Da molecular weight cut-off (Postnova Analytics) were used throughout this study.

An AF4 sample run consists of four phases: (1) injection, (2) focusing, (3) elution, and (4) rinsing. Individual pump flow rates varied between phases and shown in Table 1. Throughout Phases 1-3, the detector flow rate was held constant at 0.3 mL min^{-1} ; in Phase 4, the flow passed through the purge line to flush the system.

Ten-milliliter samples were injected into the AF4 channel using a bubble trap (Postnova Analytics). This injection volume was chosen to balance adequate UV detection with minimization of sample loss through the channel membrane during the injection and focusing steps (Schimpf and Wahlund 1997). The tip pump flow was plumbed through the bubble trap and carried the sample into the channel over 6-min. Concurrently, eluent from the focus pump was supplied to the channel 18.5-cm from the inlet (L_{FP} in Figure SM1), and a portion of this flow traveled toward the channel inlet to keep sample macromolecules in the channel. Eluent exited the channel during the injection step through the channel membrane by the action of the cross-flow pump, which acted perpendicular to the long dimension of the channel. Sample injection was followed by 6 minutes of focusing, designed to focus the sample into a uniform band near the channel inlet (at z' in Figure SM1). Next, in the transition phase, the focus pump flow was

decreased to zero as the tip pump ramped up to maintain the total flow over 1-min, followed by the elution step and 5-min of rinsing.

Following the AF4 channel outlet, the fractionated sample flowed to an inline UV-diode array detector (Agilent Technologies, G1315D), which collected UV data from 200-800 nm in 1 nm increments every 2-sec during the 20-min sample elution. UV_{254} was used to calculate the diffusion coefficient distributions of the samples. Following the UV detector, the samples were physically separated using a fraction collector (Agilent Technologies, Model 1364C). Three equal-volume fractions (denoted F1, F2, and F3 herein) were collected in 2-mL pre-washed vials beginning at 1-min elution and ending at 8-min elution. UV_{254} time series fractograms were baseline corrected using the FFF Analysis software (Postnova Analytics v. 2.03A). The fractogram data were used to determine the maximum UV_{254} peak heights (MaxUV) and area under the curves (PeakArea), which was calculated using numerical integration with Simpson's method in the freeware program R (v. 2.10.1). Calculation of the diffusion coefficient from the time-series data is detailed in Section 3.

2.5. Fluorescence

Fluorescence excitation-emission matrices (EEMs) were collected with a dual monochromator fluorescence detector (Agilent Technologies, Model G1321A) equipped with a static sample cuvette at 1-nm increments for excitation wavelengths between 200-400 nm and emission wavelengths between 270-600 nm. The fluorescence cuvette was flushed thoroughly with Milli-Q water between scans to prevent carryover and sample contamination. All scans were corrected for first- and second-order Rayleigh and Raman water scattering using a MATLAB® *Cleanscan* program developed by Zepp et al. (2004). *Cleanscan* was applied to each EEM and removed water scattering peaks and replaced them with a surface created by a 3-

dimensional Delauney interpolation algorithm. The areas of the EEMs over which *Cleanscan* was invoked are shown in Fig. SM2.

Rather than relying on the peak picking methods used in previous works (e.g. Coble (1996)), fluorescence PARAFAC modeling was used to identify the principal fluorophores and their maximum intensities, F_{MAX} , for all scatter-corrected EEMs. The EEMs were analyzed using MATLAB[®] functions contained in the *DOM-Fluor toolbox* (available for download at <http://www.models.life.ku.dk/algorithms>). First, the fluorescence data was imported into MATLAB[®] as a collection of individual EEMs, stacked into a 3-dimensional structure using the function *Loading data for DOMfluor*. PARAFAC models require the removal of outliers because they can disproportionately influence the overall model output. Outliers can be the results of measurement error (e.g. sample movement within the cuvette leading to “wrinkles” in the EEM) or can be atypical samples. Such samples were identified visually and by running the function *OutlierTest*. This test calculated and plotted leverages for each EEM, and identified those considered as possible outliers based on high leverage values relative to the other samples. For example, sample numbers 38, 81, and 100 in Fig. SM3 were identified as likely outliers. In cases where EEMs were deemed to have both measurement errors and high leverages, these samples were removed from the PARAFAC dataset. Next, the outlier program was used on the reduced dataset, and additional samples were identified as requiring further investigation after an initial estimate of the proper number of PARAFAC components. The *Split-half analysis* tool was used for this step. The function, *SplitData*, divided the EEM dataset into two pairs of halves. These halves were used in the functions *SplitHalfAnalysis* and *SplitHalfValidation* which compared the shape of components derived from each half of the dataset with the other half’s components’ shapes. When component shapes from each half were identical, the corresponding model and

number of PARAFAC components was considered robust (Stedmon and Bro 2008). Figure SM4 shows an example of one unvalidated (the 4-Component) and two validated (the 3- and 5-Component) split-half analysis models.

To ensure that all outliers were removed, questionable samples identified by the outlier test were removed from the dataset one by one and split half analysis was repeated. Samples were judged to be outliers if their removal changed the outcome of the split half analysis. This resulted in a total of 87 EEMs in the PARAFAC model. In the case that more than one set of components could be split half validated, the *CompareSpecSSE* function was used to plot the sum of squared error (SSE) versus excitation and emission wavelengths (Stedmon and Markager 2005). The SSE for excitation and emission were normalized by the sum of squares for excitation and emission and were plotted to give a visual indication of the level of residual fluorescence compared to the measured fluorescence signal (Fig. SM5). This plot showed that the 5-component model was superior to the 3-component model. As a final check, plots of loadings versus excitation and emission wavelengths for each PARAFAC component were generated and visually inspected. Stedmon and Bro (2008) suggested that these plots ideally show emission loadings with a single peak and excitation and emission loadings slightly overlapping. Discussion of these results is contained in Section 4.3.

Following the technique used by Fellman et al. (2008), the percent relative contribution of each PARAFAC component was determined using F_{MAX} values for each PARAFAC component for all 87 EEMs. For a given EEM, F_{MAX} for each component was divided by the sum of F_{MAX} for all the components (F_{MAX_TOT}). For the whole water samples and AF4-generated fractions, these quotients were averaged for each sample depth (3-, 10-, 18-m) and converted to a percentage. This procedure simplified the interpretation of the PARAFAC data, and conveys the

relative contribution of the PARAFAC components at a given sample depth for each water fraction.

3. CALCULATION

The diffusion coefficient, D_f (in $\text{cm}^2 \text{s}^{-1}$) for the AF4-fractograms was calculated using Eqn (1):

$$D_f = \frac{\lambda V_C w^2}{V^0} \quad \text{Eqn (1)}$$

In Eqn (1), λ denotes the unitless retention parameter, V_C is the cross-flow rate (4.0 mL min^{-1}), w is the experimentally determined channel thickness (0.041 cm , Section 2.3), and V^0 is the channel void volume, calculated by the product of channel thickness and the effective channel area. The effective channel area, A_{eff} , was calculated as the channel area downstream of the sample focus band, b_z , which was located 2.9 cm downstream of the channel inlet, as indicated in the channel schematic (Fig. SM1). Using similar triangles, A_{eff} was calculated to be 32 cm^2 . The effective channel area was also used to find α , a term used in the calculation of the void time, t^0 , by Eqn (2).

$$\alpha = 1 - \frac{b_0 z' - \frac{(b_0 - b_L)(z')^2}{2 \cdot L_{\text{eff}}} - y}{A_{\text{eff}}} \quad \text{Eqn (2)}$$

In Eqn (2), b_0 is the maximum channel width, b_L is the width of the narrowest part of the trapezoidal channel section, z' is the distance from the channel inlet to the focusing band, L_{eff} is the effective channel length, and y is the channel area lost by the tapered channel (3.4 cm^2). The void time, t^0 , in seconds was then calculated with Eqn (3).

$$t^0 = \frac{V^0}{V_C} \ln\left(1 + \alpha \frac{V_C}{V_{\text{OUT}}}\right) \quad \text{Eqn (3)}$$

In Eqn (3), V_{OUT} is the volumetric flow rate of the channel outlet (0.5 mL min^{-1}). The value of t^0 was divided by the time series data to determine the unitless retention ratio values, R , shown in Eqn (4), which is also equal to six times the retention parameter values, λ (Schimpf et al. 2000).

$$\frac{t^0}{t_r} = R = 6 \cdot \lambda \quad \text{Eqn (4)}$$

Values of λ were then used in Eqn (1) to determine the diffusion coefficient distribution. The hydrodynamic diameter, d_h , of the DOM was approximated from the molecular weight (MW) using Eqn (5), similar to the procedure used by Howe and Clark (2002).

$$d_h = 0.09 \cdot (MW)^{0.44} \quad \text{Eqn (5)}$$

4. RESULTS AND DISCUSSION

4.1. Water Quality Parameters

The raw water characteristics for the 24 BLW samples are reported in Table 2 along with their mean and median values. All waters had a slightly alkaline pH, low turbidity, and low to moderate alkalinity. Mean and median values were similar for pH (8.1 and 7.8), turbidity (10- and 9-NTU), conductivity (162- and 159- $\mu\text{S cm}^{-1}$), and alkalinity (61- and 62- $\text{mg L}^{-1}\text{-CaCO}_3$), reflecting the tightly bunched nature of these metrics amongst the water samples. Conversely, mean and median values differed for ammonia (0.11- and 0.05- $\text{mg L}^{-1}\text{-N}$), nitrate (0.67- and 0.90- $\text{mg L}^{-1}\text{-N}$), nitrite (16.2- and 5.6- $\mu\text{g L}^{-1}\text{-N}$), and DOC (4.4- and 2.4- $\text{mg L}^{-1}\text{-C}$), indicating these metrics were skewed by a handful of low (for nitrate) and high (for ammonia, nitrite, and DOC) values. Fig. SM6 shows a pair-wise scatter-plot for the water quality parameters. While there were no temporal trends (those with *Date*), spatial trends (those with *Depth*) were only apparent for pH, turbidity, and nitrate (second column in Fig. SM6). Values for pH were higher at 3-m than at 10- and 18-m; conversely, turbidities were lower at 3-m compared to the 10- and 18-m depths likely because of higher sediment loadings near the bottom of the reservoir.

Total iron was not reported in Table 2 because these values were below $0.33 \text{ mg L}^{-1}\text{-Fe}$, with 22 of the 24 samples below the estimated detection limit ($0.20 \text{ mg L}^{-1}\text{-Fe}$) of the Hach FerroVer test. Weishaar (2003) evaluated potential interferences of background analytes on UV_{254} and determined that a UV_{254} of 0.01 required $1 \text{ mg L}^{-1}\text{-Fe}$ total iron and in excess of $23 \text{ mg L}^{-1}\text{-N}$ nitrate. Given the iron and nitrate concentrations in the sample waters were below these thresholds, we concluded that the UV_{254} measurements (for the SUVA calculations and AF4 fractograms) were not impacted by dissolved iron and nitrate.

Interestingly, the four samples with high DOC values (those above $8 \text{ mg L}^{-1} \text{ C}$ in Table 2) all had below average alkalinity values ($< 62 \text{ mg L}^{-1}\text{-CaCO}_3$), suggesting the carbonate system controlled the alkalinity of all lake water samples and the diverse groups of weak acids present in the DOM did not contribute significantly to alkalinity. SUVA, calculated as UV_{254} divided by the product of the UV cell path length (0.01-m) and DOC, varied from 0.4- to $5.6\text{-L mg C}^{-1} \text{ m}^{-1}$. Weishaar et al. (2003) showed that SUVA had a strong positive correlation with $^{13}\text{C-NMR}$ (a direct measure of DOM aromaticity), but was weakly correlated with trihalomethane formation (a principal group of DBPs), suggesting non-aromatic compounds present in DOM mixtures contributed significantly to DBP formation. Therefore, for the waters in this study, the range of SUVA values suggest a wide array of CDOM aromaticities, but cannot be used to reliably estimate the DBP formation potential.

4.2. AF4-Fractograms

In Fig 1., AF4-fractograms were plotted as a function of elution time (t_r) and diffusion coefficient (D_f). Fig. 1A-B show the fractograms of 1.1-, 4.2-, and 10.6-kDa polystyrene sulfonate sodium salt (PSS) standards (ca. 30 mg L^{-1} in 0.001 M NaCl), which other researchers (Beckett et al. 1987; Assemi et al. 2004) have recommended as a molecular weight surrogate for

humic substances. For each PSS standard, D_f at the peak maximum was plotted against its molecular weight and compared to PSS data from other research groups (Beckett et al. 1987; Dycus et al. 1995; van Bruijnsvoort et al. 2001; Assemi et al. 2004) (Fig. 2). These data show that the D_f values determined here were bracketed by those reported in the literature. The spread in these data between research groups (approximately one-half an order of magnitude in $\log D_f$ for $\log MW$ values less than 4.0) can likely be attributed to different background electrolyte compositions.

The AF4-fractogram of Suwannee River natural organic matter (SRNOM, International Humic Substances Society, Atlanta, GA, Cat. No. 1R101N; ca. 4 mg L⁻¹ in 0.001 M NaCl) is also shown in Fig. 1A-B. This peak was broader than those of the PSS standards, with a peak maximum near that of the 4.2 kDa PSS standard ($t_r = 4.2$ min, Fig. 1A; $D_f = 2.4 \times 10^{-6}$ cm²s⁻¹, Fig. 1B) and a “shoulder-like” feature indicating the presence of CDOM smaller than 1.1 kDa PSS ($t_r = 2$ min, Fig. 1A; $D_f = 5.0 \times 10^{-6}$ cm²s⁻¹, Fig. 1B). This broad range of D_f determined here for SRNOM (~ 1.0 - 5.0×10^{-6} cm²s⁻¹) was smaller than that reported by Moon et al. (2006) of 4.1 - 5.5×10^{-6} cm²s⁻¹ (Table 3). However, when coupled with the results of the PSS standards (Fig. 2), it can be concluded that the AF4 methods used here produced similar results to those reported by other research groups, for which a variety of preparative and analytical techniques were used.

Fig. 1C-D show AF4-fractograms for BLW CDOM samples collected on July 8, 2010 at depths of 3-, 10-, and 18-m. The trends shown in Fig. 1D were typical of the other 21 fractograms (Fig. SM7), with BLW CDOM at the 10-m depth having greater UV₂₅₄ peak maximums (with the exception of the first two sampling days) than the samples collected at 3- and 18-m depths. All fractograms had a small, shoulder-like void peak at an elution time of 1.5-min followed by a larger, broad sample peak between 2- and 6-min. The grey boxes in Fig. 1C

denote the three fractions (F1-F3) that were collected for subsequent fluorescence analyses (Section 4.3). For the 24 BLW CDOM fractograms, the D_f peak maximum ranged from 3.5- to 2.8- $\times 10^{-6} \text{ cm}^2 \text{ s}^{-1}$. The peak maximums of the three PSS standards were appended as dashed lines in Fig. 1D, and indicate the BLW CDOM was most similar in diffusivity to that of the 1.1-kDa PSS standard. The approximate molecular weight range of the BLW CDOM was calculated by comparison to the PSS data. Here, the log-linear trend line for the three PSS standards (Fig. 2, $R^2 = 1$, $P < 0.02$, slope: -0.21, y-intercept: -4.86) was used with the range of D_f peak maximums (3.5- to 2.8- $\times 10^{-6} \text{ cm}^2 \text{ s}^{-1}$) to determine the molecular weight of BLW CDOM (680-1,950 Da). Using Eqn (5), this corresponded to a size range of 1.6-2.5 nm. The molecular weights and diffusivities for the BLW CDOM were compared to literature-reported values for the various humic substances (Table 3), which, on balance, indicated the results determined here were within the reported ranges of CDOM using a variety of preparative and analytical techniques. Thus, it can be concluded that BLW CDOM was composed primarily of relatively low molecular weight aromatic carbon-containing molecules (680-1,950 Da) with diffusivities between 3.5- to 2.8- $\times 10^{-6} \text{ cm}^2 \text{ s}^{-1}$. However, it should be stressed that UV_{254} was used to monitor the AF4-fractogram output, and as such, non-aromatic containing DOM was not characterized. As such, there is a possibility that colloidal DOM (3,000-100,000 Da), much larger than the fraction found here, was also present in the BLW samples, as reported by Howe and Clark (2002) in their membrane fouling study, but could not be “seen” by UV_{254} .

The AF4-fractogram data (the UV_{254} peak maximums, MaxUV, and the area under each curve, PeakArea) were compared to select water quality data (DOC and SUVA) as a function of sample date and depth. Fig. 3 shows a pair-wise scatter-plot of these data, which indicated there were no temporal trends (those with *Date*). Conversely, trends with sample *Depth* were apparent

for SUVA, MaxUV and PeakArea (the second column of Fig. 3). As indicated by the trend lines, all these metrics were on balance higher for the 10-m samples compared to the 3- and 18-m samples. Given SUVA is a surrogate for aromatic carbon (Weishaar et al. 2003), these results indicate that the nature of the CDOM pool in the Beaver Reservoir was stratified by depth over the 8-week sampling period. The strong linear relationship between MaxUV and PeakArea ($R^2 = 0.97$, $P < 0.001$) indicated that only one of these metrics needed to be determined to adequately describe the AF4-fractogram data; for simplicity, MaxUV was selected for further analyses. For the 24 lake water samples, MaxUV varied from 20-85 absorbance units (data not shown) and was uncorrelated with DOC (Fig. 3). However, MaxUV and SUVA had a weak positive correlation (Fig. 3, $R^2 = 0.21$, $P = 0.024$), suggesting that MaxUV would not be a good surrogate of CDOM aromaticity, but may be helpful in assessing CDOM reactivity in DBP studies.

4.3. Fluorescence-PARAFAC Analyses

Fluorescence excitation-emission matrices (EEMs) of the 24 whole water samples and 72 AF4-generated fractions were processed as described in Section 2.4. PARAFAC modeling began with the 96 samples, eleven of which were removed based on the protocol detailed in Section 2.4. Split half analyses on the remaining 85 samples showed that three- and five-component models were appropriate for the dataset (Fig. SM4). Fig. SM5 shows the integrated excitation and emission spectra for the sum of squared errors for three- and five-component models and the relative SSE normalized by the total sum of squares. The presence of peaks in these spectra corresponds to regions of the EEMs that are less well described by the model. The results in Fig. SM5 show that a five-component model was superior to the three-component model over the range of excitation and emission wavelengths. For the five-component model, the normalized residual excitation between 200- and 375-nm was less than 1% of the measured signal; similarly,

the normalized residual emission between 300 and 525 nm was less than 2%. As such, a 5-component PARAFAC model was selected. However, Component 3 (Fig. SM7) was present in all samples and blanks (Milli-Q water) at similar intensity (results not shown) and was therefore excluded from further analyses as it was likely a result of instrument noise. Thus, we focus the analysis on Components 1, 2, 4, and 5. These four PARAFAC components and their corresponding component loadings are shown in Fig. 4. The component loadings (Fig. 4, right-side panels) resemble the shape of organic fluorophores described by Stedmon and Bro (2008) and contain single emission peaks that slightly overlap the excitation loadings.

The four PARAFAC component EEMs (Fig. 4, left-side panels) identified by the PARAFAC model have been previously identified by other researchers using PARAFAC or peak-picking methods. The ranges of the excitation and emission maxima for these components are summarized in Table 4. Components 1, 2, and 4 have primary and secondary excitation maxima and have been identified as humic-like fluorophores using PARAFAC and peak-picking methods. Component 5 only has a primary excitation maximum and has been identified as a protein-like fluorophore in a tidal estuary (Hall et al. 2005) and lake water (Hua et al. 2007).

Fluorescence maximum (F_{MAX}) values for Components 1, 2, 4, and 5 were plotted on a percent relative contribution basis in Fig. 5. Here, the diameters of the pie charts were drawn proportional to the average maximum total fluorescence, F_{MAX_TOT} . While the Whole Water samples had larger F_{MAX_TOT} values than the AF4-generated fractions, this result is not meaningful, as the fractions were diluted by the AF4 eluent. However, regardless of water fraction, F_{MAX_TOT} was highest for the 10-m samples, indicating stratification by depth of total fluorophores. Humic-like Components 1, 2, and 4 comprised the majority of the total fluorescence for the Whole Waters, Fraction 1, and Fraction 2. Conversely, Component 5

dominated Fraction 3, indicating this protein-like fluorophore was present in relatively large-sized DOM. Further, Component 5 was in least abundance for the 10-m depth samples for all water fractions, indicating stratification by depth of the type of fluorophores.

5. CONCLUSIONS

The physicochemical properties of CDOM at three depths in the Beaver Lake Reservoir (Lowell, AR) were studied between May-July, 2010. BLW CDOM, as measured by AF4-UV₂₅₄ and SUVA, showed that the 10-m depth samples had higher intensities and SUVA values than did the 3- and 18-m depth samples. For the 24 BLW CDOM samples, the diffusion coefficient peak maximums ranged from 2.8- to $3.5 \times 10^{-6} \text{ cm}^2 \text{ s}^{-1}$, which corresponded to a molecular weight range of 680-1,950 Da and a size of 1.6-2.5 nm. As such, the BLW CDOM was comprised of relatively low molecular weight aromatic carbon-containing molecules with no measured colloidal fraction (3,000-100,000 Da). Fluorescence-PARAFAC modeling of the whole water samples and AF4-generated fractions yielded five principal components. However, Component 3 was attributed to instrument noise and discarded. PARAFAC Components 1, 2, and 4 had primary and secondary excitation maxima and resembled humic-like fluorophores identified previously by either PARAFAC or peak-picking techniques. Conversely, Component 5 had a single excitation maxima and was most similar to a protein-like fluorophore identified in estuarine and lake water samples. Samples from the 10-m sampling depth had the highest total fluorescence, echoing the AF4-UVA₂₅₄ results, and adding further weight-of-evidence to the conclusion that the BLW CDOM was stratified by depth. Further, the relative percent contribution of each fluorophore varied by depth, indicating that the type of fluorophores were stratified by depth. The stratification of BLW CDOM shown here has potentially important implications for drinking water utilities that aim to reduce formation of disinfection byproducts.

ACKNOWLEDGEMENTS

The authors gratefully acknowledge the support of the Beaver Water District (Lowell, AR) for providing access for water sampling and funds to support DRM and operation of the laboratory equipment. Dr. Soheyl Tadjiki (Postnova Analytics, Salt Lake City, UT) provided invaluable analytical guidance for the operation of the AF4 system. Funds for the laboratory equipment and support of ADP and SLC were provided by the UA as part of the start-up package for JLF. Additional support of ADP was provided by the Doctoral Academy Fellowship program (UA).

Table 1. Asymmetric flow-field flow fractionation pump flow rates.

Phase	Tip	Flow rates (mL min ⁻¹)		
		Focus	Cross-flow	Slot
Injection	2.0	2.3	4.0	0.0
Focusing	0.2	4.3	4.0	0.2
Elution	4.5	0.0	4.0	0.2
Rinsing	5.0	0.0	0.0	0.0

Table 2. Water quality parameters.

Date	Depth	pH	Turbidity	Conductivity	Alkalinity	Ammonia	Nitrate	Nitrite	DOC	SUVA
-	m	-	NTU	$\mu\text{S cm}^{-1}$	$\text{mg L}^{-1}\text{-CaCO}_3$	$\text{mg L}^{-1}\text{-N}$	$\text{mg L}^{-1}\text{-N}$	$\mu\text{g L}^{-1}\text{-N}$	$\text{mg L}^{-1}\text{-C}$	$\text{L mg}^{-1} \text{m}^{-1}$
5/27/10	3	8.0	4	231	62	0.20	0.52	166.9	3.2	2.8
	10	8.1	18	159	62	0.05	0.95	10.0	2.2	5.6
	18	8.1	7	164	60	0.46	0.86	1.3	1.3	3.0
6/15/10	3	8.2	1	158	62	0.29	0.38	12.4	2.1	2.6
	10	7.8	8	156	59	0.07	1.08	8.4	2.1	4.9
	18	7.6	9	171	63	0.04	1.04	5.2	1.7	2.8
6/22/10	3	9.1	2	153	67	0.16	0.07	11.6	2.3	2.3
	10	7.7	13	135	52	0.04	1.03	9.6	8.2	2.1
	18	7.8	9	167	60	0.04	1.08	2.3	1.5	3.1
6/29/10	3	9.3	2	141	57	0.05	BD	5.4	2.6	2.1
	10	7.7	15	137	54	0.02	1.01	9.6	2.7	5.1
	18	7.8	10	177	61	0.05	1.03	4.7	13.2	0.4
7/08/10	3	8.9	2	150	59	0.07	0.22	5.3	2.4	2.1
	10	7.6	18	147	58	0.01	0.98	4.5	24.7	0.4
	18	7.7	20	171	62	0.03	1.05	3.7	8.2	0.7
7/13/10	3	8.7	3	148	58	0.04	0.14	4.8	2.2	2.2
	10	7.7	21	173	58	0.05	0.94	5.6	2.5	4.5
	18	7.7	21	169	63	0.03	0.99	4.8	1.7	3.5
7/20/10	3	9.2	1	152	62	0.04	0.16	7.6	10.0	0.4
	10	7.7	8	150	61	0.16	0.53	5.5	2.4	4.5
	18	7.6	13	172	66	0.13	1.01	7.2	2.6	2.8
7/27/10	3	9.1	2	154	63	0.05	0.11	3.7	2.0	2.0
	10	7.9	15	171	73	0.34	0.26	19.6	2.5	3.6
	18	7.8	15	171	68	0.31	0.53	68.0	2.3	3.8
Mean	NA	8.1	10	162	61	0.11	0.67	16.2	4.4	2.8
Median	NA	7.8	9	159	62	0.05	0.90	5.6	2.4	2.8

BD – below detection

NA – not applicable

Table 3. Literature-reported diffusion coefficients for humic substances

Sample	Molecular Weight Daltons	Diffusion Coefficient $\times 10^6 \text{ cm}^2 \text{ s}^{-1}$	Reference
Suwannee River Fulvic Acid	1,340	3.4 [†]	Dycus et al. 1995
Nordic Fulvic Acid	2,137	3.3 [†]	
Nordic Humic Acid	3,264	2.7 [†]	
Suwannee stream fulvate	860	4.1	Beckett et al. 1987
Suwannee stream humate	1,490	3.2	
Trehorningen	2,900	2.4 [‡] , 2.6 [§]	Lead et al. 1999
Hellerudmyra - May	3,900	2.1 [‡] , 2.2 [§]	
Hellerudmyra - October	3,700	2.2 [‡] , 2.2 [§]	
Aurevann	2,400	2.6 [‡] , 2.7 [§]	
Maridulsvann	2,900	2.3 [‡]	
Birkenes	3,500	2.2 [‡] , 2.4 [§]	
Humex B	3,600	2.2 [‡] , 2.4 [§]	
Suwannee River Fulvic Acid	530-1,640	2.2-3.3 [†] ; 2.4-2.8 [‡] ; 2.4-3.5 [¶]	Lead et al. 2000
Suwannee River Natural Organic Matter	-	4.1-5.5 [†]	Moon et al. 2006
Suwannee River Humic Acid	-	4.5-5.8 [†]	
Suwannee River Fulvic Acid	-	3.6-4.6 [†]	
Nakdong River Natural Organic Matter	1,270	5.6 [†]	Park and Cho 2008

[†] Flow-field flow fractionation
[‡] Reverse osmosis isolation followed by fluorescence correlation spectroscopy
[§] Vacuum evaporation isolation followed by fluorescence correlation spectroscopy
[¶] Pulsed field gradient nuclear magnetic resonance (NMR)

Table 4. Characteristics of the PARAFAC components.

PARAFAC Component	Excitation Maxima nm	Emission Maxima nm	Description	Method	Sample Source	Reference
1	225-245 (315-335)	405-430	Humic-like	PARAFAC	Estuary	Hall and Kenny 2007
			Humic-like	PARAFAC	Freshwater	Stedmon and Markager 2005
2	247-267 (359-379)	455-485	Humic-like	PARAFAC	Estuary	Hall and Kenny 2007
4	374 (233)	465	Humic-like	Peak-Picking	Treated Wastewater	Worms et al. 2010
5	224-234	333-343	Protein-like	PARAFAC	Estuary	Hall et al. 2005
			Protein-like	PARAFAC	Lake Water	Hua et al. 2007

Secondary maxima are shown in parentheses

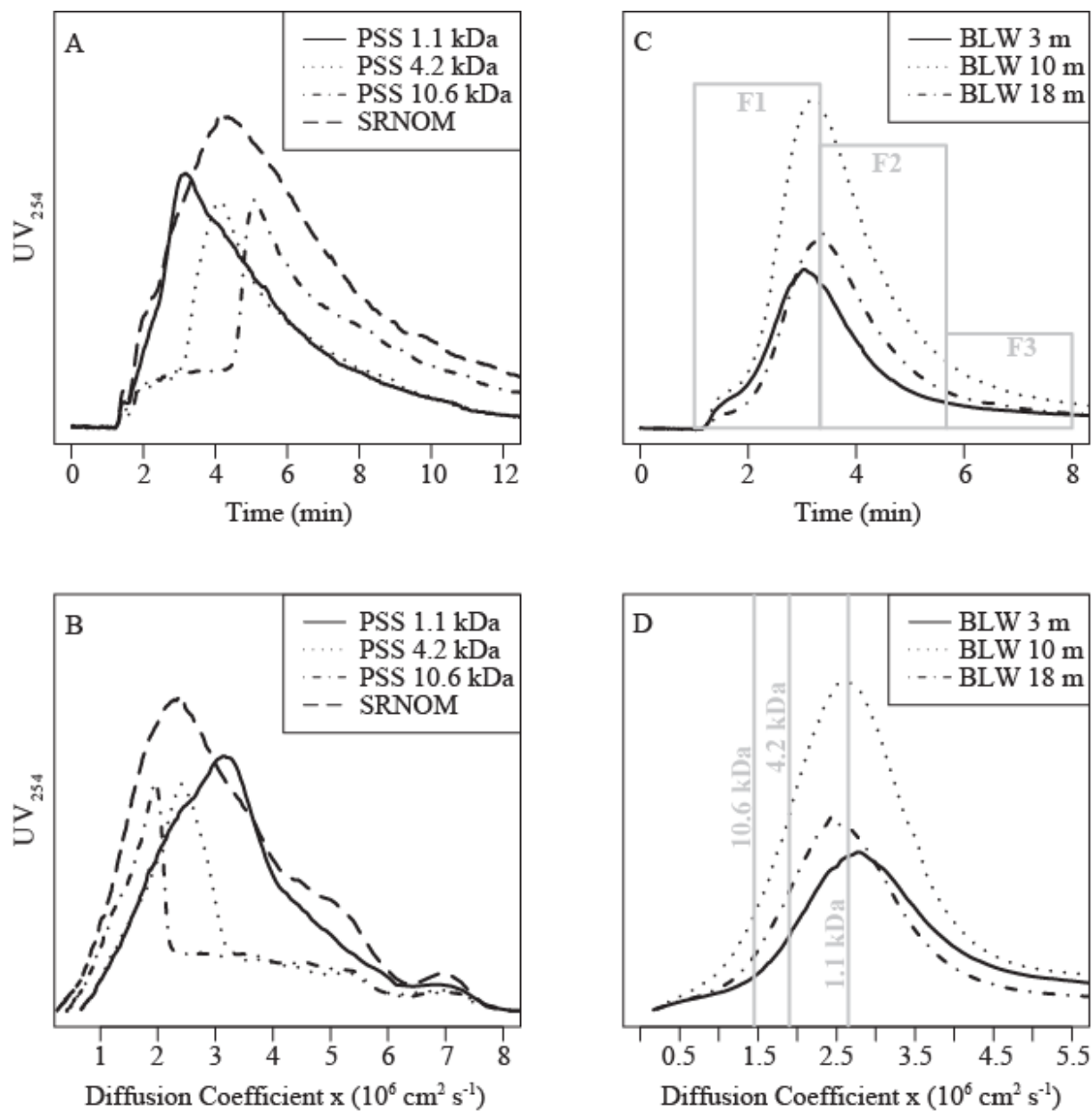


Figure 1. Asymmetric flow-field flow fractionation (AF4) fractograms of polystyrene sulfonate (PSS) standards and Suwannee River natural organic matter (SRNOM) as a function of time (Panel A) and diffusion coefficient (Panel B). AF4 fractograms of Beaver Lake Water (BLW) sampled on July 8, 2010 at depths of 3-, 10-, and 18-m as a function of time (Panel C) and diffusion coefficient (Panel D). Boxes in Panel C represent the three fractions (F1-F3) collected for subsequent fluorescence analyses. Dashed lines in Panel D represent the peak maximums of the PSS standards.

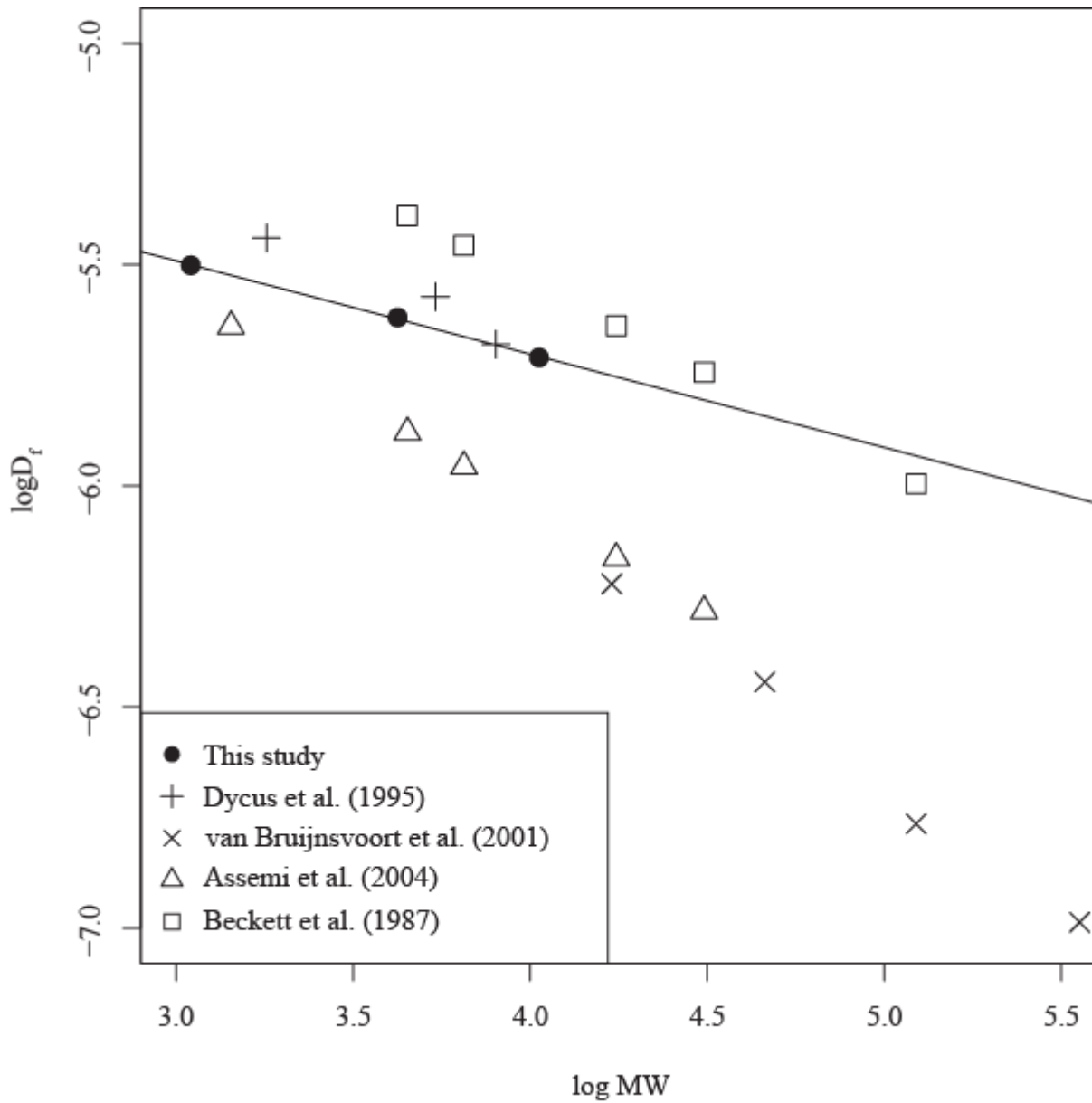


Figure 2. Diffusion coefficient, D_f , as a function of molecular weight, MW, for the polystyrene sulfonate (PSS) standards and log-linear regression line. Data from the literature is shown for comparative purposes but was not used to generate the regression line.

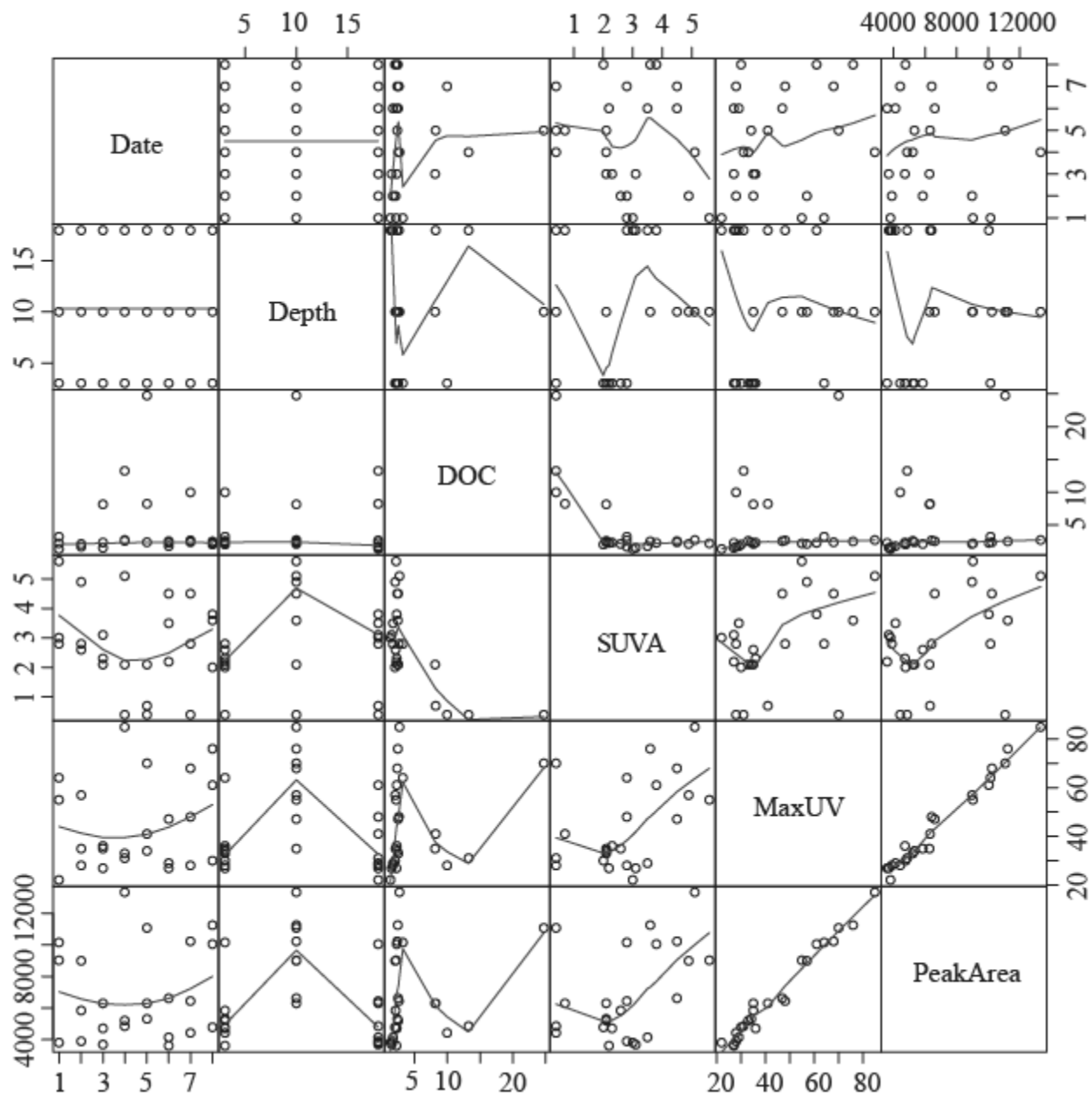


Figure 3. Pair-wise scatterplot of the asymmetric flow-field flow fractionation (AF4) fractogram data (MaxUV and PeakArea), dissolved organic carbon (DOC), specific ultraviolet absorbance (SUVA), and sample collection date and depth.

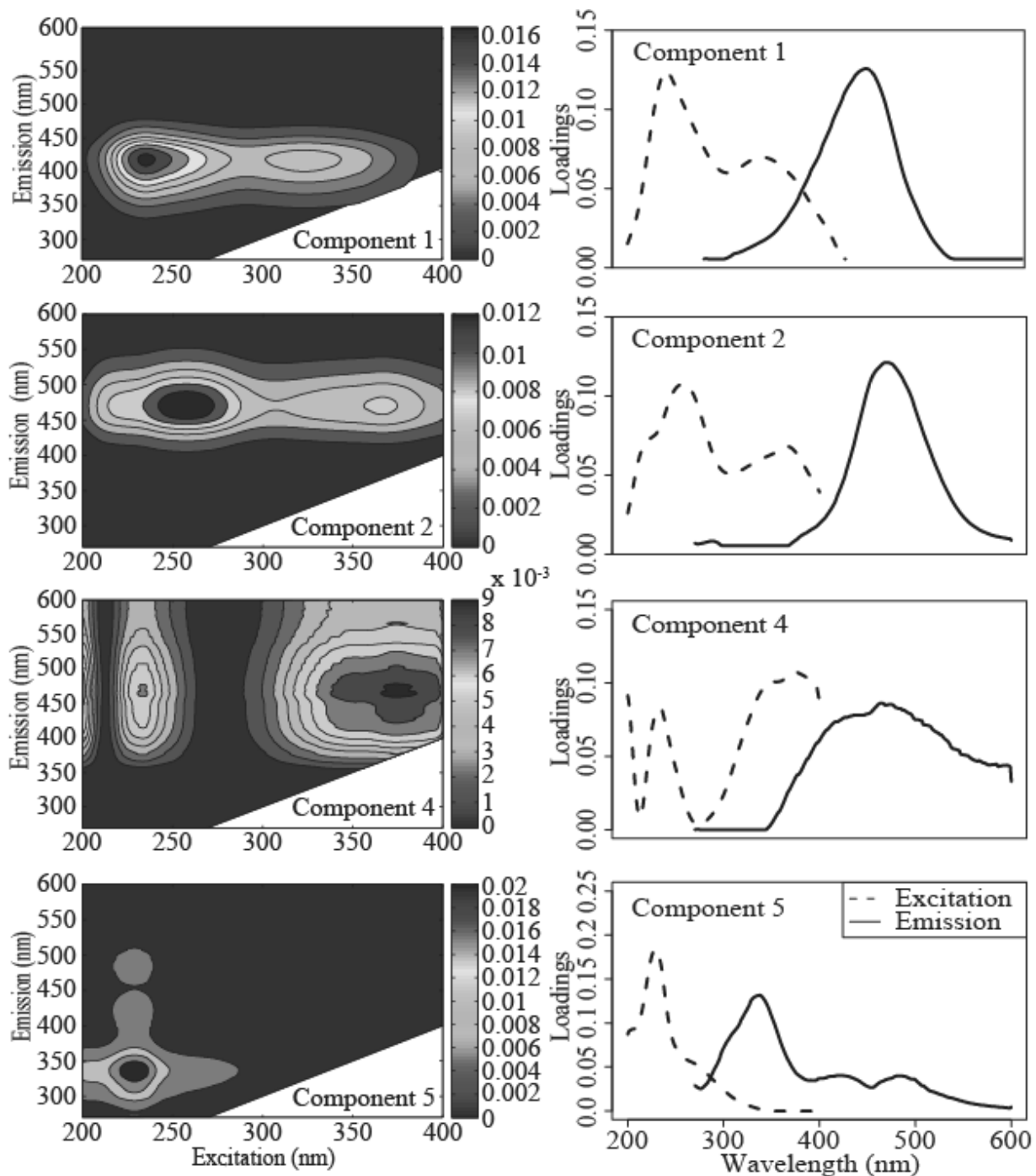


Figure 4. Fluorescence components 1, 2, 4, and 5 identified by the PARAFAC model shown as excitation-emission matrices (EEMs) in the left-side panels and their corresponding excitation and emission loadings as a function of wavelength in right-side panels.

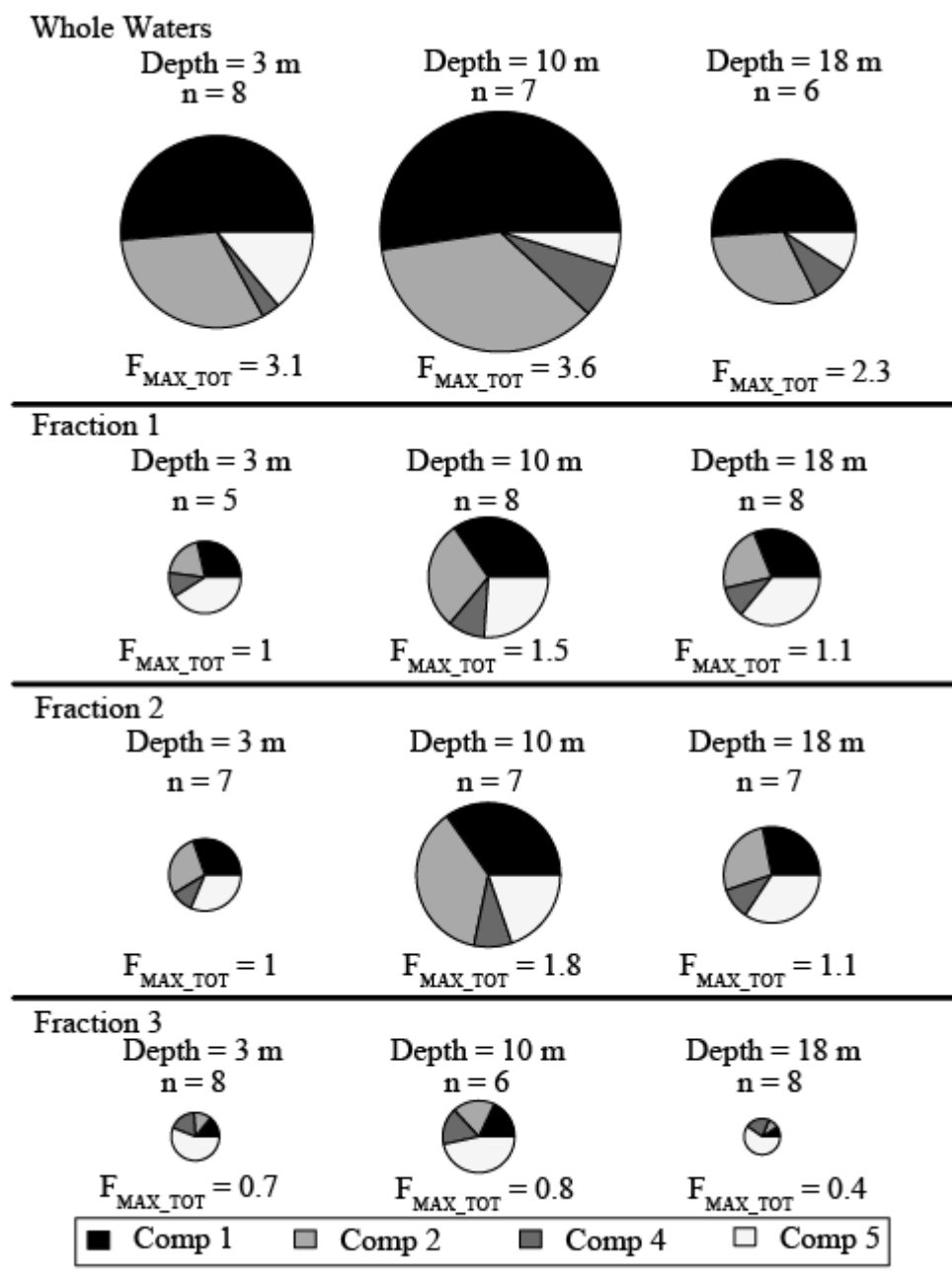


Figure 5. Relative percent contribution of PARAFAC components 1, 2, 4, and 5 for the whole waters and asymmetric flow-field flow fractionation generated fractions (Fraction 1-3) as a function of sample depth (3-, 10-, and 18-m). The diameter of pie charts was drawn proportional to the average total maximum fluorescence, F_{MAX_TOT} . The number of samples averaged, n , was appended to each pie chart.

6. REFERENCES

- Alasonati, E., Slaveykova, V. I., Gallard, H., Croue, J. P. and Benedetti, M. F., 2010. Characterization of the colloidal organic matter from the Amazonian basin by asymmetrical flow field-flow fractionation and size exclusion chromatography. *Water Research* 44 (1), 223-231.
- Andersen, C. M. and Bro, R., 2003. Practical aspects of PARAFAC modeling of fluorescence excitation-emission data. *Journal of Chemometrics* 17 (4), 200-215.
- Assemi, S., Newcombe, G., Hepplewhite, C. and Beckett, R., 2004. Characterization of natural organic matter fractions separated by ultrafiltration using flow field-flow fractionation. *Water Research* 38 (6), 1467-1476.
- Baalousha, M., Kammer, F. V. D., Motelica-Heino, M. and Le Coustumer, P., 2005. Natural sample fractionation by F1FFF-MALLS-TEM: Sample stabilization, preparation, pre-concentration and fractionation. *Journal of Chromatography A* 1093 (1-2), 156-166.
- Baalousha, M. and Lead, J. R., 2007. Characterization of natural aquatic colloids (< 5 nm) by flow-field flow fractionation and atomic force microscopy. *Environmental Science & Technology* 41 (4), 1111-1117.
- Beckett, R., Jue, Z. and Giddings, J. C., 1987. Determination of molecular weight distributions of fulvic and humic acids using flow field-flow fractionation. *Environmental Science & Technology* 21 (3), 289-295.
- Boehme, J. and Wells, M., 2006. Fluorescence variability of marine and terrestrial colloids: Examining size fractions of chromophoric dissolved organic matter in the Damariscotta River estuary. *Marine Chemistry* 101 (1-2), 95-103.
- Cabaniss, S. E., Zhou, Q. H., Maurice, P. A., Chin, Y. P. and Aiken, G. R., 2000. A log-normal distribution model for the molecular weight of aquatic fulvic acids. *Environmental Science & Technology* 34 (6), 1103-1109.
- Cawley, K. M., Hakala, J. A. and Chin, Y. P., 2009. Evaluating the triplet state photoreactivity of dissolved organic matter isolated by chromatography and ultrafiltration using an alkylphenol probe molecule. *Limnology and Oceanography-Methods* 7, 391-398.
- Chatterjee, A., 1964. Diffusion Studies of Bovine Plasma Albumin at 25° with the Help of Jamin Interference Optics. *Journal of the American Chemical Society* 86 (18), 3640-3642.
- Chu, W.-H., Gao, N.-Y., Deng, Y. and Krasner, S. W., 2010. Precursors of Dichloroacetamide, an Emerging Nitrogenous DBP Formed during Chlorination or Chloramination. *Environmental Science & Technology* 44 (10), 3908-3912.
- Coble, P. G., 1996. Characterization of marine and terrestrial DOM in seawater using excitation emission matrix spectroscopy. *Marine Chemistry* 51 (4), 325-346.

- Coble, P. G., Green, S. A., Blough, N. V. and Gagosian, R. B., 1990. Characterization of dissolved organic matter in the Black Sea by fluorescence spectroscopy. *Nature* 348 (6300), 432-435.
- Dubascoux, S., Von Der Kammer, F., Le Hecho, I., Gautier, M. P. and Lespes, G., 2008. Optimisation of asymmetrical flow field flow fractionation for environmental nanoparticles separation. *Journal of Chromatography A* 1206 (2), 160-165.
- Dycus, P. J. M., Healy, K. D., Stearman, G. K. and Wells, M. J. M., 1995. Diffusion-coefficients and molecular-weight distributions of humic and fulvic-acids determined by flow field-flow fractionation. *Separation Science and Technology* 30 (7-9), 1435-1453.
- Eaton, A. D., Clesceri, L. S., Rice, E. W. and Greenberg, A. E., Eds. (2005). Standard methods for the examination of water & wastewater. Washington, DC, American Public Health Association
- Fellman, J. B., D'Amore, D. V., Hood, E. and Boone, R. D., 2008. Fluorescence characteristics and biodegradability of dissolved organic matter in forest and wetland soils from coastal temperate watersheds in southeast Alaska. *Biogeochemistry* 88 (2), 169-184.
- Floge, S. A. and Wells, M. L., 2007. Variation in colloidal chromophoric dissolved organic matter in the Damariscotta Estuary, Maine. *Limnology and Oceanography* 52 (1), 32-45.
- Gadmar, T. C., Vogt, R. D. and Evje, L., 2005. Artifacts in XAD-8 NOM fractionation. *International Journal of Environmental Analytical Chemistry* 85 (6), 365-376.
- Giddings, J. C., 1993. Field-flow fractionation - Analysis of macromolecular, colloidal, and particulate materials. *Science* 260 (5113), 1456-1465.
- Hall, G. J., Clow, K. E. and Kenny, J. E., 2005. Estuarial Fingerprinting through Multidimensional Fluorescence and Multivariate Analysis. *Environmental Science & Technology* 39 (19), 7560-7567.
- Hall, G. J. and Kenny, J. E., 2007. Estuarine water classification using EEM spectroscopy and PARAFAC-SIMCA. *Analytica Chimica Acta* 581 (1), 118-124.
- Howe, K. J. and Clark, M. M., 2002. Fouling of microfiltration and ultrafiltration membranes by natural waters. *Environmental Science & Technology* 36 (16), 3571-3576.
- Hua, B., Dolan, F., McGhee, C., Clevenger, T. E. and Deng, B., 2007. Water-source characterization and classification with fluorescence EEM spectroscopy: PARAFAC analysis. *International Journal of Environmental Analytical Chemistry* 87 (2), 135-147.
- Hua, B., Veum, K., Yang, J., Jones, J. and Deng, B. L., 2010. Parallel factor analysis of fluorescence EEM spectra to identify THM precursors in lake waters. *Environmental Monitoring and Assessment* 161 (1-4), 71-81.

- Huguet, A., Vacher, L., Relexans, S., Saubusse, S., Froidefond, J. M. and Parlanti, E., 2009. Properties of fluorescent dissolved organic matter in the Gironde Estuary. *Organic Geochemistry* 40 (6), 706-719.
- Johnstone, D. W. and Miller, C. M., 2009. Fluorescence Excitation-Emission Matrix Regional Transformation and Chlorine Consumption to Predict Trihalomethane and Haloacetic Acid Formation. *Environmental Engineering Science* 26 (7), 1163-1170.
- Johnstone, D. W., Sanchez, N. P. and Miller, C. M., 2009. Parallel Factor Analysis of Excitation-Emission Matrices to Assess Drinking Water Disinfection Byproduct Formation During a Peak Formation Period. *Environmental Engineering Science* 26 (10), 1551-1559.
- Kitis, M., Karanfil, T., Wigton, A. and Kilduff, J. E., 2002. Probing reactivity of dissolved organic matter for disinfection by-product formation using XAD-8 resin adsorption and ultrafiltration fractionation. *Water Research* 36 (15), 3834-3848.
- Kitis, M., Karanfil, T., Kilduff, J.E., Wigton, A., 2001. The reactivity of natural organic matter to disinfection byproducts formation and its relation to specific ultraviolet absorbance. *Water Science and Technology* 43 (2), 9-16.
- Korshin, G. V., Benjamin, M. M., Chang, H. S. and Gallard, H., 2007. Examination of NOM chlorination reactions by conventional and stop-flow differential absorbance spectroscopy. *Environmental Science & Technology* 41 (8), 2776-2781.
- Krachler, R., Krachler, R. F., von der Kammer, F., Suephandag, A., Jirsa, F., Ayromlou, S., Hofmann, T. and Keppler, B. K., 2010. Relevance of peat-draining rivers for the riverine input of dissolved iron into the ocean. *Science of the Total Environment* 408 (11), 2402-2408.
- Lead, J. R., Balnois, E., Hosse, M., Menghetti, R. and Wilkinson, K. J., 1999. Characterization of Norwegian natural organic matter: Size, diffusion coefficients, and electrophoretic mobilities. *Environment International* 25 (2-3), 245-258.
- Lead, J. R., Wilkinson, K. J., Balnois, E., Cutak, B. J., Larive, C. K., Assemi, S. and Beckett, R., 2000. Diffusion coefficients and polydispersities of the Suwannee River fulvic acid: Comparison of fluorescence correlation spectroscopy, pulsed-field gradient nuclear magnetic resonance, and flow field-flow fractionation. *Environmental Science & Technology* 34 (16), 3508-3513.
- LeChevallier, M. W., Welch, N. J. and Smith, D. B., 1996. Full-scale studies of factors related to coliform regrowth in drinking water. *Applied and Environmental Microbiology* 62 (7), 2201-2211.
- Moon, J., Kim, S. H. and Cho, J., 2006. Characterizations of natural organic matter as nano particle using flow field-flow fractionation. *Colloids and Surfaces a-Physicochemical and Engineering Aspects* 287 (1-3), 232-236.

- Park, N. and Cho, J., 2008. Natural organic matter diffusivity for transport characterizations in nanofiltration and ultrafiltration membranes. *Journal of Membrane Science* 315 (1-2), 133-140.
- Prestel, H., Niessner, R. and Panne, U., 2006. Increasing the sensitivity of asymmetrical flow field-flow fractionation: Slot outlet technique. *Analytical Chemistry* 78 (18), 6664-6669.
- Reszat, T. N. and Hendry, M. J., 2005. Characterizing dissolved organic carbon using asymmetrical flow field-flow fractionation with on-line UV and DOC detection. *Analytical Chemistry* 77 (13), 4194-4200.
- Rook, J. J., 1977. Chlorination reactions of fulvic acids in natural waters. *Environmental Science & Technology* 11 (5), 478-482.
- Santschi, P. H., Roberts, K. A. and Guo, L., 2002. Organic Nature of Colloidal Actinides Transported in Surface Water Environments. *Environmental Science & Technology* 36 (17), 3711-3719.
- Schimpf, M. E., Caldwell, K. D. and Giddings, J. C., Eds. (2000). Field-flow fractionation handbook, John Wiley & Sons, Inc.
- Schimpf, M. E. and Wahlund, K. G., 1997. Asymmetrical flow field-flow fractionation as a method to study the behavior of humic acids in solution. *Journal of Microcolumn Separations* 9 (7), 535-543.
- Sen, S., Haggard, B. E., Chaubey, I., Brye, K. R., Costello, T. A. and Matlock, M. D., 2007. Sediment phosphorus release at Beaver Reservoir, northwest Arkansas, USA, 2002-2003: A preliminary investigation. *Water Air and Soil Pollution* 179 (1-4), 67-77.
- Stedmon, C. A. and Bro, R., 2008. Characterizing dissolved organic matter fluorescence with parallel factor analysis: a tutorial. *Limnology and Oceanography-Methods* 6, 572-579.
- Stedmon, C. A. and Markager, S., 2005. Resolving the variability in dissolved organic matter fluorescence in a temperate estuary and its catchment using PARAFAC analysis. *Limnology and Oceanography* 50 (2), 686-697.
- Stolpe, B., Guo, L. D., Shiller, A. M. and Hasselov, M., 2010. Size and composition of colloidal organic matter and trace elements in the Mississippi River, Pearl River and the northern Gulf of Mexico, as characterized by flow field-flow fractionation. *Marine Chemistry* 118 (3-4), 119-128.
- van Bruijnsvoort, M., Tijssen, R. and Kok, W. T., 2001. Assessment of the diffusional behavior of polystyrene sulfonates in the dilute regime by hollow-fiber flow field flow fractionation. *Journal of Polymer Science Part B: Polymer Physics* 39 (15), 1756-1765.
- Wahlund, K. G. and Giddings, J. C., 1987. Properties of an asymmetrical flow field-flow fractionation channel having one permeable wall. *Analytical Chemistry* 59 (9), 1332-1339.

- Weishaar, J. L., Aiken, G. R., Bergamaschi, B. A., Fram, M. S., Fujii, R. and Mopper, K., 2003. Evaluation of specific ultraviolet absorbance as an indicator of the chemical composition and reactivity of dissolved organic carbon. *Environmental Science & Technology* 37 (20), 4702-4708.
- Worms, I. A. M., Szigeti, Z. A. G., Dubascoux, S., Lespes, G., Traber, J., Sigg, L. and Slaveykova, V. I., 2010. Colloidal organic matter from wastewater treatment plant effluents: Characterization and role in metal distribution. *Water Research* 44 (1), 340-350.
- Yang, X., Shang, C., Lee, W., Westerhoff, P. and Fan, C. H., 2008. Correlations between organic matter properties and DBP formation during chloramination. *Water Research* 42 (8-9), 2329-2339.
- Yohannes, G., Wiedmer, S. K., Jussila, M. and Riekkola, M. L., 2005. Fractionation of Humic Substances by Asymmetrical Flow Field-Flow Fractionation. *Chromatographia* 61 (7), 359-364.
- Zepp, R. G., Sheldon, W. M. and Moran, M. A., 2004. Dissolved organic fluorophores in southeastern US coastal waters: correction method for eliminating Rayleigh and Raman scattering peaks in excitation-emission matrices. *Marine Chemistry* 89 (1-4), 15-36.

APPENDIX 1

Supporting Material for

“Coupling Asymmetric Flow-Field Flow Fractionation and Fluorescence Parallel Factor Analysis Reveals Stratification of Dissolved Organic Matter in a Drinking Water Reservoir”

The supporting material contains (1) a schematic of the asymmetric flow-field flow fractionation channel (Fig. SM1), (2) figures used to illustrate the processing of the fluorescence excitation-emission data and the various diagnostic checks that were used to verify the PARAFAC model (Figs. SM2-5), (3) a pair-wise scatter plot of the water quality data presented in Table 2, (4) the complete of AF4 fractograms (Fig. SM7), and (5) the PARAFAC Component 3 that was discarded and attributed to instrument noise (Fig. SM8).

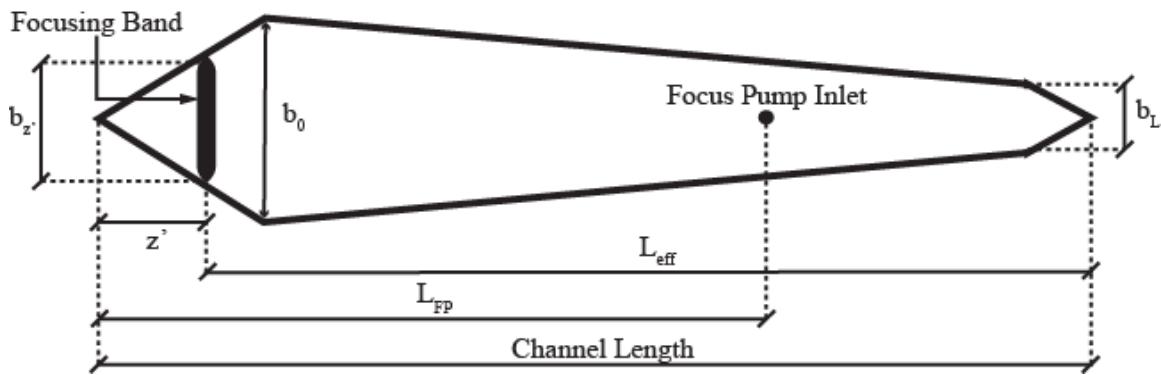


Figure SM1. Schematic of the channel for the asymmetric flow-field flow fractionation system.

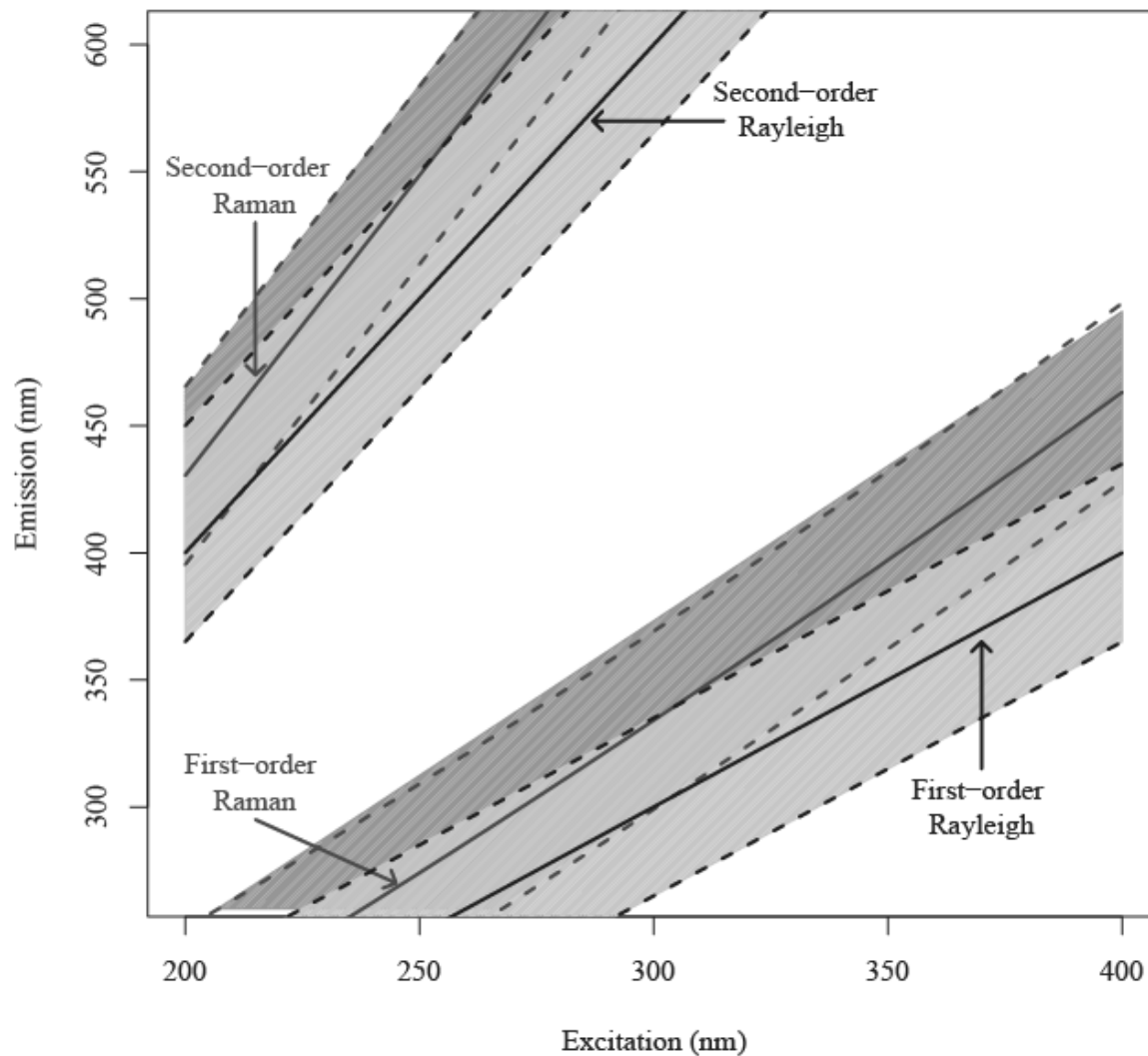


Figure SM2. Excitation-emission matrix depicting the water scattering regions excised and interpolated using the *Cleanscan* protocol. Solid lines represent the theoretical locations of the first- and second-order Rayleigh and Raman scattering regions and the shaded areas bound with dashed lines show the swath of data over which *Cleanscan* was used.

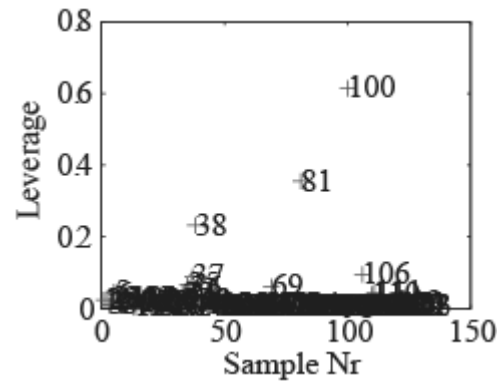


Figure SM3. Leverage plots for the excitation-emission matrices contained in the initial PARAFAC data array.

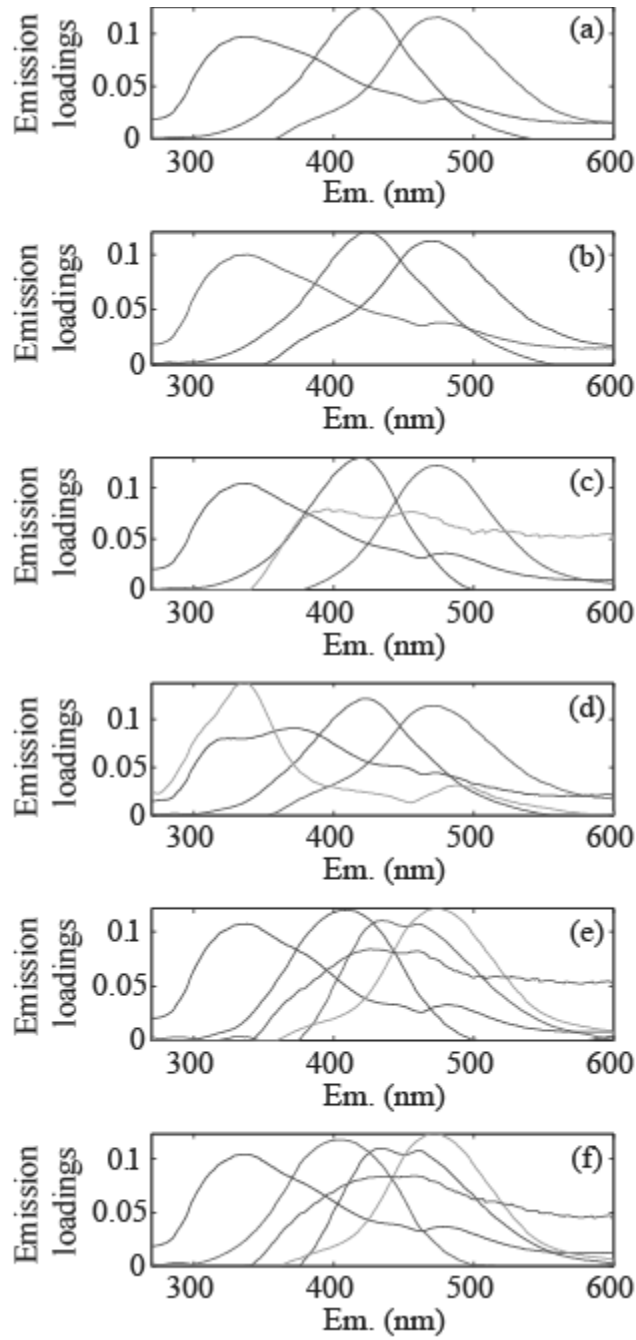


Figure SM4. Results from Split-halves Analysis for PARAFAC models containing (a, b) 3-components: validated, (c, d) 4-components: not validated, and (e, f) 5-components: validated.

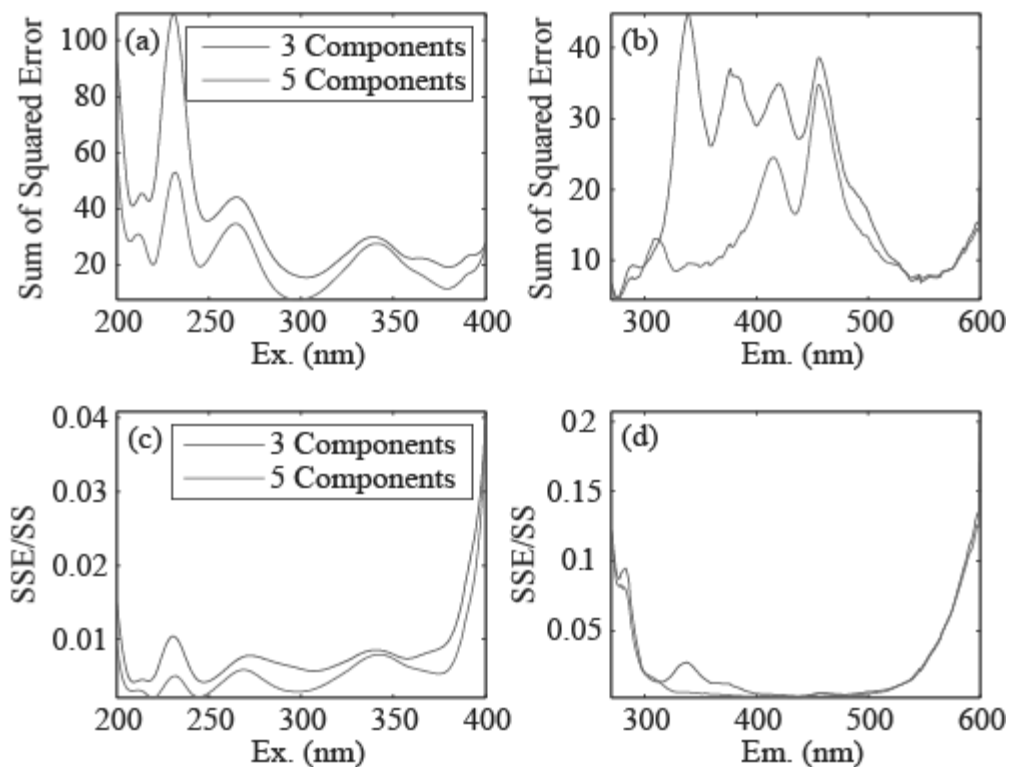


Figure SM5. Analysis of the increase in fit of the PARAFAC model to the measured EEMs: (a, b) the sum of squared error versus excitation and emission; (c, d) the sum of squared error normalized by the sum of total sum of squares versus excitation and emission.

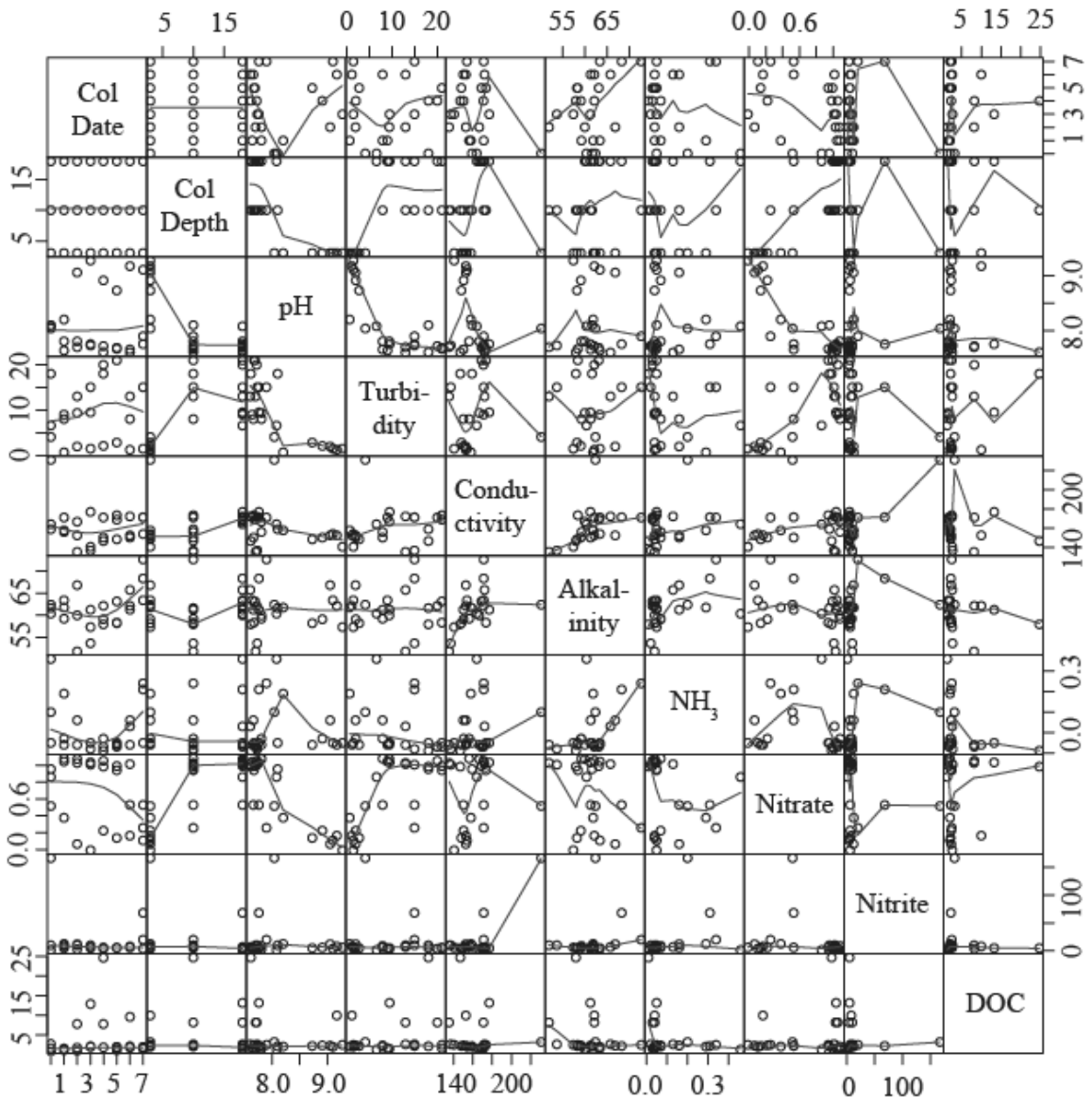


Figure SM6. Pair-wise scatter plot of the water quality parameters.

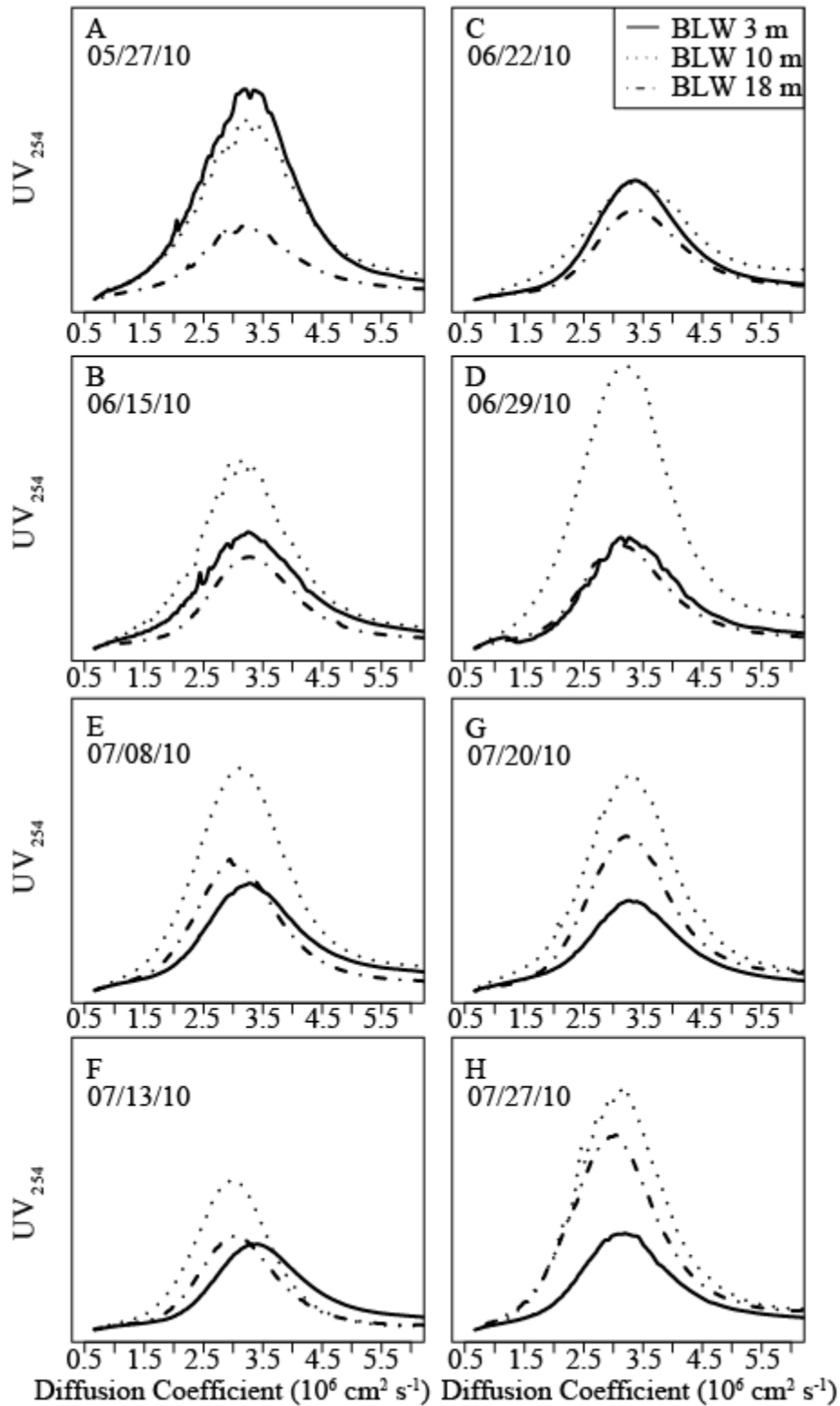


Figure SM7. Asymmetric flow-field flow fractionation (AF4) diffusion coefficient fractograms of Beaver Lake Water (BLW) chromophoric dissolved organic matter (CDOM) sampled between 05/27/10 and 07/27/10 at depths of 3-, 10-, and 18-m below the water surface.

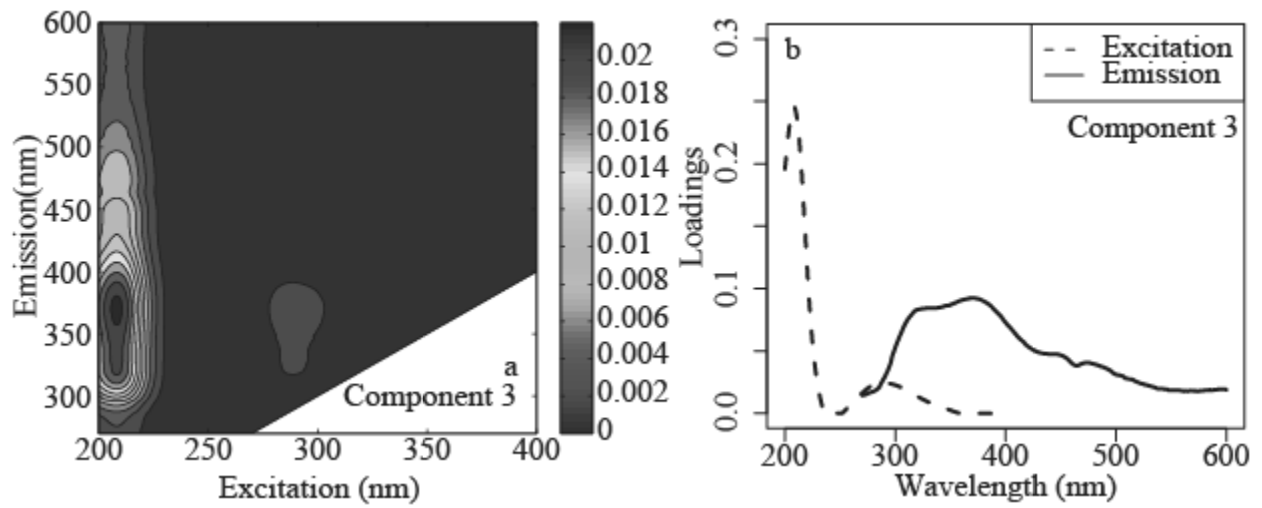
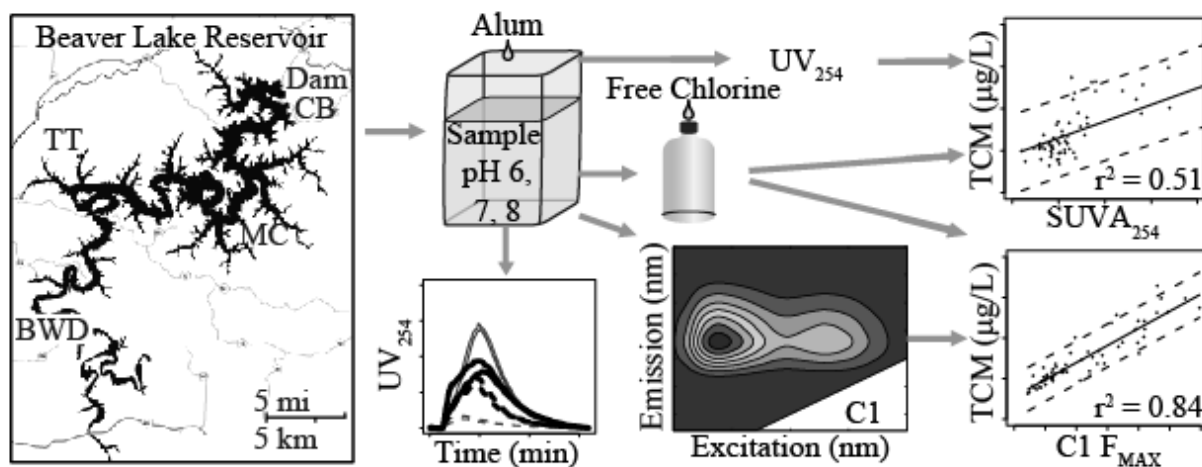


Figure SM8. The PARAFAC Component 3, which was attributed to instrument noise: (a) excitation-emission matrix and (b) the corresponding loadings plot.

CHAPTER 3

Improving on $SUVA_{254}$ Using Fluorescence-PARAFAC Analysis and Asymmetric Flow-Field Flow Fractionation for Assessing Disinfection Byproduct Formation and Control



ABSTRACT

Several challenges with disinfection byproduct (DBP) control stem from the complexity and diversity of dissolved organic matter (DOM), which is ubiquitous in natural waters and reacts with disinfectants to form DBPs. Fluorescence parallel factor (PARAFAC) analysis and asymmetric flow-field flow fractionation (AF4) were used in combination with free chlorine DBP formation potential (DBPFP) tests to study the physicochemical DOM properties and DBP formation in raw- and alum-coagulated waters. Enhanced coagulation with alum became more effective at removing DBP-precursors as the pH decreased from 8 to 6. AF4-UV₂₅₄ fractograms indicated enhanced coagulation at pH 6 preferentially removed larger DOM, whereas no preferential size removal occurred at pH 8. Fluorescence-PARAFAC analysis revealed the presence of one protein-like and three humic-like fluorophore groups; stronger linear correlations were found between chloroform and the maximum intensity (F_{MAX}) of a humic-like fluorophore ($r^2 = 0.84$) than with SUVA₂₅₄ ($r^2 = 0.51$). This result indicated that the fluorescence-PARAFAC approach used here was an improvement on SUVA₂₅₄, i.e., fluorescence-based measurements were stronger predictors of chloroform formation.

KEYWORDS

Enhanced coagulation; dissolved organic matter; chloroform; drinking water; pH effects

ABBREVIATIONS

AF4 (asymmetric flow-field flow fractionation); BWD (Beaver Water District); CB (Carroll Boone Water District); DBPFP (disinfection byproduct formation potential); DBPs (disinfection byproducts); DOC (dissolved organic carbon); DOM (dissolved organic matter); DWTPs (drinking water treatment plants); EEMs (excitation-emission matrices); F_{MAX} (fluorophore maximum intensity); GFF (glass fiber filters); HDPE (high-density polyethylene); MC (Madison

County Regional Water District); NOM (natural organic matter); PARAFAC (parallel factor analysis); SUVA₂₅₄ (specific ultraviolet absorbance at 254 nm); TDN (total dissolved nitrogen); THMs (trihalomethanes); TN (total nitrogen); TOC (total organic carbon); TT (Benton/Washington Regional Public Water Authority, Two Ton); UV₂₅₄ (ultraviolet absorbance at 254 nm).

1. INTRODUCTION AND MOTIVATION

Disinfection of drinking water has been crucial in the protection of public health since the early twentieth century, but is not without challenges. Rook (1976) reported the formation of haloforms following chlorination of natural waters from reactions with natural organic matter (NOM), which is ubiquitous in surface and ground waters. Trihalomethanes (THMs) are the most abundant group of DBPs formed during chlorination and have been linked to increased cancer risk (Cantor et al. 1998) and adverse reproductive outcomes (Nieuwenhuijsen et al. 2000). The sum of the four THMs was regulated in drinking water under the United States Environmental Protection Agency (USEPA) Stage 1 Disinfectants/Disinfection Byproducts Rule with THM regulations becoming more stringent following the promulgation of the Stage 2 Rule. Other potentially harmful DBPs (e.g. haloacetonitriles) can form upon chlorination but are currently unregulated.

Drinking water treatment plants (DWTPs) use a two-pronged approach to curb DBPs: (1) alter the disinfectant (e.g., switch from free chlorine to chloramines) and/or (2) remove more NOM (e.g., enhanced coagulation). Despite this, a 1997 survey showed that 20 of 100 DWTPs exceeded the USEPA maximum contaminant level for total THMs, 80 µg/L (Arora et al. 1997). Many DWTPs have switched disinfectants, which can decrease formation of regulated DBPs, but can produce unintended consequences (e.g. increased occurrence of nitrification and corrosion in

distribution systems (Zhang et al. 2008)). A safer but typically more expensive approach to curb DBPs is the use of enhanced coagulation with alum or another metal salt. The dominant coagulation mechanism depends on particle concentration, as well as coagulant dose and speciation, which is controlled in part by the solution pH (Yang et al. 2010). DWTPs attempt to operate enhanced coagulation with alum at the optimum pH for sweep coagulation, pH 6 to 8 (Amirtharajah 1990). The effectiveness of coagulation for DBP precursor removal is dependent on precursor properties, and tends to be highest between pH 5 and 6 (Chow et al. 2009). However, a fraction of NOM is typically recalcitrant to alum coagulation (Drikas et al. 2003) and can subsequently react with chlorine to form DBPs.

NOM exists in natural waters in the milligram per liter range, and is a mixture derived from terrestrial and aquatic sources (Rosario-Ortiz et al. 2007). NOM comprises humic substances, carboxylic acids, carbohydrates, amino acids, and proteins and can contain aromatic and aliphatic moieties along with hydrophilic and hydrophobic regions (Yohannes et al. 2005), the diversity of which presents challenges for removal. Further, NOM is present in a range of sizes, adding another level of complexity. There is limited understanding of the physicochemical characteristics of NOM especially following processes like enhanced coagulation, which, if augmented, may lead to improved NOM removal and reductions in DBP formation.

To predict DBP formation, specific ultraviolet absorbance ($SUVA_{254}$) is routinely correlated with DBPs (Ates et al. 2007). $SUVA_{254}$ is calculated as the ratio of ultraviolet absorbance at 254 nm (UV_{254}) and the product of the dissolved organic carbon (DOC) and UV cell path length. This metric requires minimal sample preparation (e.g., filtration) and commonly available analytical equipment. Filtration removes interfering particles, and the resultant NOM can be operationally defined as dissolved organic matter (DOM). In this work, DOM was defined

as the NOM that passed a 1- μm pore size glass fiber filter (GFF). While SUVA_{254} has been of some value in assessing DBP formation, not all DOM is sensitive to UV light (Kitis 2001). Further, SUVA_{254} cannot be used to predict DBPFP successfully in waters with low SUVA_{254} values (Ates et al. 2007) and strong correlations between SUVA_{254} and DBPs are water dependent (Weishaar et al. 2003).

To improve DOM characterizations, fluorescence indices and excitation emission matrices (EEMs) have been investigated. Although not all DOM components fluoresce, EEMs provide a more detailed description of DOM than SUVA_{254} . Fluorescence EEMs have been used to (1) identify a water's source (Hall et al. 2005), and (2) to reveal DOM variations by season (Miller and McKnight 2010) and sampling depth (Pifer et al. 2011). In the past, a sample's fluorescence components were identified by peak picking methods (Coble et al. 1990), but the development of parallel factor analysis (PARAFAC) for EEMs (Andersen and Bro 2003) standardized this process. PARAFAC resolves arrays of EEMs into components, or groups of fluorophores with common excitation-emission signatures. PARAFAC components are typically humic-like and protein-like fluorophores (Stedmon and Bro 2008) which some evidence suggests may correlate to formation of specific DBPs (Johnstone et al. 2009).

Due to the complexity of DOM, researchers have attempted to fractionate it chemically (e.g. resin adsorption (Hua and Reckhow 2007)) and physically (e.g. size exclusion chromatography (Vuorio et al. 1998)) prior to analysis. However, these techniques can produce artifacts due to pH perturbations, sample pre-concentration, and interactions of DOM with the stationary phase, all of which can confound inferences regarding DBP formation. Conversely, asymmetric flow-field flow fractionation (AF4), which has been used to physically characterize DOM in natural waters (Schimpf and Wahlund 1997; Guéguen and Cuss 2011), operates in a

manner that can overcome many of these limitations. AF4 separates macromolecules, colloids, and particles between 1 nm and 100 μm in size on the basis of diffusivity (Giddings 1993). The sample molecules elute from the channel in order of increasing size, and a continuous size distribution, or fractogram, is produced and detected by UV₂₅₄. AF4-UV₂₅₄ has several benefits over traditional physical characterization techniques, including that it requires a low sample volume (10 mL) and minimal sample pretreatment (i.e. filtration through a GFF). As such, AF4-UV₂₅₄ fractograms can be obtained before and after jar tests, allowing estimation of the changes in DOM size distributions.

Here, fluorescence-PARAFAC analysis and AF4-UV₂₅₄ were applied to study DOM removal by enhanced coagulation and DBP formation during chlorination. The primary objectives were to use these physicochemical characterization techniques to (1) distinguish spatial and temporal variation in the character and treatability of DOM, (2) identify impacts of alum coagulation on DOM and DBP formation as a function of pH, and (3) improve on SUVA₂₅₄ as a predictor of DBP formation. Lake water samples were collected from the intake structures of four DWTPs in Northwest Arkansas between May-August, 2011. Jar tests with alum were conducted at pH 6, 7, and 8, and were followed by DBP formation potential (DBFPF) tests with free chlorine. AF4-UV₂₅₄ fractograms were collected from raw water samples and after alum coagulation, providing estimates of the relative amounts and sizes of DOM remaining. Fluorescence-PARAFAC identified humic-like and protein-like DOM components and was used to track preferential removal of these components. DBFPF tests provided a means to evaluate the effectiveness of enhanced coagulation and to compare the strength of correlations between SUVA₂₅₄ and DBFPF with those between fluorescence-PARAFAC components and DBFPF.

2. MATERIALS AND METHODS

2.1. Site description

Beaver Lake, the primary drinking water source for the approximately 500,000 residents of Northwest Arkansas, was used as the sampling site for this study. Beaver Lake is used by four DWTPs: Beaver Water District (BWD), Benton/Washington Regional Public Water Authority, commonly known as Two Ton (TT), Carroll Boone Water District (CB), and Madison County Regional Water District (MC). Beaver Lake has a surface area of 103-km², an average depth of 18-m, and a hydraulic retention time of 1.5 years (Sen et al. 2007). Beaver Lake is located on the White River and is fed by Richland Creek, War Eagle Creek, and Brush Creek. All four rivers drain mostly forested or agricultural lands with increasing urbanization. Fig. S1 shows the location of the four DWTPs on Beaver Lake.

2.2. Sample collection and handling

Water samples were collected from the four DWTPs on May 13, May 31, June 28, July 14, and August 4, 2011 as detailed in the Supplementary Data. All samples were transported to the University of Arkansas and stored in the dark at 4°C until use.

Glassware and plastic ware were prepared as described in Pifer et al. (2011). All chemicals used were ACS-reagent grade. Aqueous solutions were prepared using water with a resistivity of 18.2 MΩ-cm (Milli-Q water) generated by a Milli-Q Integral 3 (Millipore) or a Barnstead NANOpure Diamond (Thermo Scientific).

2.3. Water Quality Tests

Raw water pH, alkalinity, conductivity, turbidity, total ammonia, and UV₂₅₄ were measured. Next, 600 mL aliquots of sample were filtered through GFFs as described in Pifer et al. (2011) and total dissolved nitrogen (TDN) and dissolved organic carbon (DOC) were

measured using Shimadzu TOC/TN analyzers. $SUVA_{254}$ was calculated by dividing UV_{254} (normalized by the UV cell path length in meters) by DOC in mg/L. Details on the measurements of bromide and dissolved and particulate phosphorus are in the Supplementary Data.

2.4. Jar Tests

For each raw water sample, 1-L aliquots were adjusted to pH 6.0, 7.0, and 8.0 using 1 N hydrochloric acid or 1 N sodium hydroxide, and jar tests with alum (aluminum sulfate octadecahydrate) were conducted on each pH-adjusted sample. An eight-position magnetic stir plate with variable speed control (Challenge Technology, Springdale, AR) and rectangular plastic jars were used for the enhanced coagulation tests. Magnetic stir bars (5-cm in length) with ring-collared ends were used to minimize breakup of the floc. An alum dose of 60 mg/L was used throughout to evaluate the impact of coagulation pH on DOM removal and subsequent DBP formation, rather than determine the optimum alum dose. Alum and 2-6 mL of a 10.6 g/L sodium carbonate solution were added simultaneously to minimize pH drift during the 30 seconds of rapid mixing (~200 rpm). The flocculation time was 30 minutes, with a mixing speed of 40 rpm. The samples were allowed to settle quiescently for at least 30 minutes before the supernatant was decanted. The supernatant was filtered as described in Pifer et al. (2011), pH was measured, and two 250-mL portions were collected in amber glass jars with screw-top lids. Raw water from each DWTP was also filtered and stored in two 250-mL jars. One jar of each raw and alum-coagulated water was stored in the dark at 4°C until DOC, TDN, and UV_{254} were measured and AF4- UV_{254} fractograms and fluorescence EEMs were collected.

2.5. Disinfection byproducts

DBPFP was measured following Standard Methods 5710-B (Eaton et al. 2005) with modifications. One 250-mL jar of each filtered raw water and filtered alum-coagulated water was adjusted to pH 7.0 ± 0.2 using a phosphate buffer and chlorinated using a stock 5,000 mg/L sodium hypochlorite solution at doses resulting in chlorine residuals between 2.6 and 8.1 mg/L as Cl_2 after seven days in the dark at room temperature. After the seven day hold time, chlorine residuals were measured using DPD total chlorine reagent powder pillows (Hach Company) and a spectrophotometer (Shimadzu UV-Vis 2450). Ammonium chloride was added to 30-mL aliquots of each sample to slow DBP formation reactions without destroying haloacetonitriles species. The chlorine residual of the remaining 220-mL sample was quenched using sodium sulfite and the samples were stored at 4°C in the dark until pH, DOC, TDN, and UV_{254} were measured and AF4- UV_{254} fractograms and fluorescence EEMs were collected.

Following quenching, DBPs were immediately extracted from the 30 mL aliquots by liquid/liquid extraction following EPA 551.1 with modifications. Pentane was used as the extraction solvent, and 1,1,1-trichloroethane was added to the pentane as the internal standard (Wahman 2006). Concentrations of chloroform, bromodichloromethane, dibromochloromethane, bromoform, dichloroacetonitrile, trichloroacetonitrile, dibromoacetonitrile, and 1,1,1-trichloro-2-propanone were measured in triplicate on a gas chromatograph (Shimadzu GC-2010) with an electron capture detector and a J&W DB-1 column (Agilent Technologies). The column was initially held at 32°C for one minute, and was increased by $2^\circ\text{C}/\text{min}$ increments until it reached 50°C and was held for ten minutes. The oven temperature increased by $2^\circ\text{C}/\text{minute}$ to 160°C and was held constant for five minutes. A 10-point standard curve from 1 to $100 \mu\text{g}/\text{L}$ was used to

quantify the DBPs, and blanks and check standards were run after every twelfth injection for quality control.

2.6. Asymmetric flow-field flow fractionation

AF4 fractograms were collected on the July 14, 2011 filtered raw and alum treated samples at pH 6 and 8 using the instrumentation and methods described in Pifer et al. (2011) with the following modifications. Polyethersulfone (PES) membranes with a 1,000 Da molecular weight cut-off were used in the separation channel to achieve a stable channel pressure. Elution time was extended to 15 minutes when necessary to capture the tail of the sample peaks, and the rinse time was extended to 10 minutes with focus pump and tip pump flowrates of $3 \text{ mL}\cdot\text{min}^{-1}$ to thoroughly flush the AF4-channel and minimize the height of the void peak. Phosphate-carbonate buffer solutions at pH 6 and 8 were used as eluent to ensure that pH during fractionation remained at the coagulation pH. The conductivity of the pH 8 eluent was modified with sodium chloride to match that of the pH 6 eluent ($470 \mu\text{S cm}^{-1}$). The raw water samples were run with pH 6 and pH 8 buffers so that calculated removal percentages would reflect the impacts of coagulation only. Duplicate samples were run to ensure consistency in DOM separation and detector performance.

2.7. Fluorescence-PARAFAC analysis

Fluorescence EEMs were collected for each filtered raw water, alum-treated water, and chlorinated sample (160 EEMs total). To achieve numerical stability of the PARAFAC model, thirty-three EEMs obtained from filtered raw Beaver Lake water sampled between May 2010 and May 2011 were added to the array. After three outliers were removed, the resulting 190-EEM dataset formed the basis for a PARAFAC model. A 5-component PARAFAC model was obtained and validated using split halves analysis. Details of the PARAFAC modeling process

are provided in the Supplementary Data and complete descriptions of EEM collection, scatter correction, and PARAFAC analyses can be found in Pifer et al. (2011).

3. RESULTS AND DISCUSSION

3.1. Raw Water Parameters

Raw water parameters are summarized in Table S1. Discussion of pH, turbidity, conductivity, alkalinity, TDN, total phosphorus, and trophic state index are contained in the Supplementary Data. $SUVA_{254}$ values varied spatially by DWTP and temporally throughout the sampling period. At the BWD, $SUVA_{254}$ was high initially (11.6-L mg⁻¹ m⁻¹ on 5/13/11) and subsequently dropped to values between 2.6- and 4.9-L mg⁻¹ m⁻¹; at TT, $SUVA_{254}$ was also high initially (12.4-L mg⁻¹ m⁻¹ on 5/13/11), but was erratic thereafter with values between 3.0- and 11.1-L mg⁻¹ m⁻¹. In contrast, $SUVA_{254}$ values at CB and MC had smaller ranges and were between 1.4- and 5.8-L mg⁻¹ m⁻¹ throughout the sample period. A late April rainfall event (28-cm of rainfall in Northwest Arkansas between April 24-26, 2011 (NOAA Satellite and Information Service 2011)) may explain some of the variation in $SUVA_{254}$, as increased runoff may have carried large amounts of humic-like material (e.g., DOM rich in UV₂₅₄ absorbing groups) to the lake, disproportionately impacting BWD and TT before being diluted or degraded prior to reaching the intakes at MC and CB. Interestingly, DOC varied temporally and no correlation was found between raw water DOC and $SUVA_{254}$ ($r^2 = 0.06$), suggesting varying aromatic content (as measured by UV₂₅₄) in the Beaver Lake DOM throughout the sampling period.

3.2. AF4-UV₂₅₄ Fractograms

AF4-UV₂₅₄ fractograms for pH 6 and 8 samples collected on 7/14/11 are shown in duplicate in Fig. 1 for the four sampling locations as a function of time. AF4 separates DOM macromolecules on the basis of diffusivity, and as such samples elute with time in order of

increasing particle size (or decreasing diffusivity). The fractograms had a void peak at approximately 2-minutes, and with the exception of the TT raw water samples, the void and sample peaks were similar in height and location within each pair of duplicates, indicating the AF4-channel was flushed sufficiently between samples and the method was reproducible. For the TT raw water samples at a given pH, the void peak height increased from one run to the next, possibly indicating sample carryover, however the sample peak (around 5-min elution time) was relatively unaffected.

The AF4-UV₂₅₄ fractograms in Fig. 1 demonstrated the impact of alum coagulation pH on DOM removal. For the BWD, CB, and MC samples, the AF4-UV₂₅₄ peak maxima for the raw water DOM occurred between 4.8- and 5.6-minutes. For TT, the relatively large void peak obscured the location and height of the AF4-UV₂₅₄ DOM peak maximum. For the raw waters, the AF4-UV₂₅₄ peak heights at pH 6 were higher than those at pH 8. Alum coagulation at pH 6 resulted in average reductions between 86-91% based on AF4-UV₂₅₄ peak heights for the BWD, CB, and MC samples. In contrast, coagulation at pH 8 reduced the AF4-UV₂₅₄ peak height by 28% for BWD, 36% for MC, and 43% for CB. These findings were supported by Yang et al. (2010) who reported increased removal of UV₂₅₄ as coagulation pH decreased from 8 to 6. Coagulation also produced shifts in the time to peak maximum between the raw and alum-treated samples, but the time-shifts were larger at pH 6 (1.8-2.3 minutes) than at pH 8 (0.5 minutes). Given the AF4 fractograms are presented in order of increasing DOM size, this result indicated preferential removal of larger-sized DOM at pH 6, but relatively uniform, albeit less, removal of all DOM size fractions at pH 8.

Although AF4-UV₂₅₄ fractionation provides insight into changes in the physical properties of DOM with changes in pH, it is important to note that not all molecules absorb light

uniformly at 254 nm and that the fractograms presented here do not provide a complete picture of the DOM size distribution. Future work should explore the use of other inline detectors (e.g., DOC) for DOM size characterizations following separation by AF4.

3.3. Fluorescence-PARAFAC Analysis

A 5-component PARAFAC model was validated for an array of 190 EEMs, consisting of raw- and alum-treated waters from the four DWTPs. However, one component, previously identified as fluorometer instrument noise due to its presence at similar intensity in both samples and Millipore water blanks (Pifer et al. 2011), was ignored and, as such, a 4-component model was used here. The excitation and emission maxima of each component were listed in Table 1 and shown as EEMs in Fig. S2. Components 1 and 4 were previously identified as a humic-like fluorophore groups (Pifer et al. 2011). Component 2 was similar to protein-like fluorophores reported by Dubnick et al. (2010) and Marhaba and Lippincott (2000). These protein-like moieties contain nitrogen in their structures and as such may be of importance in the formation of nitrogen containing DBPs. Component 3 appeared to be a combination of previously identified humic-like fluorophores, including the C peak reported by Coble (1996).

Fig. 2 shows the fluorescence intensity data of the peak maxima (F_{MAX}) for each component as a function of sampling date, DWTP, and treatment (raw water and following alum coagulation at pH 6, 7, and 8). In general, for each sampling date and location, F_{MAX} was highest for raw waters and decreased following alum coagulation. Further, for the alum treated samples, F_{MAX} increased with increasing pH between 6 and 8, implying lowering the net negative surface charge on the DOM by decreasing the pH enhanced DOM removal. Component 1 was the most abundant fluorophore group of the raw- and treated-water samples, and was removed to the greatest extent by alum coagulation. To further aid in the interpretation of these data, the relative

percent contributions and percent removals of component 1 relative to the total F_{MAX} were calculated (Table 2). The percent contribution increased with increasing coagulation pH for all sample locations, indicating it was removed to a greater extent relative to the other fluorophore groups as the pH decreased. Further, F_{MAX} percent removal decreased with increasing pH at all sampling locations (e.g., 76%, 65%, and 41% removal at pH 6, 7, and 8, respectively for the four DWTPs together). For all components, the F_{MAX} data were pooled and averaged for the four DWTPs and five sampling dates and reported with their corresponding standard deviations in Table S2. Components 2, 3, and 4 had similar contributions (13-17%) to raw water fluorescence, but were removed to varying extents. The standard deviations of the percent removals for components 2 and 3 were too large to permit meaningful inferences with regard to trends with pH. Component 4 had similar percent removals and pH dependence as component 1, suggesting these fluorophore groups were more effectively removed during coagulation at lower pH. Overall, alum coagulation at pH 6 provided the best removal of all fluorescence-PARAFAC components. Regardless of pH, alum coagulation appeared to preferentially remove the humic-like components 1 and 4 compared to the protein-like component 2 and the humic-like component 3.

3.4. Disinfection Byproducts

DBPFP was measured for chlorinated raw and alum coagulated samples. Out of the eight DBPs in the standard curve, only chloroform, dichloroacetonitrile, bromodichloromethane, and 1,1,1-trichloro-2-propanone formed at quantifiable levels. The absence of dibromochloromethane, bromoform, and dibromoacetonitrile was not unexpected because the bromide concentrations in the raw water samples were low ($<0.05 \text{ mg L}^{-1}$). Fig. 3 shows the concentrations of chloroform, dichloroacetonitrile, bromodichloromethane, and 1,1,1-trichloro-2-

propanone in units of micrograms per liter as each DBP for each sampling date, DWTP, and treatment. Due to select large deviations in the check standards, the chloroform data from 5/31/11 was excluded from subsequent regression analyses. The chlorinated CB pH 8 sample for 7/14/11 was lost during the extraction procedure and was not included in Fig. 3 or used in regression analyses. With these exclusions, all chloroform data used in the regression analyses had check standards within $\pm 13\%$. The other DBPs formed at concentrations less than $10 \mu\text{g L}^{-1}$ in the raw and treated waters, which was too low to permit meaningful regression analyses.

Although pH control of all alum treated samples was effected with sodium carbonate, some drift occurred. The pH of each sample immediately following the decanting step of the jar tests was indicated at the top of each bar in Fig. 3.

As expected, chloroform was the dominant DBP in all raw- and alum treated-waters and formed in concentrations between 30 and $175 \mu\text{g/L}$. There was temporal and spatial variability in chloroform formation potential in the raw water samples. For example, on 5/13/11, chloroform ranged from $58 \mu\text{g/L}$ at CB to $149 \mu\text{g/L}$ at TT; similarly, chloroform at CB ranged from $58 \mu\text{g/L}$ on 5/13/11 to $128 \mu\text{g/L}$ on 7/14/11. These results suggest that (1) the location of the source water intake structure within a watershed can be an important aspect of DBP control strategies, and (2) the reactivity of precursors at a given location can shift quite rapidly. For chloroform, average percent removals and associated standard deviations for each DWTP are shown in Table 3 as a function of coagulation pH. The data for each DWTP and the pooled data (e.g., the four DWTPs and five sampling dates) indicate that alum treatment decreased chloroform formation, which was positively correlated with coagulation pH ($r^2=0.67$). Dichloroacetonitrile formation potentials ranged from 0.5 to $7.5 \mu\text{g/L}$, bromodichloromethane ranged from 3.5 to $10 \mu\text{g/L}$, and 1,1,1-trichloro-2-propanone ranged between 0.1 to $7.5 \mu\text{g/L}$, with one extreme case of $17.3 \mu\text{g/L}$.

Dichloroacetonitrile, bromodichloromethane, and 1,1,1-trichloro-2-propanone were removed to lower extents (8-35%), and were uncorrelated with coagulation pH (Table S3). Overall, these results indicate that decreasing coagulation pH may be a useful tool for DBP reduction in treated Beaver Lake water where chloroform dominates the total DBP formation during chlorination.

3.5. Correlations between DBP formation and DOM properties

Linear correlations were sought between DBPFP and DOM properties such as $SUVA_{254}$, chlorine demand, and F_{MAX} for the individual PARAFAC components. There were weak, positive correlations (Fig. 4) between chloroform and $SUVA_{254}$ ($r^2=0.51$) and chlorine demand ($r^2=0.58$). Correlations between chloroform and PARAFAC F_{MAX} components 2 and 3 were weak ($r^2 < 0.40$, data not shown). Stronger linear correlations were found between chloroform and PARAFAC F_{MAX} component 1 ($r^2 = 0.84$, Fig. 4) and component 4 ($r^2 = 0.76$, Fig. S3); in these plots, linear best-fit regression lines were shown along with 95% prediction intervals. This result indicates that the fluorescence-PARAFAC approach used here was an improvement on $SUVA_{254}$, i.e., fluorescence-based measurements were more quantitatively representative of chloroform precursors. F_{MAX} values from component 1 could be used to predict subsequent formation of chloroform for the waters from the four DWTPs and treatments (raw water and alum coagulation at pH 6, 7, and 8). This correlation suggests that humic-like fluorophores were important chloroform precursors and was particularly strong at low F_{MAX} values (e.g., alum treated waters), indicating that this metric may be useful in optimizing DBP control strategies such as enhanced coagulation. Similarly, Johnstone et al. (2009) used PARAFAC on raw- and alum-treated waters and found multi-linear regression correlations ($r^2 = 0.77$) between chloroform and the combination of two other PARAFAC components (one humic-like and one protein-like fluorophore group).

No correlations were found with dichloroacetonitrile, bromodichloromethane, and 1,1,1-trichloro-2-propanone and SUVA₂₅₄ ($r^2 < 0.26$, data not shown), perhaps due to the low concentrations of these three DBPs in the raw and treated waters. Interestingly, dichloroacetonitrile, a nitrogen containing DBP, was uncorrelated to the protein-like Component 2 as well as the three humic-like components, suggesting that predicting formation of nitrogen containing DBPs by fluorescence-based techniques may be challenge. Bromodichloromethane was uncorrelated with any of the PARAFAC components ($r^2 < 0.21$), perhaps due to the low bromide concentrations in the source waters, which prevented bromodichloromethane formation at levels similar to chloroform. Similarly, although 1,1,1-trichloro-2-propanone has been identified as a chloroform precursor (Suffet et al. 1976), it was uncorrelated with the PARAFAC components and chloroform. Studies are needed with an array of water sources (e.g., varying bromide and DOC) and treatment types (e.g., ion exchange) to determine if the F_{MAX} correlations determined here were source water specific or if they could be applied broadly.

4. CONCLUSIONS

AF4-UV₂₅₄ and fluorescence-PARAFAC characterizations of raw and alum coagulated Beaver Lake water samples provided the following insights into DOM removal using enhanced coagulation and DBPFP with free chlorine:

- Spatial and temporal variation of DOM chemical properties within Beaver Lake impacted DBP formation.
- AF4-UV₂₅₄ data indicated that DOM was of similar size throughout Beaver Lake and that coagulation at pH 6 preferentially removed larger DOM whereas that at pH 8 removed all DOM size fractions uniformly, although to a lesser extent.

- Fluorescence-PARAFAC analyses identified the presence of three humic-like fluorophore groups and one protein-like fluorophore group in Beaver Lake water.
- Humic-like PARAFAC component 1 was more strongly correlated ($r^2 = 0.84$) to chloroform formation potential compared to $SUVA_{254}$ ($r^2 = 0.51$) and was preferentially removed by alum coagulation.
- AF4-UV₂₅₄, fluorescence-PARAFAC, $SUVA_{254}$, and DBPFP showed that alum coagulation at pH 6 removed DOM more effectively than at pH 8.

ACKNOWLEDGEMENTS

The authors gratefully acknowledge the support of the Beaver Water District (Lowell, AR) for running the DOC samples. Soluble reactive phosphorus was measured in J. Thad Scott's lab at UA. Funding for ADP was provided by UA as part of the start-up package for JLF and by the Doctoral Academy Fellowship program (UA).

Table 1 – Maxima locations and characteristics of the fluorescence-PARAFAC components.

Component	Excitation Maxima (nm)	Emission Maxima (nm)	Identification
1	238 (329)	430	Humic-like (Pifer et al. 2011)
2	231	362	Protein-like (Marhaba and Lippincott 2000; Dubnick et al. 2010)
3	344 (203, 228)	426	Humic-like (Coble 1996)
4	395 (269, 213)	471	Humic-like (Pifer et al. 2011)

Values in parentheses are secondary and tertiary Excitation maxima

Table 2 – Average percent contribution and percent removal of fluorescence-PARAFAC component 1 as a result of alum coagulation as a function of coagulation pH and sampling location.

Treatment	BWD	TT	CB	MC	All
Average Contribution					
Raw	53 ± 8	50 ± 4	54 ± 2	55 ± 4	53 ± 5
Alum, pH 6	40 ± 3	38 ± 7	33 ± 7	38 ± 2	37 ± 5
Alum, pH 7	41 ± 6	44 ± 3	42 ± 3	40 ± 3	42 ± 4
Alum pH 8	48 ± 2	48 ± 5	46 ± 5	46 ± 4	47 ± 4
Average Removal					
Alum, pH 6	74 ± 9	79 ± 8	80 ± 6	73 ± 5	76 ± 7
Alum, pH 7	65 ± 8	68 ± 10	62 ± 11	63 ± 13	65 ± 10
Alum pH 8	44 ± 18	42 ± 24	38 ± 7	42 ± 11	41 ± 15

Values are averages ± standard deviations.

BWD is the Beaver Water District, TT is the Benton/Washington Regional Public Water Authority (Two Ton), CB is the Carroll Boone Water District, MC is the Madison County Regional Water District, and All represents combined data from the four sampling locations.

Table 3 – Average percent removal of chloroform as a result of alum coagulation as a function of coagulation pH and sampling location.

Coagulation pH	BWD	TT	CB	MC	All
pH 6	60 ± 4	64 ± 12	61 ± 11	58 ± 6	62 ± 8
pH 7	53 ± 4	55 ± 14	48 ± 11	52 ± 11	52 ± 10
pH 8	40 ± 6	41 ± 15	28 ± 3	37 ± 11	37 ± 9

Values are averages ± standard deviations

BWD is the Beaver Water District, TT is the Benton/Washington Regional Public Water Authority (Two Ton), CB is the Carroll Boone Water District, MC is the Madison County Regional Water District, and All represents combined data from the four sampling locations.

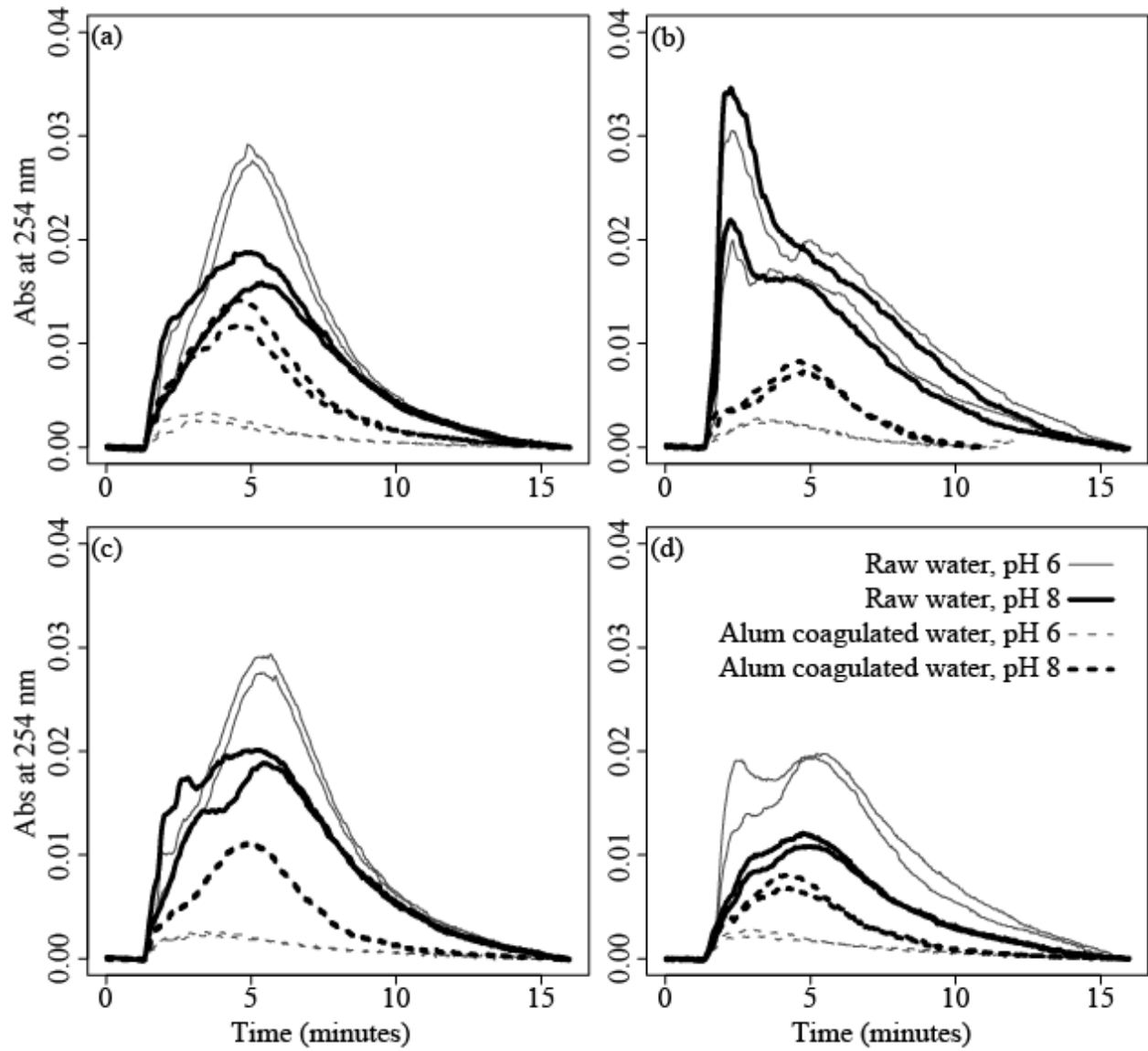


Fig. 1 – AF4-UV₂₅₄ fractograms in duplicate for (a) Beaver Water District, (b) Two Ton, (c) Carroll-Boone, and (d) Madison County samples from July 14, 2011.

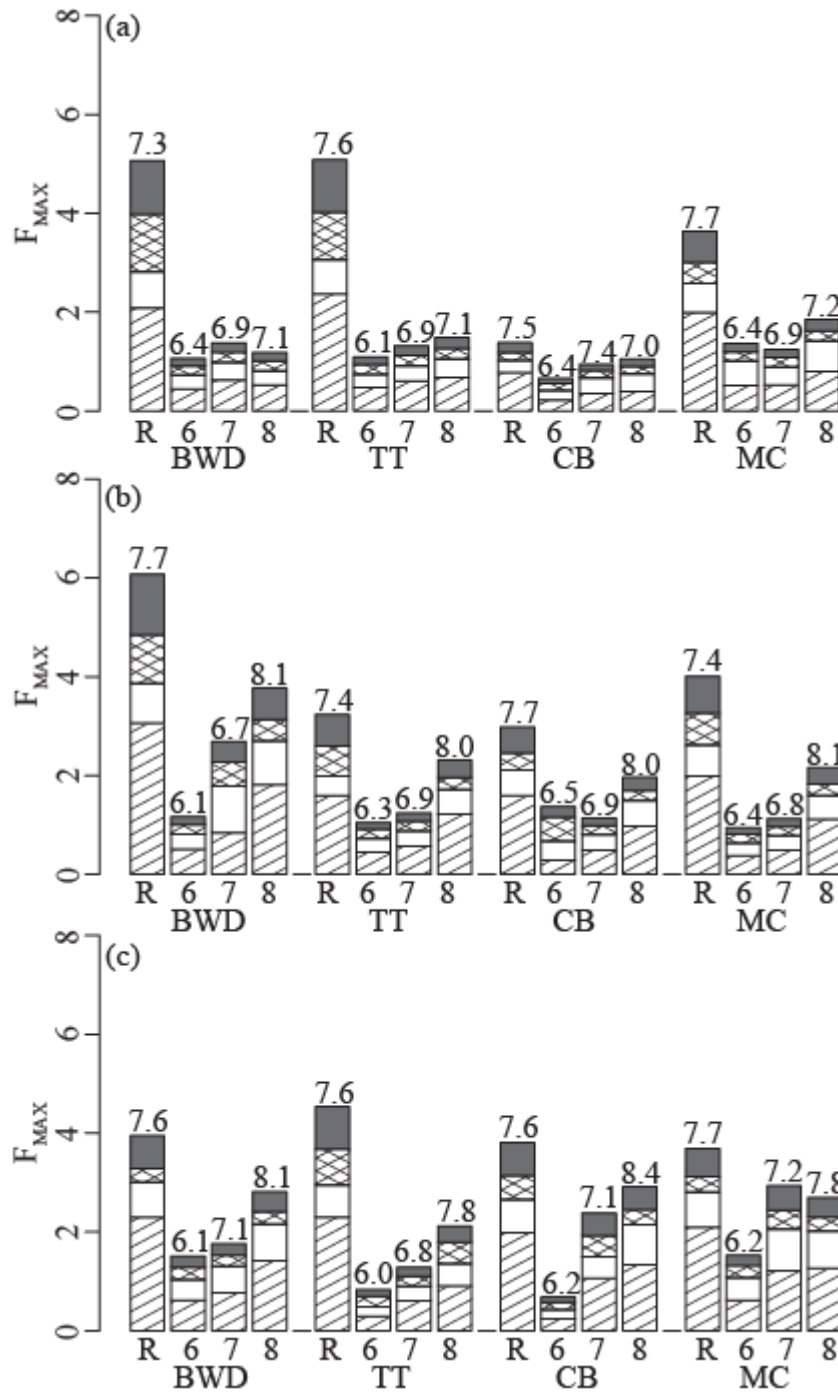


Fig. 2 – Fluorescence-PARAFAC component maximums (F_{MAX}) by drinking water treatment plant and treatment for sample dates: (a) May 13, 2011, (b) May 31, 2011, (c) June 28, 2011, (d) July 14, 2011, and (e) August 4, 2011. R indicates a raw water sample, and 6, 7, and 8 indicate the target coagulation pH values; the number above each bar indicates the measured pH of the sample after alum coagulation. BWD is the Beaver Water District, TT is the Benton/Washington Regional Public Water Authority (commonly referred to as Two Ton), CB is the Carroll-Boone Water District, and MC is the Madison County Regional Water District. Fluorescence-PARAFAC components are indicated as follows: \square component 1, \square component 2, \boxtimes component 3, and \blacksquare component 4.

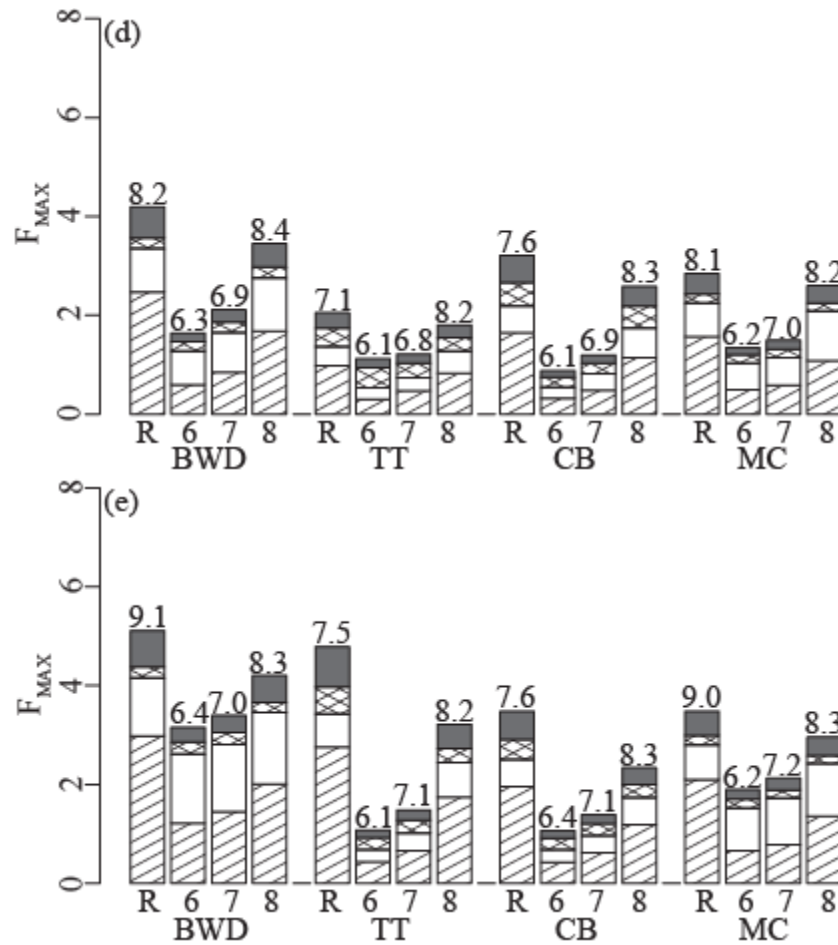


Fig. 2, continued – Fluorescence-PARAFAC component maximums (F_{MAX}) by drinking water treatment plant and treatment for sample dates: (a) May 13, 2011, (b) May 31, 2011, (c) June 28, 2011, (d) July 14, 2011, and (e) August 4, 2011. R indicates a raw water sample, and 6, 7, and 8 indicate the target coagulation pH values; the number above each bar indicates the measured pH of the sample after alum coagulation. BWD is the Beaver Water District, TT is the Benton/Washington Regional Public Water Authority (commonly referred to as Two Ton), CB is the Carroll-Boone Water District, and MC is the Madison County Regional Water District. Fluorescence-PARAFAC components are indicated as follows: component 1, component 2, component 3, and component 4.

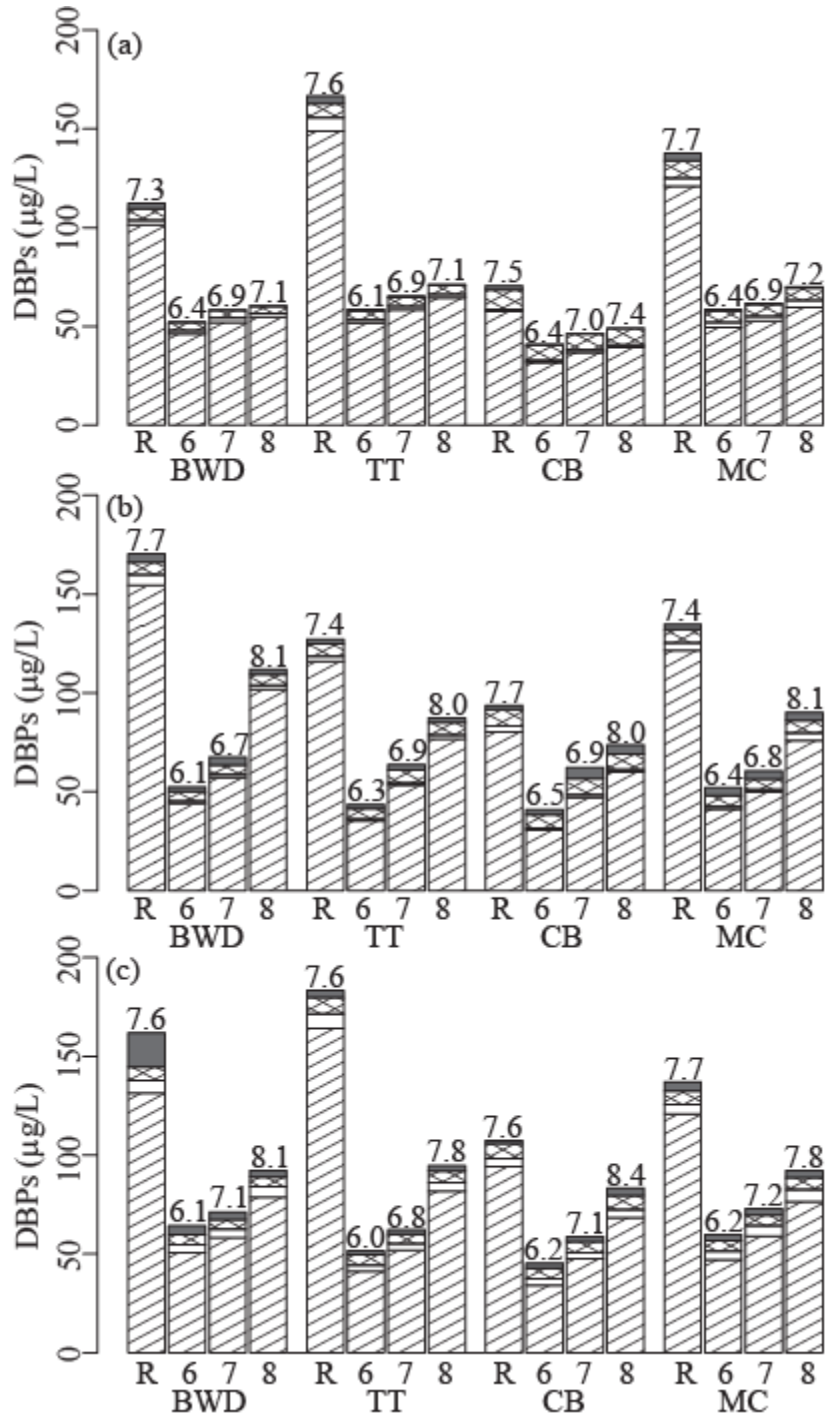


Fig. 3 - Disinfection byproducts (DBPs) in µg/L as each DBP formed during free chlorine formation potential tests by drinking water treatment plant and treatment for sample dates: (a) May 13, 2011, (b) May 31, 2011, (c) June 28, 2011, (d) July 14, 2011, and (e) August 4, 2011. R indicates a raw water sample, and 6, 7, and 8 indicate the target coagulation pH values; the number above each bar indicates the measured pH of the sample after alum coagulation. DBPs are indicated as follows: \square chloroform (TCM), \square dichloroacetonitrile (DCAN), \boxtimes bromodichloromethane (BDCM), and \blacksquare 1,1,1-trichloro-propanone (TCP).

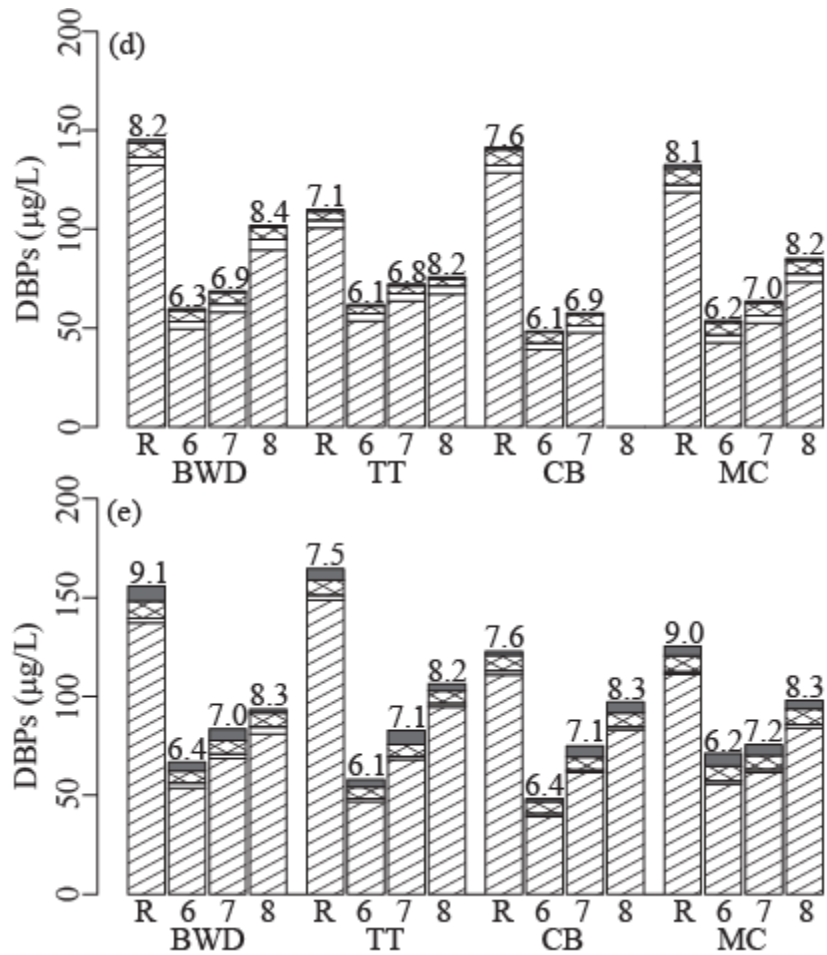


Fig. 3, continued - Disinfection byproducts (DBPs) in µg/L as each DBP formed during free chlorine formation potential tests by drinking water treatment plant and treatment for sample dates: (a) May 13, 2011, (b) May 31, 2011, (c) June 28, 2011, (d) July 14, 2011, and (e) August 4, 2011. R indicates a raw water sample, and 6, 7, and 8 indicate the target coagulation pH values; the number above each bar indicates the measured pH of the sample after alum coagulation. DBPs are indicated as follows: chloroform (TCM), dichloroacetonitrile (DCAN), bromodichloromethane (BDCM), and 1,1,1-trichloro-propanone (TCP).

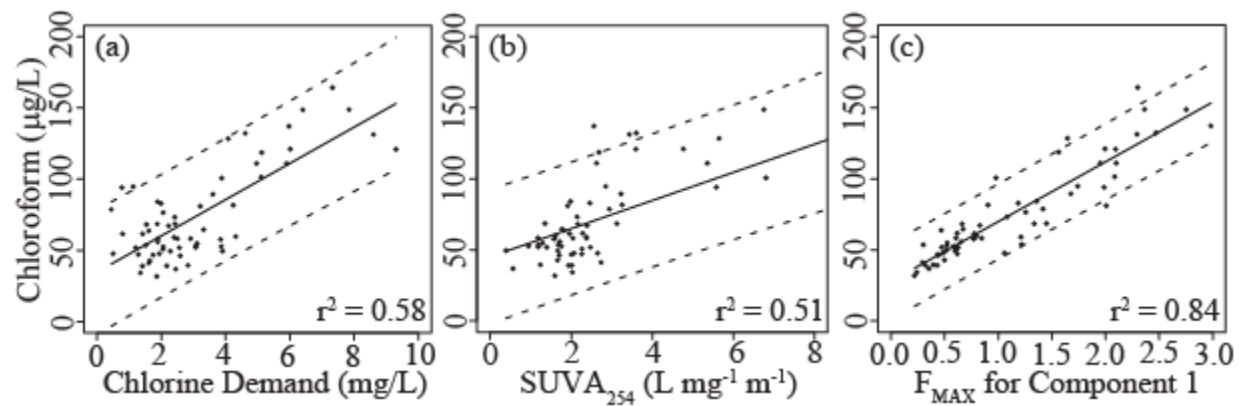


Fig. 4 – Correlations between chloroform formed during the free chlorine disinfection byproduct formation potential tests and (a) chlorine demand, (b) SUVA_{254} , and (c) F_{MAX} for Component 1. The solid lines are the linear model fits to the experimental data. The dashed lines are the upper and lower 95% prediction intervals for the linear models.

5. REFERENCES

- Amirtharajah, A., 1990. Coagulation: Rejuvenation for a Classical Process. *Water Engineering & Management* 137 (12), 25.
- Andersen, C. M. and Bro, R., 2003. Practical aspects of PARAFAC modeling of fluorescence excitation-emission data. *Journal of Chemometrics* 17 (4), 200-215.
- Arora, H., LeChevallier, M. W. and Dixon, K. L., 1997. DBP occurrence survey. *Journal American Water Works Association* 89 (6), 60-68.
- Ates, N., Kitis, M. and Yetis, U., 2007. Formation of chlorination by-products in waters with low SUVA-correlations with SUVA and differential UV spectroscopy. *Water Research* 41 (18), 4139-4148.
- Cantor, K. P., Lynch, C. F., Hildesheim, M. E., Dosemeci, M., Lubin, J., Alavanja, M. and Craun, G., 1998. Drinking water source and chlorination byproducts I. Risk of bladder cancer. *Epidemiology* 9 (1), 21-28.
- Chow, C. W. K., van Leeuwen, J. A., Fabris, R. and Drikas, M., 2009. Optimised coagulation using aluminium sulfate for the removal of dissolved organic carbon. *Desalination* 245 (1-3), 120-134.
- Coble, P. G., 1996. Characterization of marine and terrestrial DOM in seawater using excitation emission matrix spectroscopy. *Marine Chemistry* 51 (4), 325-346.
- Coble, P. G., Green, S. A., Blough, N. V. and Gagosian, R. B., 1990. Characterization of dissolved organic matter in the Black Sea by fluorescence spectroscopy. *Nature* 348 (6300), 432-435.
- Drikas, M., Chow, C. W. K. and Cook, D., 2003. The impact of recalcitrant organic character on disinfection stability, trihalomethane formation and bacterial regrowth: An evaluation of magnetic ion exchange resin (MIEX (R)) and alum coagulation. *Journal of Water Supply Research and Technology-Aqua* 52 (7), 475-487.
- Dubnick, A., Barker, J., Sharp, M., Wadham, J., Lis, G., Telling, J., Fitzsimons, S. and Jackson, M., 2010. Characterization of dissolved organic matter (DOM) from glacial environments using total fluorescence spectroscopy and parallel factor analysis. *Annals of Glaciology* 51 (56), 111-122.
- Eaton, A. D., Franson, M. A. H., American Public Health Association., American Water Works Association. and Water Environment Federation., 2005. Standard methods for the examination of water & wastewater. Washington, DC, American Public Health Association.
- Giddings, J. C., 1993. Field-Flow Fractionation: Analysis of Macromolecular, Colloidal, and Particulate Materials. *Science* 260 (5113), 1456-1465.

- Guéguen, C. and Cuss, C. W., 2011. Characterization of aquatic dissolved organic matter by asymmetrical flow field-flow fractionation coupled to UV-Visible diode array and excitation emission matrix fluorescence. *Journal of Chromatography A* 1218 (27), 4188-4198.
- Hall, G. J., Clow, K. E. and Kenny, J. E., 2005. Estuarial Fingerprinting through Multidimensional Fluorescence and Multivariate Analysis. *Environmental Science & Technology* 39 (19), 7560-7567.
- Hua, G. and Reckhow, D. A., 2007. Characterization of Disinfection Byproduct Precursors Based on Hydrophobicity and Molecular Size. *Environmental Science & Technology* 41 (9), 3309-3315.
- Johnstone, D. W., Sanchez, N. P. and Miller, C. M., 2009. Parallel Factor Analysis of Excitation-Emission Matrices to Assess Drinking Water Disinfection Byproduct Formation During a Peak Formation Period. *Environmental Engineering Science* 26 (10), 1551-1559.
- Kitis, M., Karanfil, T., Kilduff, J.E., Wigton, A., 2001. The reactivity of natural organic matter to disinfection byproducts formation and its relation to specific ultraviolet absorbance. *Water Science and Technology* 43 (2), 9-16.
- Marhaba, T. F. and Lippincott, R. L., 2000. Application of fluorescence technique for rapid identification of DOM fractions in source waters. *Journal of Environmental Engineering-Asce* 126 (11), 1039-1044.
- Miller, M. P. and McKnight, D. M., 2010. Comparison of seasonal changes in fluorescent dissolved organic matter among aquatic lake and stream sites in the Green Lakes Valley. *J. Geophys. Res.* 115, G00F12.
- Nieuwenhuijsen, M. J., Toledano, M. B., Eaton, N. E., Fawell, J. and Elliott, P., 2000. Chlorination disinfection byproducts in water and their association with adverse reproductive outcomes: a review. *Occupational and Environmental Medicine* 57 (2), 73-85.
- NOAA Satellite and Information Service (2011).
- Pifer, A. D., Miskin, D. R., Cousins, S. L. and Fairey, J. L., 2011. Coupling asymmetric flow-field flow fractionation and fluorescence parallel factor analysis reveals stratification of dissolved organic matter in a drinking water reservoir. *Journal of Chromatography A* 1218 (27), 4167-4178.
- Rook, J. J., 1976. Haloforms in drinking water. *Journal American Water Works Association* 68 (3), 168-172.
- Rosario-Ortiz, F. L., Snyder, S. A. and Suffet, I. H., 2007. Characterization of dissolved organic matter in drinking water sources impacted by multiple tributaries. *Water Research* 41 (18), 4115-4128.

- Schimpf, M. E. and Wahlund, K. G., 1997. Asymmetrical flow field-flow fractionation as a method to study the behavior of humic acids in solution. *Journal of Microcolumn Separations* 9 (7), 535-543.
- Sen, S., Haggard, B., Chaubey, I., Brye, K., Costello, T. and Matlock, M., 2007. Sediment Phosphorus Release at Beaver Reservoir, Northwest Arkansas, USA, 2002–2003: A Preliminary Investigation. *Water, Air, & Soil Pollution* 179 (1), 67-77.
- Stedmon, C. A. and Bro, R., 2008. Characterizing dissolved organic matter fluorescence with parallel factor analysis: a tutorial. *Limnology and Oceanography-Methods* 6, 572-579.
- Suffet, I. H., Brenner, L. and Silver, B., 1976. Identification of 1,1,1-trichloroacetone (1,1,1-trichloropropanone) in two drinking waters: a known precursor in haloform reaction. *Environmental Science & Technology* 10 (13), 1273-1275.
- Vuorio, E., Vahala, R., Rintala, J. and Laukkanen, R., 1998. The evaluation of drinking water treatment performed with HPSEC. *Environment International* 24 (5-6), 617-623.
- Wahman, D. G. (2006). Cometabolism of trihalomethanes by nitrifying biofilters under drinking water treatment plant conditions. *Civil, Architectural, and Environmental Engineering*. Austin, The University of Texas at Austin. **Ph.D**: 398.
- Weishaar, J. L., Aiken, G. R., Bergamaschi, B. A., Fram, M. S., Fujii, R. and Mopper, K., 2003. Evaluation of specific ultraviolet absorbance as an indicator of the chemical composition and reactivity of dissolved organic carbon. *Environmental Science & Technology* 37 (20), 4702-4708.
- Yang, Z., Gao, B. and Yue, Q., 2010. Coagulation performance and residual aluminum speciation of $Al_2(SO_4)_3$ and polyaluminum chloride (PAC) in Yellow River water treatment. *Chemical Engineering Journal* 165 (1), 122-132.
- Yohannes, G., Wiedmer, S. K., Jussila, M. and Riekkola, M. L., 2005. Fractionation of Humic Substances by Asymmetrical Flow Field-Flow Fractionation. *Chromatographia* 61 (7), 359-364.
- Zhang, Y., Griffin, A. and Edwards, M., 2008. Nitrification in premise plumbing: Role of phosphate, pH and pipe corrosion. *Environmental Science & Technology* 42 (12), 4280-4284.

APPENDIX 2

Supplementary Data for

“Improving on SUVA₂₅₄ Using Fluorescence-PARAFAC Analysis and Asymmetric Flow-Field Flow Fractionation for Assessing Disinfection Byproduct Formation and Control”

1. MATERIALS AND METHODS

1.1. Sample collection and handling.

At the BWD, the samples were collected from intake depth at the plant's intake structure using a 6-L Van Dorn bottle (Wildco, Model 1960-H65, Yulee, FL) and transferred to pre-rinsed (Milli-Q water) 9-L HDPE carboys. At TT and CB, raw water samples were collected in the 9-L HDPE carboys from taps within the DWTPs following a few minutes of flushing. At MC, samples were collected directly from Beaver Lake next to the plant's intake structure using the carboys.

1.2. Water Quality Tests.

Bromide was measured in filtered samples using a Dionex DX-120 ion chromatograph with an IonPac AS4A-SC column according to EPA 300.0. To measure particulate phosphorus concentrations, raw water samples were filtered through acid-rinsed GFFs, which were then digested with a 2% (w/v) persulfate solution to convert particulate phosphorus to soluble reactive phosphorus. For dissolved phosphorus measurements, the filtrate was collected and refrigerated until analysis. The soluble reactive phosphorus of the digested samples and filtrate was quantified on a Trilogy fluorometer with Spreadsheet Interface Software for Trilogy software (Turner Designs) following Standard Methods 4500-P (Eaton et al. 2005). Total phosphorus (TP) was obtained by summing particulate phosphorus and dissolved phosphorus.

1.3. Fluorescence-PARAFAC analysis.

Fluorescence excitation-emission matrices (EEMs) were collected for a given sample in 1 nm increments between 200 and 400 nm for excitation and 270 and 600 nm for emission. The scans were scatter-corrected using *Cleanscan* for MATLAB (Zepp et al. 2004). PARAFAC modeling, using the DOM-Fluor toolbox (available for download at

<http://www.models.life.ku.dk/algorithms>), identified groups of fluorophores that made up the EEMs. The model requires removal of outlier samples because they can bias the model. A combination of visual identification and the function *OutlierTest* was used to ensure that outliers were removed. The PARAFAC model was validated using *SplitHalfAnalysis* and *SplitHalfValidation*.

2. RESULTS AND DISCUSSION

2.1. Raw Water Parameters.

Throughout the sampling period, all four DWTPs had raw waters with slightly alkaline pH, with a range of 7.1-8.9 and a mean of 7.7. For the first sampling date (5/13/11), BWD and TT had high turbidity (~120 NTU) and low alkalinity (~33 mg L⁻¹-CaCO₃), likely due to 28-cm of rainfall in Northwest Arkansas between April 24-26, 2011 (NOAA Satellite and Information Service 2011). Turbidities decreased thereafter to values less than 20 NTU for the last three sampling dates, with the exception of TT on 5/31/11 (60 NTU). Values of alkalinity remained consistent throughout the sampling period, with a range of 33-56 mg L⁻¹-CaCO₃. Bromide and ammonia concentrations were consistently below the practical quantitation limits or method detection limits (0.05 mg L⁻¹ as Br and 0.1 mg L⁻¹ as N, respectively) and were not reported in Table S1.

TDN measurements were low throughout the sampling period, with a range of 0.36-1.47 mg L⁻¹-N, and had no consistent spatial or temporal trends. TP was highest for BWD, TT, and MC in the 5/13/11 samples, suggesting that the runoff from the heavy rainfall event carried a significant phosphorus load that did not make it to CB prior to sampling. TP and TDN were uncorrelated throughout the sampling period, suggesting varying sources of these limiting nutrients throughout Beaver Lake. Trophic state index (TSI) was calculated from TP using log-

linear regression equations developed by Carlson (1977). The TSI for BWD, TT, and MC was highest on 5/13/11 (>70) and lowest on 6/28/11 (<50) where each increase in TSI major division (e.g., from 40-50 to 50-60) represents a doubling of algal biomass. For all four DWTPs, the average TSI based was 51, with a high for the BWD (56) and a low of CB (46), suggesting only a modest spatial trophic gradient.

Table S1 – Raw water quality parameters for Beaver Lake samples

Sampling Date	Location	pH	Turbidity (NTU)	Conductivity ($\mu\text{S cm}^{-1}$)	Alkalinity (mg L^{-1} - CaCO_3)	TDN (mg L^{-1} -N)	TP ($\mu\text{g L}^{-1}$ -P)	TSI	DOC (mg L^{-1})	SUVA ₂₅₄ ($\text{L mg}^{-1} \text{m}^{-1}$)
5/13/11	BWD	7.3	125	108	33	0.98	105	71	3.2	11.6
	TT	7.6	120	110	34	0.91	100	71	3.6	12.4
	CB	7.5	3	174	64	0.52	14	42	2.2	1.6
	MC	7.7	36	138	51	0.80	113	72	2.9	4.8
5/31/11	BWD	7.7	81	105	37	0.90	79	67	5.9	4.9
	TT	7.4	37	121	46	1.12	47	60	5.9	3.0
	CB	7.7	11	154	58	0.80	22	49	6.7	1.4
	MC	7.4	33	123	38	1.47	91	69	9.4	2.2
6/28/11	BWD	7.6	4	87	49	0.65	7	32	2.3	3.4
	TT	7.3	60	79	43	1.07	15	43	2.4	11.1
	CB	7.6	12	100	54	0.77	15	43	2.0	5.8
	MC	8.6	4	90	52	0.64	4	24	1.8	3.6
7/14/11	BWD	8.2	2	144	50	0.36	23	49	2.0	3.6
	TT	7.1	12	145	33	0.85	11	39	1.4	6.8
	CB	7.6	12	162	54	0.67	13	41	2.3	5.6
	MC	8.1	1	154	54	0.29	10	37	2.1	2.7
8/4/11	BWD	8.3	2	141	56	0.58	46	59	2.8	2.6
	TT	7.2	14	135	46	1.11	32	54	2.2	6.8
	CB	7.1	10	161	56	0.99	32	54	2.0	5.4
	MC	8.9	1	150	54	0.54	23	49	2.3	2.6
Mean		7.7	29	129	48	0.80	33	51	1.5	5.1
Median		7.6	12	137	51	0.80	23	49	1.2	4.2

TDN – total dissolved nitrogen; TP – total phosphorus; TSI – trophic state index calculated from TP; DOC – dissolved organic carbon; SUVA₂₅₄ – specific ultraviolet absorbance at 254 nm; BWD – Beaver Water District; TT – Two Ton; CB – Carroll Boone; MC – Madison Country.

Table S2 – Average contribution and removal percentages for each fluorescence-PARAFAC component

Treatment	Component 1	Component 2	Component 3	Component 4
Average Contribution				
Raw	53 ± 5	17 ± 3	13 ± 5	17 ± 2
pH 6	37 ± 5	30 ± 7	19 ± 7	14 ± 2
pH 7	42 ± 4	30 ± 7	15 ± 4	14 ± 2
pH 8	47 ± 4	27 ± 5	11 ± 4	14 ± 1
Average Removal				
pH 6	76 ± 7	39 ± 26	37 ± 37	72 ± 13
pH 7	65 ± 10	22 ± 29	36 ± 32	61 ± 18
pH 8	41 ± 15	-7 ± 29	34 ± 26	41 ± 19
Values are averages ± standard deviations				

Table S3 – Average percent removal from alum coagulation as a function of pH for each disinfection byproduct

Treatment	TCM	DCAN	BDCM	TCP
pH 6	62 ± 8	29 ± 30	24 ± 7	35 ± 42
pH 7	52 ± 10	25 ± 33	22 ± 11	9 ± 79
pH 8	37 ± 9	8 ± 35	17 ± 11	14 ± 79
Values are averages ± standard deviations				

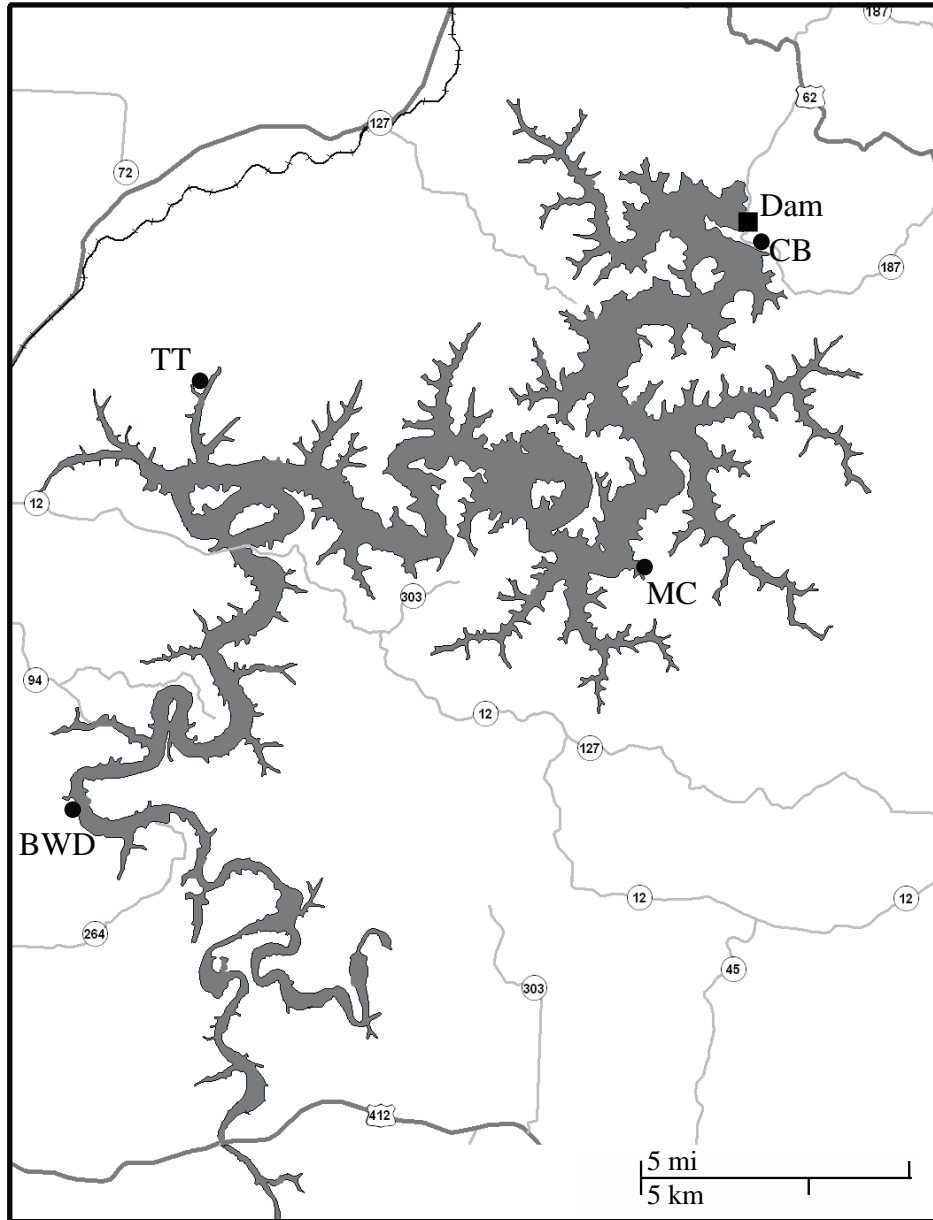


Fig. S1 – Map of Beaver Lake Reservoir in Northwest Arkansas. The locations of the four drinking water treatment plants that take source water from Beaver Lake are noted, where BWD is the Beaver Water District, TT is the Benton/Washington Regional Public Water Authority (commonly referred to as Two Ton), CB is the Carroll-Boone Water District, and MC is the Madison County Regional Water District.

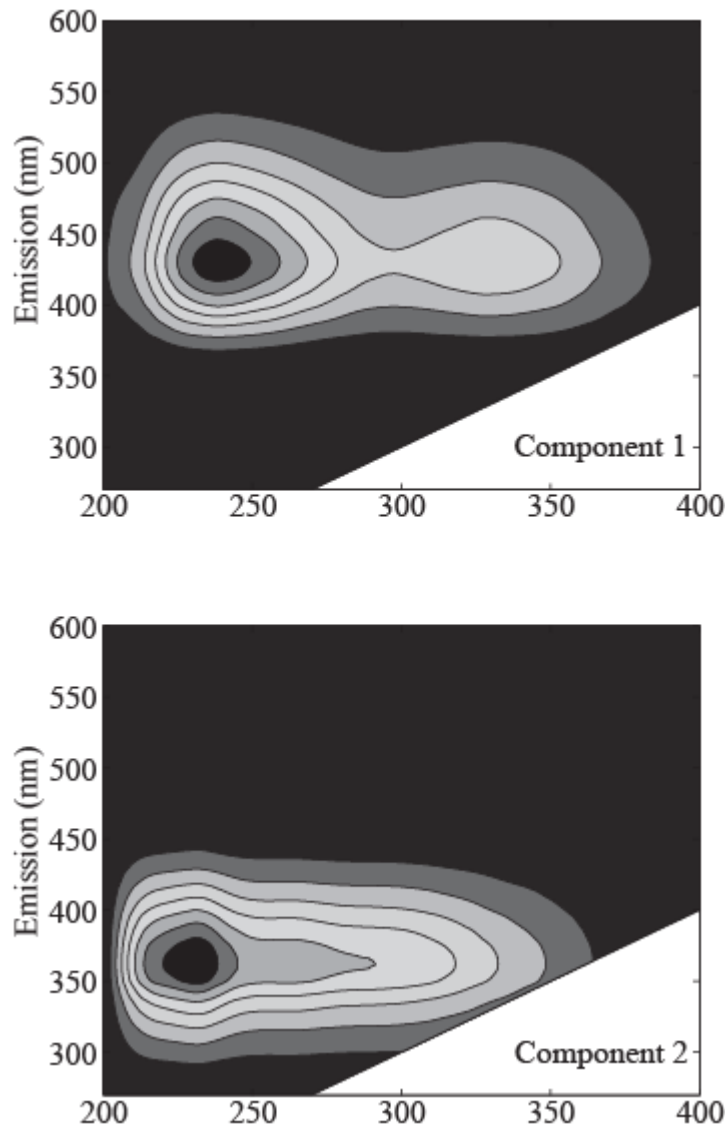


Fig. S2 – Fluorescence-PARAFAC component excitation-emission matrices (EEMs) for the array of 190 EEMs consisting of raw and alum-coagulated waters from the four drinking water treatment plants.

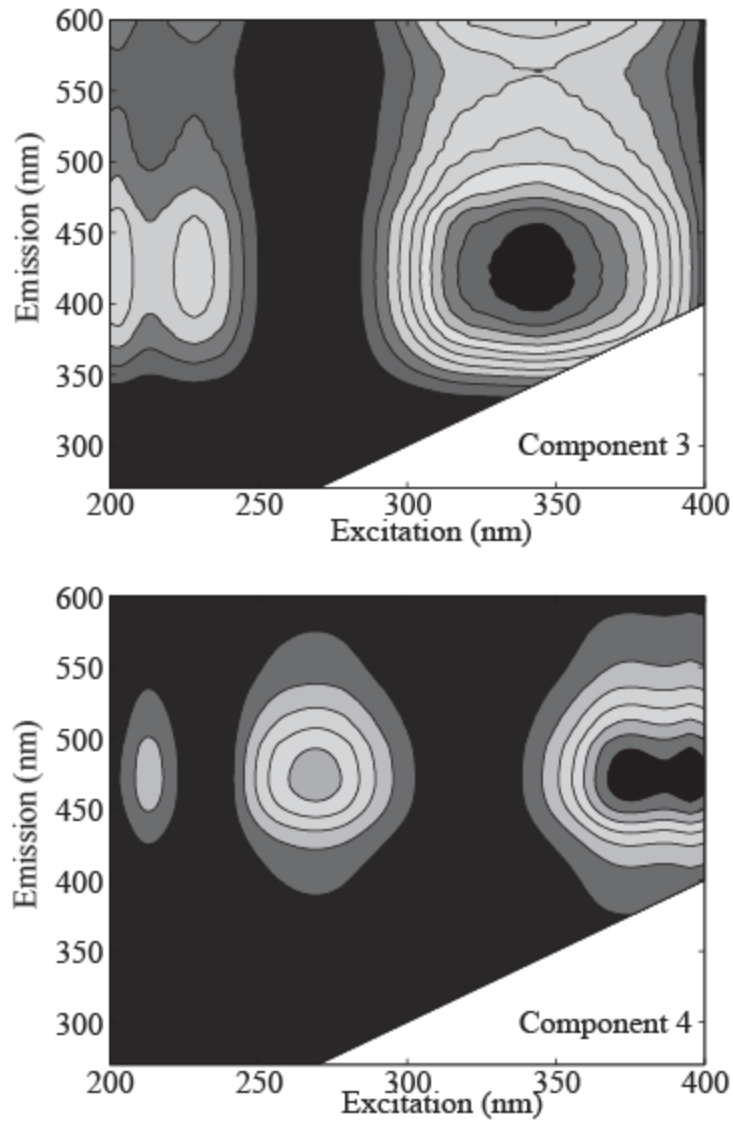


Fig. S2, continued – Fluorescence-PARAFAC component excitation-emission matrices (EEMs) for the array of 190 EEMs consisting of raw and alum-coagulated waters from the four drinking water treatment plants.

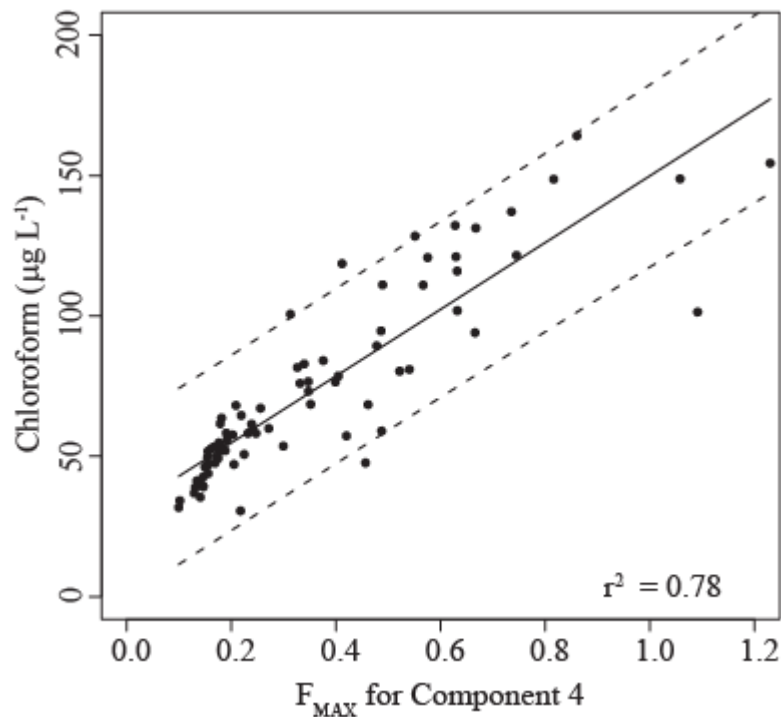


Fig. S3 – Correlations between chloroform formed during the free chlorine disinfection byproduct formation potential tests and F_{MAX} for Component 4. The solid lines are the linear model fits to the experimental data. The dashed lines are the upper and lower 95% prediction intervals for the linear models.

3. REFERENCES

Carlson, R. E., 1977. Trophic state index for lakes. *Limnology and Oceanography* 22 (2), 361-369.

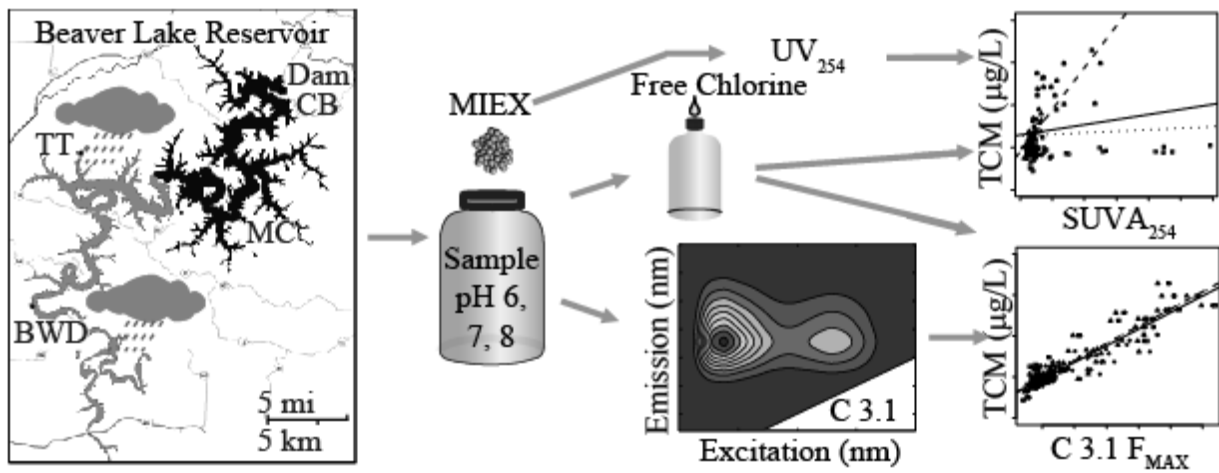
Eaton, A. D., Franson, M. A. H., American Public Health Association., American Water Works Association. and Water Environment Federation., 2005. Standard methods for the examination of water & wastewater. Washington, DC, American Public Health Association.

NOAA Satellite and Information Service (2011).

Zepp, R. G., Sheldon, W. M. and Moran, M. A., 2004. Dissolved organic fluorophores in southeastern US coastal waters: correction method for eliminating Rayleigh and Raman scattering peaks in excitation-emission matrices. *Marine Chemistry* 89 (1-4), 15-36.

CHAPTER 4

Tracking Disinfection Byproduct Precursor Removal by Magnetic Ion Exchange Resin and Alum Coagulation Using Fluorescence-PARAFAC



ABSTRACT

Removal of disinfection byproduct (DBP) precursors by magnetic ion exchange (MIEX[®]) resin at pH 6, 7, and 8 was evaluated using DBP formation potential (DBPFP) tests. Chloroform was the predominant DBP and its formation potential (FP) was reduced the greatest extent (75-82%) by MIEX[®] treatment, with no apparent trends with treatment pH. Fluorescence excitation emission matrices (EEMs) were collected from raw and MIEX[®]-treated samples. Parallel factor (PARAFAC) analysis was used to decompose the EEMs into principal component fluorophore groups, each with a maximum intensity, F_{MAX} . This model was compared to a second model from a previously reported alum coagulation study and to a third model resulting from the combination of EEMs from both MIEX[®]- and alum-treated samples. The combined model's F_{MAX} values for two humic-like fluorophore groups were more strongly correlated with chloroform FP ($r^2 = 0.87$ and 0.83) than specific ultraviolet absorbance at 254 nm ($SUVA_{254}$, with $r^2 = 0.03$). The three chloroform- F_{MAX} models showed no statistically significant differences (p values for slopes and intercepts were greater than 0.5 and 0.1, respectively). The models also allowed identification of 2 components that had elevated F_{MAX} values from a heavy rainfall event (28 cm from April 24-26, 2011), but these were uncorrelated to chloroform FP. The corresponding $SUVA_{254}$ values were also elevated and chloroform FP predictions based on them were inaccurate. These results highlight the applicability of fluorescence-PARAFAC models to multiple DBP precursor removal processes and suggest that F_{MAX} may be a more selective metric than $SUVA_{254}$ for choosing and optimizing DBP precursor removal processes. In addition, the results indicate the usefulness of F_{MAX} values for predicting changes in DBPFP resulting from heavy rainfall events.

KEYWORDS

Enhanced coagulation; anion exchange; drinking water; dissolved organic matter; chloroform; extreme weather events

ABBREVIATIONS

BWD (Beaver Water District); CB (Carroll Boone Water District); DBP (disinfection byproduct); DBPFP (DBP formation potential); DOC (dissolved organic carbon); DOM (dissolved organic matter); DWTPs (drinking water treatment plants); EEMs (excitation and emission matrices); F_{MAX} (maximum fluorescence intensity); GFFs (glass fiber filters); HAA5 (five regulated haloacetic acids); MC (Madison County Regional Water District); MIEX[®] (magnetic ion exchange); N-DBPs (nitrogen-containing DBPs); NOM (natural organic matter); PARAFAC (parallel factor analysis); $SUVA_{254}$ (specific ultraviolet absorbance at 254 nm); THM4 (four regulated trihalomethanes); TT (Benton-Washington Regional Public Water Authority, commonly referred to as Two Ton); USEPA (United States Environmental Protection Agency); UV_{254} (ultraviolet absorbance at 254 nm)

1. INTRODUCTION AND MOTIVATION

Disinfection byproducts (DBPs) are a concern in finished drinking waters due to their suspected carcinogenic (Cantor et al. 1998) and teratogenic properties (Nieuwenhuijsen et al. 2000). The United States Environmental Protection Agency (USEPA) currently regulates 11 DBPs (four trihalomethanes (THM4), five of the nine haloacetic acids (HAA5), chlorite, and bromate) in finished drinking waters under the Stage 2 Disinfection/Disinfection By-Product Rule. Other DBPs, including nitrogen-containing DBPs (N-DBPs), are being considered for regulation due to high toxicities relative to THM4 and HAA5. Despite nearly 40 years of DBP

research, DBP control remains an ongoing challenge at many drinking water treatment plants (DWTPs).

DBPs form when drinking water disinfectants (e.g., chlorine, chloramines, ozone, etc.) react with natural organic matter (NOM). DBP speciation and concentrations are influenced by the disinfectant used and the quantity and characteristics of NOM. NOM is ubiquitous in natural waters and is a complex chemical mixture consisting largely of organic carbon. NOM is derived from both terrestrial and aquatic sources, and its physical and chemical properties can vary temporally (Miller and McKnight 2010) and spatially (Pifer et al. 2011). Upon introduction to an aquatic environment, NOM can be altered through biotic and abiotic processes. As such, NOM exists as a dynamic carbon pool, which makes it difficult for DWTPs to control DBP formation in finished drinking water.

DWTPs attempt to curb DBPs by changing their disinfectant and/or removing more DBP precursors (i.e., NOM). Changing disinfectants can result in formation of different DBPs with potentially higher toxicities and/or increased corrosion in the distribution system (Zhang et al. 2008; Zhang et al. 2009). As such, enhanced DBP-precursor removal has received renewed interest in recent years.

Although enhanced coagulation is the most common method for improving NOM removal in DWTPs, alternatives such as anion exchange have been investigated (Bolto et al. 2002). Typical ion exchange processes are operated in pressurized columns which require prefiltration to prevent column plugging (Drikas et al. 2002). The Commonwealth Scientific & Industrial Research Organization and Orica Australia Pty Ltd developed magnetic ion exchange (MIEX[®]) resin, an anion exchange resin that has a high selectivity for NOM and can be employed in completely mixed reactors (Drikas et al. 2002).

An extensive body of research exists regarding the ability of MIEX[®] to reduce DBP formation potential (DBPFP) (Drikas et al. 2003; Singer et al. 2007; Jarvis et al. 2008). However, additional research is needed to better understand the capabilities and limitations of MIEX[®]. In particular, the impact of source water pH during MIEX[®] treatment has not been extensively documented. Some have speculated that pH has an effect on the removal of DBP-precursors by MIEX[®] due to changes in the protonation state of the acid/base NOM functional groups (Neale and Schafer 2009), but a significant research gap regarding the optimum operating pH for MIEX[®] treatment remains.

Optimization of DBP precursor removal is often based on specific ultraviolet absorbance (SUVA₂₅₄), the ultraviolet absorbance at 254 nm (UV₂₅₄) in units of m⁻¹ normalized by dissolved organic carbon (DOC). This measurement requires filtration, and is thus taken on the portion of NOM operationally defined as dissolved organic matter (DOM). SUVA₂₅₄ can be obtained using equipment common at DWTPs and is the most common parameter used to predict DBP formation (Ates et al. 2007). Unfortunately, not all DOM is sensitive to UV₂₅₄ (Kitis et al. 2001) and the relationships between DBPs and SUVA₂₅₄ are source water dependent (Weishaar et al. 2003) and unreliable at low SUVA₂₅₄ values (Ates et al. 2007).

Fluorescence spectroscopy has become a common DOM characterization technique. It is sensitive to aromatic and unsaturated aliphatic compounds, but is subject to quenching by dissolved oxygen and metal ions (Senesi 1990). Fluorescence spectroscopy has the benefits of higher sensitivity and selectivity relative to absorbance measurements. Fluorescence excitation and emission matrices (EEMs) decomposed into fluorescent components using parallel factor analysis (PARAFAC) have been used to identify DOM components in natural waters (Stedmon et al. 2003) and DBP precursors in raw waters (Hua et al. 2010). Although only a fraction of

DOM fluoresces, DBPFP was correlated to the maximum fluorescence intensities (F_{MAX}) of PARAFAC components for raw and alum treated samples from two watersheds. These correlations were stronger than the corresponding DBPFP-SUVA₂₅₄ correlations (Johnstone et al. 2009; Pifer and Fairey 2012). However, correlations between PARAFAC components and DBPFP have not been tested after alternative treatments or across source waters.

The objectives of this study were to examine the impacts of pH on MIEX[®] treatment, evaluate the effects of a heavy rainfall event on DOM properties, compare DOM removal achieved with alum coagulation (Pifer and Fairey 2012) with that of MIEX[®] treatment, and test the consistency of DBPFP-PARAFAC component correlations when applied to alum coagulated and MIEX[®] treated waters. A DBP precursor surrogate that behaves consistently between treatments would be a valuable tool to help DWTPs select and optimize treatment processes to reduce DBPs. Raw source waters were collected monthly from May to August 2011 from four DWTPs located on the Beaver Lake reservoir in Northwest Arkansas. These samples underwent MIEX[®] treatment and alum coagulation (the alum coagulation experiments are published in Pifer and Fairey (2012)). For the MIEX[®] experiments, treatment was conducted at pH 6, 7, or 8, and the water was filtered and underwent DBPFP tests with free chlorine. Fluorescence-PARAFAC Models 1-3 were constructed using EEMs from 1) Dataset 1, raw and MIEX[®] treated water, 2) Dataset 2, raw and alum coagulated water samples (Pifer and Fairey 2012), and 3) Dataset 3, the combination of the first two datasets. The resultant F_{MAX} values for individual PARAFAC components in Models 1-3 were correlated with DBPFP. These correlations were compared with each other and to correlations between SUVA₂₅₄ and DBPFP.

MATERIALS AND METHODS

2.1. Sampling Locations

Raw water samples (18 L each) were collected on May 13, 2011, June 28, 2011, July 14, 2011, and August 4, 2011, at the intake of four DWTPs on the Beaver Lake reservoir: Beaver Water District (BWD), Benton-Washington Regional Public Water Authority, commonly referred to as Two Ton (TT), Carroll Boone Water District (CB), and Madison County Regional Water District (MC). These sampling locations were selected to assess the spatial variability of DBP-precursors on Beaver Lake and determine the impact of this variability on MIEX treatment and DBP formation. These raw water samples were also used in a parallel alum coagulation study (Pifer and Fairey 2012).

2.2. Water Quality Tests

All glassware, with the exception of volumetric flasks, was washed with a solution of tap water and Alconox detergent, rinsed multiple times with Milli-Q water (18.2 M Ω -cm), and baked for 30 minutes at 400°C. Volumetric flasks and plastic-ware were washed with an Alconox and tap water solution, rinsed with Milli-Q water and air-dried at room temperature. For vacuum filtration, 1-micron glass fiber filters (GFFs) were pre-combusted (400°C for 30 min) and pre-rinsed (1-L Milli-Q water). Therefore, in this work DOM is operationally defined as the portion of NOM passing a 1-micron GFF.

Raw water quality parameters, i.e., pH, alkalinity, turbidity, DOC, total dissolved nitrogen, ammonia, and total phosphorus, were measured as part of the alum coagulation study (Pifer and Fairey 2012), and a description of the methods can be found in its Supplementary Data. UV₂₅₄ measurements were taken on filtered samples following Standard Methods 5910-B (Eaton et al. 2005) on the UV-Vis 2450, which was blanked with Milli-Q water before the first

sample and after every six samples. Thereafter, $SUVA_{254}$ was calculated by dividing the UV_{254} absorbance by the product of the UV cell path length (0.01 m) and the DOC concentration (mg/L).

2.3. MIEX[®] Experiments

MIEX[®] resin (Orica Watercare, Watkins, CO) was obtained in a 5% brine solution. The resin was prepared by decanting with glass Pasteur pipettes and rinsing with Milli-Q water until the conductivity of the supernatant, measured with a four-cell conductivity probe (Accumet), was less than or equal to 1 mS/cm. The MIEX[®] resin/Milli-Q water slurry was transferred to a 10 mL graduated cylinder and allowed to settle for approximately 10 minutes before use. A resin dose of 6 mL/L was chosen for all MIEX[®] treatments based on preliminary experiments that showed significant DOC reduction (greater than 50%).

MIEX[®] experiments were conducted at pH 6, 7, and 8. To control pH, 10 mL of phosphate buffer (68.1 g/L KH_2PO_4 and 11.7 g/L NaOH) was added to each 490 mL raw water sample. The pH of the samples was further adjusted using HCl or NaOH. The samples were transferred to 500 mL amber glass bottles, and glass pipettes were used to deliver settled resin to the pH-buffered raw water samples. The samples were tumbled end-over-end at 45 rpm for approximately 18 hours, a time sufficient to ensure equilibrium was achieved based on preliminary experiments (data not shown). The samples were filtered using 1 μ m GFFs before further analyses.

2.4. Disinfection Byproduct Formation Potential Tests

DBPFP tests were conducted on 250 mL portions of raw and MIEX[®]-treated water samples according to Standard Methods 5710 B with modifications. The samples were adjusted to pH 7.0 with phosphate buffer and spiked with NaOCl solution such the chlorine residual was

between 3 and 7 mg/L as Cl₂ after 7 days in the dark at 25°C. Chlorine residuals were measured using DPD total chlorine powder pillows (Hach Company) and a UV-Vis 2450 spectrophotometer (Shimadzu) calibrated at a wavelength of 552 nm with a standard curve between 1.0 and 7.0 mg/L as Cl₂. Precisely 30 mL of each chlorinated sample were taken for DBP analysis, and the remainder was quenched by sodium sulfate and reserved for further analyses. The 30 mL portions were quenched using ammonium chloride to preserve haloacetonitriles, and DBPs were extracted by liquid-liquid extraction following EPA 551.1 with modifications described in Pifer and Fairey (2012). The extraction solvent and internal standard were combined as 0.5 mg/L 1,1,1-trichloroethane in pentane (Wahman 2006). A GC-2010 with an electron capture detector (Shimadzu Corp.) was used to quantify DBPs. A standard curve (1, 2, 5, 10, 20, 40, 60, 80, and 100 µg/L) containing eight DBPs (chloroform, dichlorobromomethane, dibromochloromethane, bromoform, 1,1,1-trichloro-2-propanone, dichloroacetonitrile, trichloroacetonitrile, and dibromoacetonitrile) was run prior to the samples. Blanks and 10 µg/L check standards were run after every twelfth injection, and all check standards were within ± 25% of the standard concentration, considered to be acceptable based on EPA 551.1.

2.5. Fluorescence-PARAFAC Analysis

Fluorescence EEMs of 200 raw and MIEX[®]-treated waters were collected using a dual monochromator fluorescence detector (Agilent Technologies, Model G1321A) at excitation wavelengths from 200 to 400 nm and emission wavelengths from 270 to 600 nm, each in 1-nm increments. EEMs were corrected for Raleigh and Raman scattering using *Cleanscan* in MATLAB (Zepp et al. 2004). Three PARAFAC models were constructed for this work using three datasets. Model 1 was based on Dataset 1 (200 EEMs total), which contained the corrected

EEMs from the MIEX[®] experiments combined with raw Beaver Lake Water EEMs to improve stability of the model. Model 2 was based on Dataset 2, which contained 190 EEMs from raw and alum coagulated waters and was described in detail by Pifer and Fairey (2012). Model 3 was based on Dataset 3, which contained the EEMs used in Models 1 and 2 (378 EEMs). PARAFAC modeling was done in MATLAB using the DOM-Fluor toolbox (available for download at <http://www.models.life.ku.kd/algorithms>). The PARAFAC algorithm decomposed the datasets into their principal fluorophore groups (called components) and reported the signatures of these fluorophore groups, and the F_{MAX} values for each component in each sample. All models were validated using the *SplitHalfAnalysis* and *SplitHalfValidation* functions. Additional details of the PARAFAC procedure are provided elsewhere (Pifer et al. 2011; Pifer and Fairey 2012).

RESULTS AND DISCUSSION

3.1. Raw Water Parameters

Raw water parameters are presented and discussed in the Supplementary Data of Pifer and Fairey (2012). $SUVA_{254}$, often considered the most useful predictor of DBP formation, ranged from 0.3-12.4 L mg⁻¹ m⁻¹, with a mean of 4.8 L mg⁻¹ m⁻¹. Along with turbidity, $SUVA_{254}$ spiked at BWD and TT following a heavy rainfall event (28 cm from April 24-26, 2011, NOAA Satellite and Information Service), suggesting the runoff material was rich in aromatic organics.

3.2. Fluorescence-PARAFAC Analysis

The EEMs in Dataset 1 resulted in a 5-component PARAFAC model, but one component was identified as instrument noise (EEM not shown) based on a previous study (Pifer et al. 2011), leaving a 4-component model for analysis. The locations of the excitation and emission maxima for these components are listed in Table 1 as C1.1, C1.2, C1.3, and C1.4. Based on the location of the excitation and emission maxima, components 1.1, 1.2, and 1.4 were identified as

humic-like fluorophore groups (Pifer et al. 2011), and were correlated to the formation of THM4 (Pifer and Fairey 2012). Component 1.3 had an emission maximum less than 400 nm, and has been identified as a protein-like fluorophore group (Marhaba and Lippincott 2000; Dubnick et al. 2010). Such fluorophores contain nitrogen and may play a role in the formation of N-DBPs.

Model 2, based on Dataset 2 EEMs, was also a five component model with three humic-like components, 1 protein-like component, and 1 noise component, and component EEMs and a description of the model was previously published (Pifer and Fairey 2012). C2.1, C2.2, C2.3 and C2.4 were equivalent to C1.1, C1.3, C1.2, and C1.4, respectively.

A 6-component model was validated by split half analysis for Dataset 3, likely due to the increased number of samples, and showed improvement over a valid 5-component model in terms of sum of squared error. As before, one component was identified as instrument noise, leaving five meaningful components. C3.1, C3.3, and C3.5 were equivalent to C1.1, C1.3, and C1.2, respectively. The combination of F_{MAX} from two humic-like components, C3.2 and C3.4, were strongly correlated to F_{MAX} from C1.4 ($r^2 = 0.95$, data not shown). For consistency, Model 3 was used in comparisons between samples.

Figure 1 contains the F_{MAX} values for Model 3 as a function of sampling date, location, and treatment. The total F_{MAX} values for the raw water samples for each DWTP and sampling date were higher than for the corresponding treated waters. This indicated that both alum and MIEX[®] resin removed portions of DOM from raw water. As in Model 2 (Pifer and Fairey 2012), the alum-treated samples showed increasing DOM removal with decreasing pH (Fig. 1e-h). However, there was no apparent impact of treatment pH for the MIEX[®]-treated samples (Fig. 1a-d). The absence of a F_{MAX} removal trend by pH for MIEX[®] treatment may indicate that the

portions of DOM removed by ion exchange are relatively insensitive to pH changes between 6 and 8 (Boyer et al. 2008).

F_{MAX} for components 3.4 and 3.5 were highest in the BWD and TT samples from May 13, 2011, which suggested that they were related to the heavy rainfall event. There were no consistent trends with sampling date or location, so Table 2 summarizes the average contribution of each Model 3 component to the total F_{MAX} and the average percent removal of each component by each treatment. Component 3.1 (humic-like) was the largest contributor to each sample's overall fluorescence before and after treatment, and was removed by alum and MIEX[®] treatment for all sample locations. Alum treatment at pH 6 performed similarly to MIEX[®] at pH 6, 7 and 8, but removal percentages for alum at pH 7 and 8 were lower for all locations. Component 3.2 (humic-like) was mostly (>80%) removed by MIEX[®] treatment at pH 6-8 and alum coagulation at pH 6, and to a lesser extent by alum at pH 7 and 8. Component 3.3 (protein-like), component 3.4 (humic-like), and component 3.5 (humic-like) were more significant contributors to the total F_{MAX} of the samples after MIEX[®] treatment, indicating that MIEX[®] treatment preferentially removed the other components. The resistance of components 3.4 and 3.5 were highlighted in the BWD and TT samples following the heavy rainfall event (May 13, 2011) where their raw water F_{MAX} values were highest. Interestingly, alum treatment at pH 6, 7, and 8 was more effective at removing components 3.4 and 3.5 than MIEX[®]. For the remaining samples, the percent removals of components 3.4 and 3.5 for both alum and MIEX[®] were inconsistent, as noted by the high standard deviations of these values from the mean. Negative values for the average percent removals indicate that the treatments achieved little-to-no removal.

3.3. Specific Ultraviolet Absorbance

SUVA₂₅₄ and DOC values for MIEX[®]-treated samples are shown in Figure 2 by sampling date, location, and treatment. SUVA₂₅₄ was highest in the May 13, 2011 MIEX[®]-treated samples from BWD and TT following the heavy rainfall event. The DOC values were between 0.70 and 2.15 mg L⁻¹ as C in the MIEX[®]-treated samples throughout the study, so it appears that while MIEX effectively reduced DOC in the May 13 samples, it did not remove a group of UV₂₅₄-absorbing compounds. High F_{MAX} values for components 3.4 and 3.5 in the MIEX[®]-treated samples also indicate that a specific group of compounds was resistant to MIEX[®] treatment.

3.4. Disinfection Byproduct Formation Potential

Of the eight DBPs screened, only three – chloroform, dichloroacetonitrile, and bromodichloromethane – formed consistently at detectable levels (>1 µg/L) in the raw and MIEX[®]-treated samples (Fig. 3). There were no spatial or temporal trends in DBPFP, so the concentrations and percent reduction in FP with MIEX[®] treatment for each DBP were averaged and listed in Table 3. Similar data for alum-treated samples were shown and discussed in Pifer and Fairey (2012). Chloroform was the dominant DBP, and its FP was reduced to the greatest extent by MIEX[®] treatment. Similar to the fluorescence-PARAFAC component data (Fig. 1 and Table 2), no pH trends in DBP formation were apparent during MIEX[®] treatment. Interestingly, bromodichloromethane concentrations *increased* in several instances following MIEX[®] treatment, suggesting that chemicals (such as bromide ion) leached from the resin were DCBM precursors. This was a potentially troubling result considering the bromine-substituted DBPs are generally considered to be more toxic than fully chlorinated DBPs.

3.5. Correlations Between DBPs and DBP-Precursor Properties

Fig. 4 shows correlations between chloroform FP and $SUVA_{254}$ (Fig. 4a) and fluorescence-PARAFAC components 1.1, 2.1, and 3.1 (Fig. 4b). The plot of chloroform FP versus $SUVA_{254}$ for Dataset 1 showed no linear relationship ($r^2 = 0.00$) indicating that the $SUVA_{254}$ data was not a good predictor for chloroform formation for raw and MIEX[®] treated water samples. These correlations were influenced by the May 13, 2011 MIEX[®]-treated samples from BWD and TT following the heavy rainfall event, which had high $SUVA_{254}$ but low chloroform FP. This indicates that the UV_{254} -sensitive species in these samples are not chloroform precursors. Chloroform FP was weakly correlated to $SUVA_{254}$ for Dataset 2 ($r^2 = 0.52$). The $SUVA_{254}$ values for the May 13, 2011 alum-treated samples from BWD and TT were similar to those throughout the study (Pifer and Fairey 2012), which suggests that alum was more effective at removing the species that were UV_{254} -absorbing but not DBP-precursors. Despite this, $SUVA_{254}$ for Dataset 3 was uncorrelated to chloroform FP ($r^2=0.03$).

Correlations were developed between the F_{MAX} data from Datasets 1-3 and the individual DBP concentrations. Chloroform FP was positively correlated with F_{MAX} for Components 1.1, 2.1, and 3.1 with r^2 values of 0.89, 0.84, and 0.87, respectively, and the linear models are shown in Figure 4b. The slopes and intercepts of the three models were not significantly different ($p > 0.5$ for slopes, $p > 0.1$ for intercepts), which indicates that fluorescence-PARAFAC components could be used to predict DBPFP following different NOM removal processes and be used by DWTPs to choose and optimize DBP precursor removal processes. Chloroform FP was also positively correlated to component 3.2 ($r^2=0.83$), another humic-like component. The lack of correlation ($r^2= 0.20$) between the protein-like component 3.3 and any of the nitrogen containing DBPs was not unexpected due to the low formation potentials of these DBPs ($< 8 \mu\text{g/L}$).

Components 3.4 and 3.5 were uncorrelated to DBPFP ($r^2 = 0.10$ and 0.23 , respectively), which was expected based on the similarity of their behavior in the May 13, 2011 samples to that of $SUVA_{254}$. This result indicates that fluorescence-PARAFAC was a valuable tool for measuring DBP-precursor surrogates because the algorithm is able to differentiate between components that are strongly correlated to DBP formation (e.g., components 3.1 and 3.2) and those contributing to high UV_{254} -absorbance but not DBPFP (e.g., components 3.4 and 3.5). Also, the importance of sample size for PARAFAC models is suggested by a comparison between Models 1 and 3. Although C1.4 and C3.2 are strongly correlated to chloroform FP, C3.4 is not, and the larger sample size in Dataset 3 likely allowed PARAFAC to separate C3.2 and C3.4.

CONCLUSIONS

MIEX[®] treatment followed by DBPFP tests and the comparison of fluorescence-PARAFAC models constructed from MIEX[®]- and alum-treated samples led to the following conclusions on DBP precursor properties and treatability:

- Fluorescence-PARAFAC analysis of Dataset 3 identified four humic-like components and one protein-like component in the raw and treated waters.
- Chloroform was the predominant DBP formed during the DBPFP tests in the raw and MIEX[®] treated waters. MIEX[®] treatment (with fresh resin at 6 mL/L) reduced the TCM formation potential by approximately 50%, with no quantifiable pH effect (between pH 6 and 8).
- On average, bromodichloromethane FP increased following MIEX[®] treatment, indicating the resin or chemicals (e.g., bromide) from its polymer shell may be a source of DBP precursors.

- F_{MAX} for two humic-like components from Dataset 3 were more strongly correlated to TCM formation potential ($r^2 = 0.87$ and 0.83) than $SUVA_{254}$ ($r^2 = 0.03$), indicating fluorescence-PARAFAC analysis was a more reliable predictor of DBP formation in alum- and MIEX-treated waters.
- Although $SUVA_{254}$ and F_{MAX} for components 3.4 and 3.5 were high in the May 13, 2011 MIEX[®]-treated samples from BWD and TT and appeared to be impacted by the heavy rainfall event, the chloroform FP for these samples was moderate. This highlights the effectiveness of fluorescence-PARAFAC because it was able to isolate these components when $SUVA_{254}$ could not distinguish them from other UV_{254} -sensitive DBP precursors.
- Chloroform- F_{MAX} correlations associated with Datasets 1-3 were statistically similar, indicating that DBPFP- F_{MAX} correlations were applicable to the two NOM removal processes investigated.

ACKNOWLEDGEMENTS

We thank personnel at the four drinking water treatment plants on Beaver Lake for access to their source water and Orica Watercare (Watkins, CO) for providing the MIEX[®] resin. The authors gratefully acknowledge the support of Central Arkansas Water (Little Rock, AR) for running the DOC samples.

Table 1 – Maxima location and characteristics of the fluorescence-PARAFAC components

Component	Excitation Maxima (nm)	Emission Maxima (nm)	Identification*
Model 1			
C1.1	237 (329)	429	Humic-like
C1.2	346 (229, 203)	427	Humic-like
C1.3	214 (298)	372	Protein-like
C1.4	398 (270, 212)	474	Humic-like
Model 2*			
C2.1	238 (329)	430	C1.1
C2.2	231	362	C1.3
C2.3	344 (203,228)	426	C1.2
C2.4	395 (269, 213)	471	C1.4
Model 3			
C3.1	238 (329)	428	C1.1
C3.2	271 (371, 212)	456	C1.4
C3.3	229	359	C1.3
C3.4	371 (229)	481	C1.4
C3.5	322 (209)	396	C1.2

Values in parentheses are secondary and tertiary Excitation Maxima
*Pifer and Fairey (2012)

Table 2 – Average contribution and percent removal for each fluorescence-PARAFAC component as a function of treatment

Treatment	C3.1	C3.2	C3.3	C3.4	C3.5
Average Contribution					
Raw	51 ± 5	17 ± 2	13 ± 3	10 ± 5	9 ± 3
MIEX [®] , pH 6	31 ± 7	4 ± 1	21 ± 4	25 ± 6	20 ± 4
MIEX [®] , pH 7	33 ± 8	5 ± 2	21 ± 4	22 ± 7	19 ± 5
MIEX [®] , pH 8	35 ± 7	5 ± 2	22 ± 5	21 ± 7	18 ± 4
Alum, pH 6	38 ± 3	8 ± 3	25 ± 8	16 ± 6	14 ± 4
Alum, pH 7	41 ± 3	11 ± 3	24 ± 7	12 ± 4	12 ± 3
Alum, pH 8	44 ± 3	14 ± 3	23 ± 6	9 ± 4	10 ± 3
Average Percent Removal					
MIEX [®] , pH 6	82 ± 5	94 ± 3	49 ± 14	10 ± 25	32 ± 14
MIEX [®] , pH 7	76 ± 7	88 ± 5	35 ± 29	-10 ± 68	11 ± 51
MIEX [®] , pH 8	78 ± 7	90 ± 4	45 ± 18	21 ± 27	36 ± 19
Alum, pH 6	73 ± 8	83 ± 9	27 ± 34	28 ± 35	40 ± 29
Alum, pH 7	61 ± 11	67 ± 17	10 ± 35	28 ± 35	32 ± 29
Alum, pH 8	41 ± 16	42 ± 20	-22 ± 37	27 ± 31	28 ± 24
Values are averages ± standard deviations					

Table 3 – Average formation potential and percent reduction in formation potential as a function of treatment

	Chloroform	Dichloroacetonitrile	Bromodichloromethane
Average Formation Potential ($\mu\text{g/L}$)			
Raw	120 \pm 25	4 \pm 2	8 \pm 1
MIEX [®] , pH 6	44 \pm 10	3 \pm 1	14 \pm 2
MIEX [®] , pH 7	49 \pm 12	3 \pm 1	13 \pm 2
MIEX [®] , pH 8	46 \pm 9	3 \pm 1	15 \pm 3
Alum, pH 6	46 \pm 7	3 \pm 1	6 \pm 1
Alum, pH 7	56 \pm 8	3 \pm 1	6 \pm 1
Alum, pH 8	73 \pm 14	3 \pm 2	6 \pm 1
Average Percent Reduction			
MIEX [®] , pH 6	63 \pm 9	20 \pm 24	-86 \pm 31
MIEX [®] , pH 7	58 \pm 11	16 \pm 21	-76 \pm 38
MIEX [®] , pH 8	61 \pm 9	21 \pm 24	-97 \pm 29
Alum, pH 6*	62 \pm 8	29 \pm 30	24 \pm 7
Alum, pH 7*	52 \pm 10	25 \pm 33	22 \pm 11
Alum, pH 8*	37 \pm 9	8 \pm 35	17 \pm 11

Values are averages \pm standard deviations

*From Pifer and Fairey (2012)

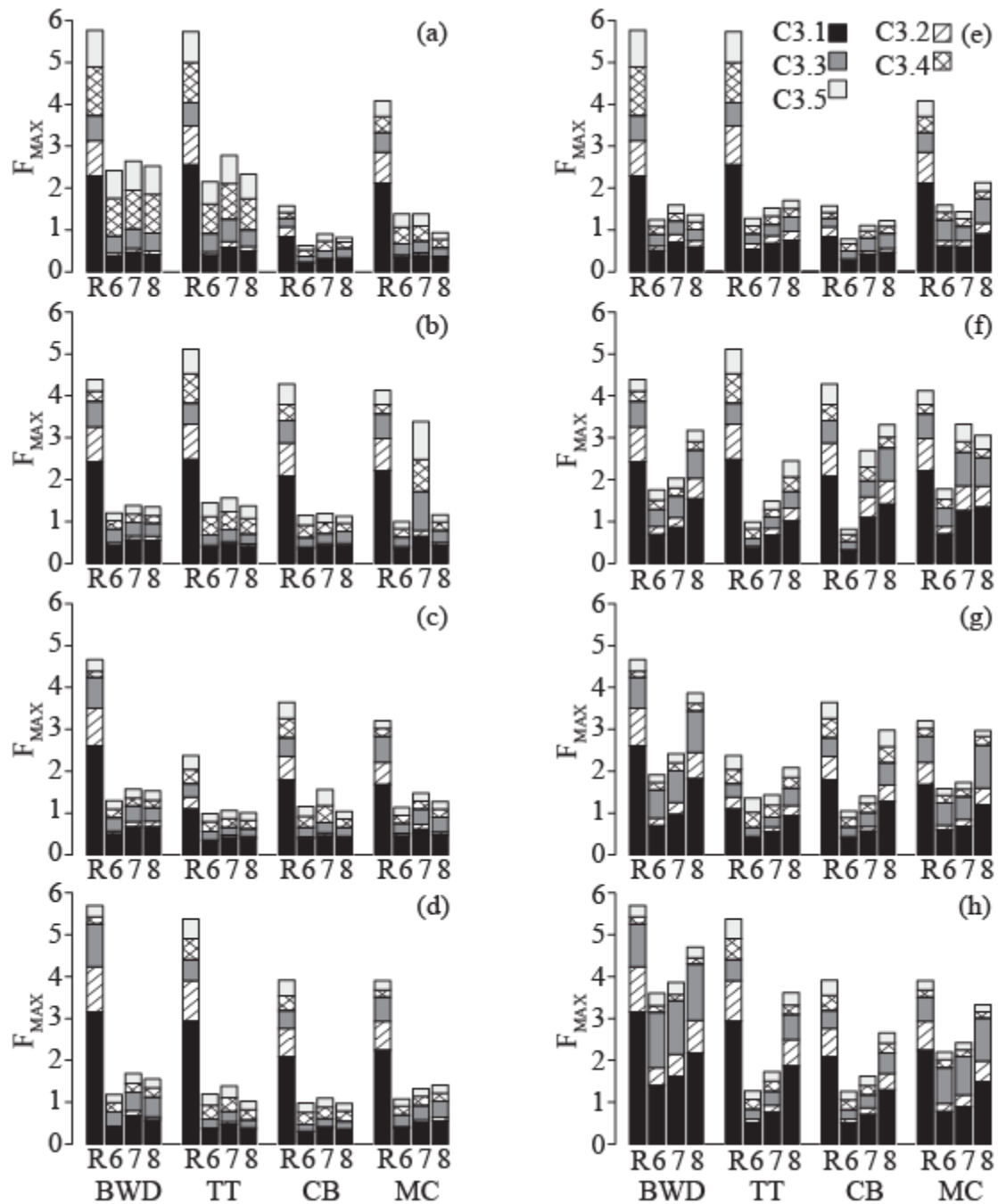


Fig. 1 – Fluorescence-PARAFAC component maxima (F_{MAX}) by sampling location and treatment for sample dates of (a,e) May 13, 2011, (b,f) June 28, 2011, (c,g) July 14, 2011, and (d,h) August 4, 2011. Panels (a-d) are for MIEX[®] treatment, and (e-h) are for alum coagulation. R indicates a raw water sample, and 6, 7, and 8 indicate the target treatment pH. BWD is the Beaver Water District, TT is Two Ton, CB is the Carroll-Boone Water District, and MC is the Madison County Regional Water District.

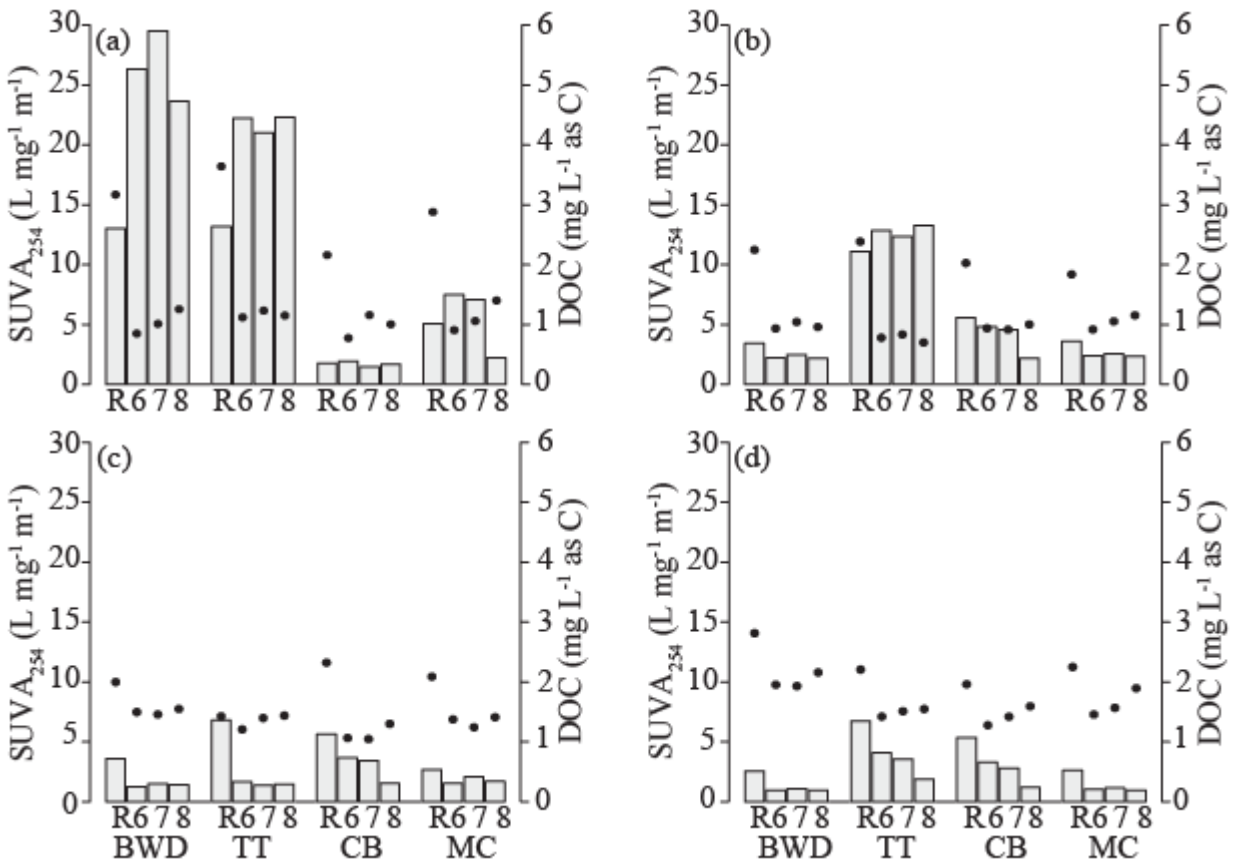


Fig. 2 – Specific ultraviolet absorbance at 254 nm (SUVA₂₅₄) by sampling location and treatment for the sample dates (a) May 13, 2011, (b) June 28, 2011, (c) July 14, 2011, and (d) August 4, 2011. R indicates a raw water sample, and 6, 7, and 8 indicate the target pH for MIEX[®] treatment. BWD is the Beaver Water District, TT is Two Ton, CB is the Carroll-Boone Water District, and MC is the Madison County Regional Water District. The filled circles represent dissolved organic carbon (DOC) in mg/L as C.

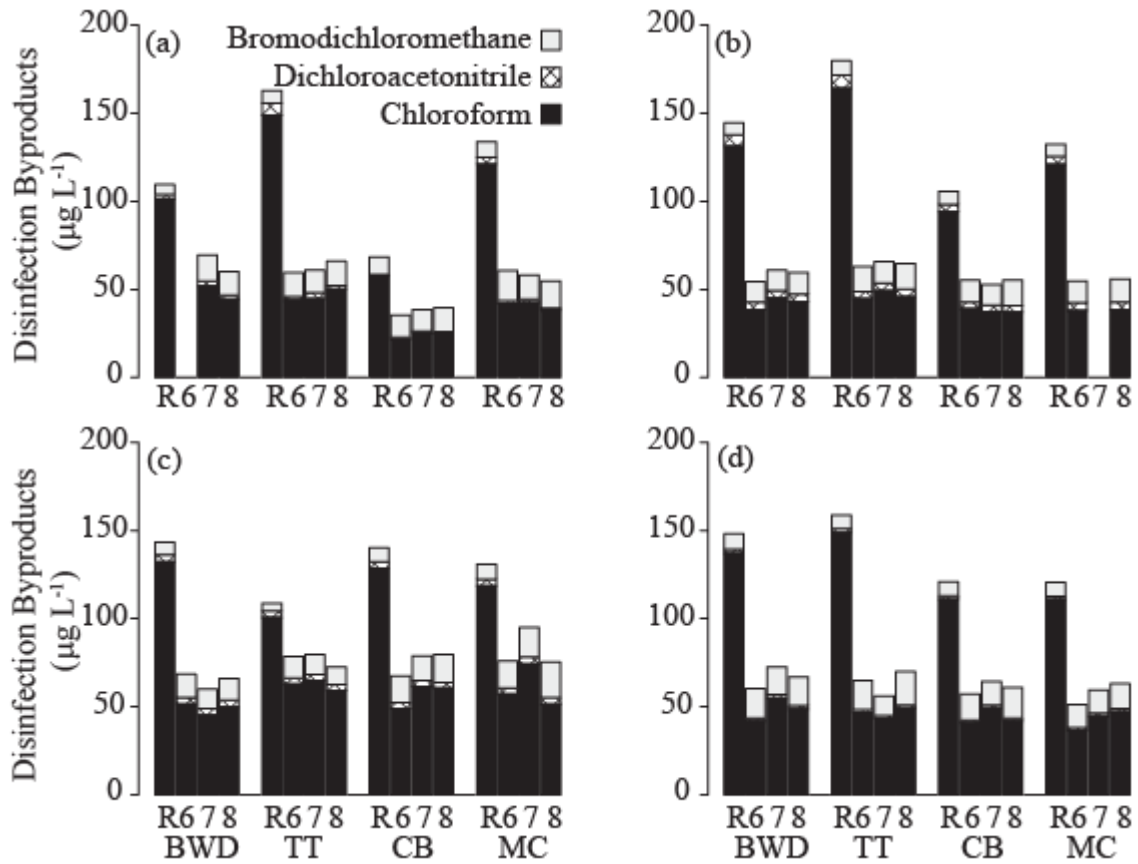


Fig. 3 – Disinfection byproducts (DBPs) in $\mu\text{g/L}$ as each DBP formed during free chlorine formation potential tests by DWTP and treatment for the sample dates: (a) May 13, 2011, (b) June 28, 2011, (c) July 14, 2011, and (d) August 4, 2011. R indicates a raw water sample, and 6, 7, and 8 indicate the target pH for MIEX[®] treatment. BWD is the Beaver Water District, TT is Two Ton, CB is the Carroll-Boone Water District, and MC is the Madison County Regional Water District.

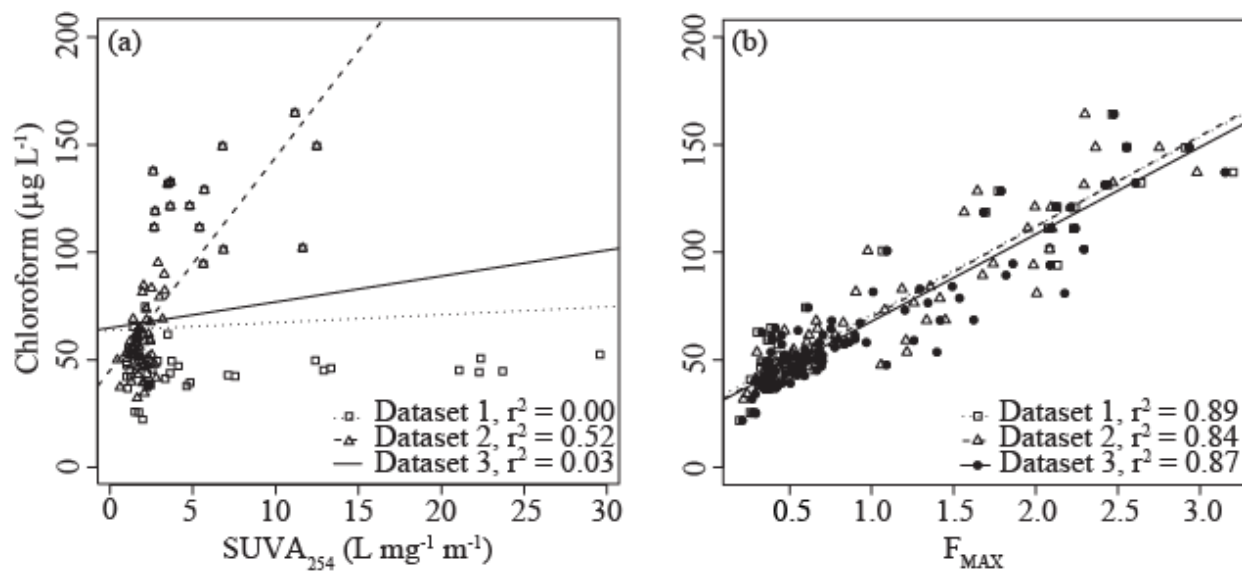


Fig. 4 – Correlations between chloroform formed during the free chlorine disinfection byproduct formation potential tests and (a) SUVA_{254} , (b) F_{MAX} for Components 1.1, 2.1, and 3.1.

REFERENCES

- Ates, N., Kitis, M. and Yetis, U., 2007. Formation of chlorination by-products. in waters with low SUVA-correlations with SUVA and differential UV spectroscopy. *Water Research* 41 (18), 4139-4148.
- Bolto, B., Dixon, D., Eldridge, R., King, S. and Linge, K., 2002. Removal of natural organic matter by ion exchange. *Water Research* 36 (20), 5057-5065.
- Boyer, T. H., Singer, P. C. and Aiken, G. R., 2008. Removal of dissolved organic matter by anion exchange: Effect of dissolved organic matter properties. *Environmental Science & Technology* 42 (19), 7431-7437.
- Cantor, K. P., Lynch, C. F., Hildesheim, M. E., Dosemeci, M., Lubin, J., Alavanja, M. and Craun, G., 1998. Drinking water source and chlorination byproducts I. Risk of bladder cancer. *Epidemiology* 9 (1), 21-28.
- Drikas, M., Chow, C. W. K. and Cook, D., 2003. The impact of recalcitrant organic character on disinfection stability, trihalomethane formation and bacterial regrowth: An evaluation of magnetic ion exchange resin (MIEX (R)) and alum coagulation. *Journal of Water Supply Research and Technology-Aqua* 52 (7), 475-487.
- Drikas, M., Morran, J. Y., Pelekani, C., Hepplewhite, C. and Bursill, D. B., 2002. Removal of natural organic matter - a fresh approach. *Water Science and Technology: Water Supply* 2 (1), 71-79.
- Dubnick, A., Barker, J., Sharp, M., Wadham, J., Lis, G., Telling, J., Fitzsimons, S. and Jackson, M., 2010. Characterization of dissolved organic matter (DOM) from glacial environments using total fluorescence spectroscopy and parallel factor analysis. *Annals of Glaciology* 51 (56), 111-122.
- Eaton, A. D., Franson, M. A. H., American Public Health Association., American Water Works Association. and Water Environment Federation., 2005. *Standard methods for the examination of water & wastewater*. Washington, DC, American Public Health Association.
- Hua, B., Veum, K., Yang, J., Jones, J. and Deng, B. L., 2010. Parallel factor analysis of fluorescence EEM spectra to identify THM precursors in lake waters. *Environmental Monitoring and Assessment* 161 (1-4), 71-81.
- Jarvis, P., Mergen, M., Banks, J., McIntosh, B., Parsons, S. A. and Jefferson, B., 2008. Pilot scale comparison of enhanced coagulation with magnetic resin plus coagulation systems. *Environmental Science & Technology* 42 (4), 1276-1282.

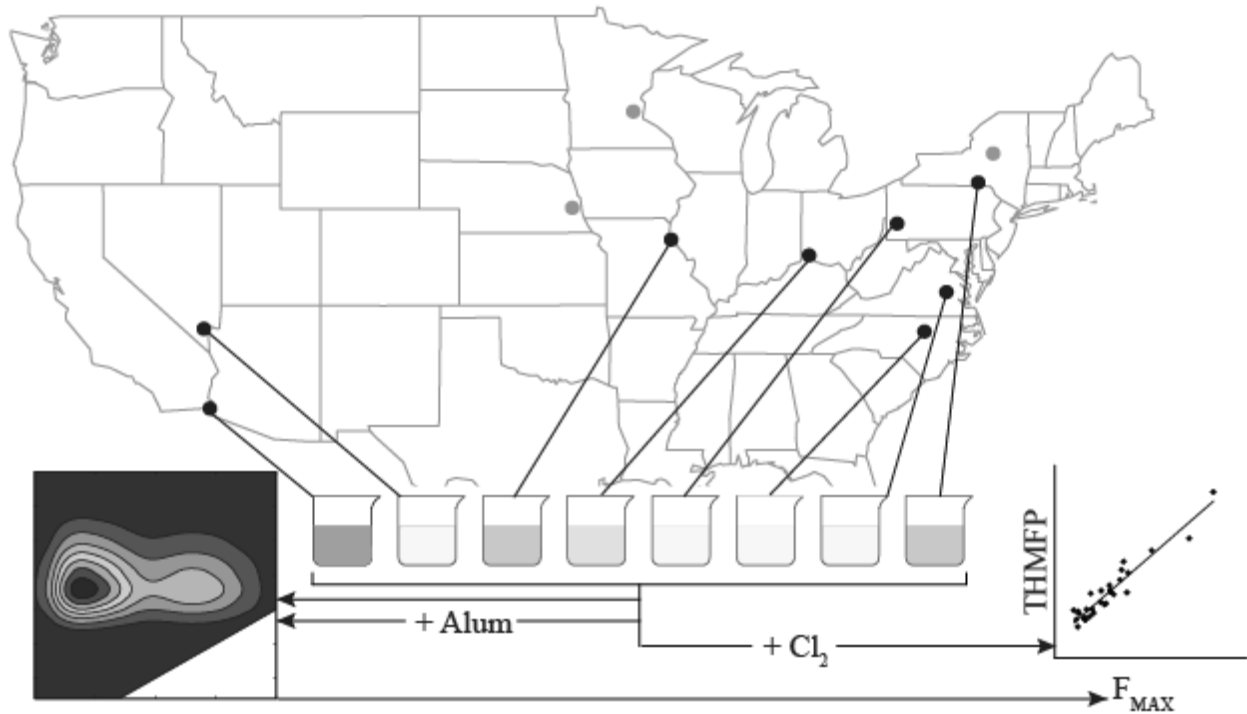
- Johnstone, D. W., Sanchez, N. P. and Miller, C. M., 2009. Parallel Factor Analysis of Excitation-Emission Matrices to Assess Drinking Water Disinfection Byproduct Formation During a Peak Formation Period. *Environmental Engineering Science* 26 (10), 1551-1559.
- Kitis, M., Karanfil, T., Kilduff, J. E. and Wigton, A., 2001. The reactivity of natural organic matter to disinfection byproducts formation and its relation to specific ultraviolet absorbance. *Water Science and Technology* 43 (2), 9-16.
- Marhaba, T. F. and Lippincott, R. L., 2000. Application of fluorescence technique for rapid identification of DOM fractions in source waters. *Journal of Environmental Engineering-Asce* 126 (11), 1039-1044.
- Miller, M. P. and McKnight, D. M., 2010. Comparison of seasonal changes in fluorescent dissolved organic matter among aquatic lake and stream sites in the Green Lakes Valley. *Journal of Geophysical Research-Biogeosciences* 115.
- Neale, P. A. and Schafer, A. I., 2009. Magnetic ion exchange: Is there potential for international development? *Desalination* 248 (1-3), 160-168.
- Nieuwenhuijsen, M. J., Toledano, M. B., Eaton, N. E., Fawell, J. and Elliott, P., 2000. Chlorination disinfection byproducts in water and their association with adverse reproductive outcomes: a review. *Occupational and Environmental Medicine* 57 (2), 73-85.
- Pifer, A. D. and Fairey, J. L., 2012. Improving on SUVA₂₅₄ using fluorescence-PARAFAC analysis and asymmetric flow-field flow fractionation for assessing disinfection byproduct formation and control. *Water Research* 46 (9), 2927-2936.
- Pifer, A. D., Miskin, D. R., Cousins, S. L. and Fairey, J. L., 2011. Coupling asymmetric flow-field flow fractionation and fluorescence parallel factor analysis reveals stratification of dissolved organic matter in a drinking water reservoir. *Journal of Chromatography A* 1218 (27), 4167-4178.
- Senesi, N., 1990. Molecular and quantitative aspects of the chemistry of fulvic-acid and its interactions with metal-ions and organic-chemicals. 2. The fluorescence spectroscopy approach. *Analytica Chimica Acta* 232 (1), 77-106.
- Singer, P. C., Schneider, M., Edwards-Brandt, J. and Budd, G. C., 2007. MIEX for removal of DBP precursors: Pilot-plant findings. *Journal American Water Works Association* 99 (4), 128-139.

- Stedmon, C. A., Markager, S. and Bro, R., 2003. Tracing dissolved organic matter in aquatic environments using a new approach to fluorescence spectroscopy. *Marine Chemistry* 82 (3-4), 239-254.
- Wahman, D. G. (2006). Cometabolism of trihalomethanes by nitrifying biofilters under drinking water treatment plant conditions. Civil, Architectural, and Environmental Engineering. Austin, The University of Texas at Austin. **Ph.D**: 398.
- Weishaar, J. L., Aiken, G. R., Bergamaschi, B. A., Fram, M. S., Fujii, R. and Mopper, K., 2003. Evaluation of Specific Ultraviolet Absorbance as an Indicator of the Chemical Composition and Reactivity of Dissolved Organic Carbon. *Environmental Science & Technology* 37 (20), 4702-4708.
- Zepp, R. G., Sheldon, W. M. and Moran, M. A., 2004. Dissolved organic fluorophores in southeastern US coastal waters: correction method for eliminating Rayleigh and Raman scattering peaks in excitation-emission matrices. *Marine Chemistry* 89 (1-4), 15-36.
- Zhang, Y., Griffin, A. and Edwards, M., 2008. Nitrification in premise plumbing: Role of phosphate, pH and pipe corrosion. *Environmental Science & Technology* 42 (12), 4280-4284.
- Zhang, Y., Griffin, A., Rahman, M., Camper, A., Baribeau, H. and Edwards, M., 2009. Lead Contamination of Potable Water Due to Nitrification. *Environmental Science & Technology* 43 (6), 1890-1895.

CHAPTER 5

Assessing Fluorescence-PARAFAC as a Disinfection Byproduct Formation Potential

Surrogate in Drinking Water Sources from Diverse Watersheds



ABSTRACT

Disinfection byproduct (DBP) control in drinking water treatment plants (DWTPs) could be improved by the use of broadly applicable DBP surrogates to optimize treatment processes. Fluorescence-PARAFAC components were evaluated as total trihalomethane formation potential (TTHMFP) surrogates using source waters from eleven DWTPs within watersheds comprising 6 of the 12 dominant soil orders in the United States. Raw water samples were alum coagulated at pH 6, 7, and 8, and underwent TTHMFP tests using free chlorine. Dissolved organic matter (DOM) from the samples was characterized before and after alum treatment by asymmetric flow-field flow fractionation coupled to an ultraviolet absorbance detector (AF4-UV₂₅₄), specific ultraviolet absorbance at 254 nm (SUVA₂₅₄), and fluorescence-PARAFAC. AF4-UV₂₅₄ showed that alum coagulation preferentially removed the relatively large chromophoric DOM fraction at pH 6 relative to pH 8. TTHMFP was correlated to SUVA₂₅₄ and maximum fluorescence intensity (F_{MAX}, from PARAFAC). The TTHMFP-SUVA₂₅₄ correlations were weak ($r^2 = 0.15$, 10 DWTPs) relative to TTHMFP-F_{MAX} correlations ($r^2 = 0.91$ for 8 DWTPs, $r^2 = 0.77$, 1.00 for 2 individual DWTPs), which indicated that F_{MAX} was a stronger TTHMFP surrogate than SUVA₂₅₄ and could be applied across a diverse set of water sources (10 of 11 DWTPs).

1. INTRODUCTION

Disinfection byproducts (DBPs) form from reactions between disinfectants (particularly free chlorine) and natural organic matter (NOM) during disinfection. DBPs have been associated with adverse health risks (Cantor et al. 1998; Nieuwenhuijsen et al. 2000), which prompted the United States Environmental Protection Agency (USEPA) to regulate certain groups of DBPs, such as trihalomethanes (THMs), in finished drinking water. As such, the removal of NOM, a primary pool of DBP precursors, prior to disinfection is an important part of drinking water

treatment. Not all NOM reacts to form DBPs (Beggs and Summers 2011), and selective removal of DBP precursors has been impossible in part due to difficulties in relating physicochemical NOM properties to DBP formation (Bond et al. 2010).

NOM is a complex mixture including humic substances and proteins derived from terrestrial and aquatic sources and therefore is subject to spatial (Stedmon et al. 2003) and temporal (Miller and McKnight 2010) variability. An array of techniques has been employed to characterize NOM and relate NOM properties (e.g. hydrophobicity (Kitis et al. 2002)) to DBP formation. Size characterizations using size exclusion chromatography (Chow et al. 2008) and asymmetric flow-field flow fractionation (AF4) (Pifer and Fairey 2012) have been used to evaluate the effectiveness of alum coagulation for NOM removal. However, bulk NOM characterizations are preferred by DWTPs due to the ease and low cost of obtaining them. Metrics including total organic carbon (TOC), dissolved organic carbon (DOC, the portion of TOC passing a 0.45 μm filter), and ultraviolet absorbance at 254 nm (UV_{254}) have been used to estimate NOM quantity and reactivity, and correlated to DBP formation. However, TOC and DOC are of limited use because not all NOM is reactive. UV_{254} has been related to the aromatic content of NOM (Korshin et al. 2009), and has been normalized by DOC to give specific UV_{254} (SUVA_{254}), which is commonly used to optimize NOM removal processes for DBP control. SUVA_{254} has successfully predicted DBP formation, but is ineffective for low SUVA_{254} waters (Ates et al. 2007), such as treated waters still containing DBP precursors. Also, SUVA_{254} -DBP correlations are source-water dependent (Weishaar et al. 2003; Chow et al. 2008) which decreases its value as a surrogate.

Recently, fluorescence excitation emission matrices (EEMs) have been used to characterize NOM. Because EEMs are data-rich, statistical algorithms such as parallel factor

analysis (PARAFAC) have been used to resolve fluorophore groups (components) from EEMs (Andersen and Bro 2003). Fluorescence-PARAFAC has been used to characterize NOM from diverse sources (Murphy et al. 2006) and strong correlations between components and DBP formation have been reported (Johnstone et al. 2009; Pifer and Fairey 2012) for individual watersheds. Fluorescence-PARAFAC could be a significant improvement over $SUVA_{254}$ as a DBP surrogate, but its applicability to a variety of source waters remains unknown.

The objectives of this work were to (1) investigate the impacts of alum coagulation on the physicochemical properties of NOM (e.g., AF4 was used to size NOM in raw and alum-treated waters), (2) assess fluorescence-PARAFAC components as surrogates of DBP formation potential (FP) in water samples collected from diverse sources, and (3) compare DBPFP-component correlations with DBPFP- $SUVA_{254}$ correlations. Raw water samples were collected from the intakes of eleven DWTPs in the United States. Because aquatic NOM is influenced by nearby soils (Eswaran et al. 1993; Aiken and Cotsaris 1995), the sampling locations were chosen such that 6 of the 12 soil orders were represented. To further increase the sample variety, samples were taken from rivers, reservoirs, and one surface water-influenced aquifer. The raw waters were subjected to alum coagulation (at pH 6, 7, and 8) and chlorination, and fluorescence-PARAFAC components in raw and alum-coagulated waters were correlated to DBPFP.

2. EXPERIMENTAL

2.1. Sample collection and handling.

Raw water samples were collected from the intakes of eleven DWTPs (Table 1). The DWTPs and the principal cities they serve were: City of Binghamton Water Treatment Plant (BNY, Binghamton, NY); Miller Treatment Plant (COH, Cincinnati, OH); Hannibal Water Treatment Plant (HMO, Hannibal, MO); Platte River Water Treatment Plant (LNE, Lincoln,

NE); River Mountains Water Treatment Facility (LNV, Las Vegas, NV); Fridley Softening Plant (MMN, Minneapolis, MN); Hays Mine Water Treatment Plant (PPA, Pittsburgh, PA); E.M. Johnson Water Treatment Plant (RNC, Raleigh, NC); Richmond Water Treatment Plant (RVA, Richmond, VA); Hinckley Reservoir Water Treatment Plant (UNY, Utica, NY); and Main Street Water Treatment Facility (YAZ, Yuma, AZ). Sampling locations were chosen based on the dominant soil order (Table 1) within each watershed (Natural Resource Conservation Service) and the type of water source (i.e., river, lake, or groundwater under direct influence of surface water). At each DWTP, two pre-cleaned 9-L HDPE carboys were filled headspace free with raw water and overnight shipped on ice to the University of Arkansas and stored at 4°C in the dark until analysis.

2.2. Glassware and reagents.

Glassware and plastic-ware were washed in a solution of Alconox detergent in tap water and rinsed using water with a resistivity of 18.2 MΩ-cm (Milli-Q water), produced by a Milli-Q Integral 3 (Millipore). Non-precision glassware in contact with organic solvents was baked at 400°C for 30 minutes, and other non-precision glassware was dried at 105°C. Plastic-ware was dried at 80°C, and precision glassware was dried at room temperature. Glass fiber filters (GFFs) with a nominal pore size of 1 micron were used for vacuum filtration. GFFs were pre-combusted (400°C for 30 minutes) and pre-rinsed with 1 L of Milli-Q water. As such, dissolved organic matter (DOM) and DOC were operationally defined as the organic matter or carbon, respectively, which passed through 1 micron GFFs. All chemicals were ACS grade and all aqueous solutions were prepared in Milli-Q water.

2.3. Water quality tests.

Raw water pH, alkalinity, and turbidity were measured as described by Pifer et al. (2011), and conductivity was measured after filtration on a Malvern Zetasizer Nano ZS90. For raw and alum-treated samples, UV_{254} was measured on a Shimadzu UV-Vis 2450 spectrophotometer with a 1-cm pathlength low volume quartz cell following Standard Methods 5910-B (Eaton et al. 2005). DOC was measured on a Sievers 900 Portable TOC Analyzer with a practical quantification limit (PQL) of $4 \mu\text{g L}^{-1}$. $SUVA_{254}$ was calculated as $UV_{254} (\text{m}^{-1})$ divided by DOC (mg L^{-1}). Bromide (PQL = $60 \mu\text{g L}^{-1}$) and sulfate (PQL = $160 \mu\text{g L}^{-1}$) were measured on a Dionex DX-120 ion chromatograph with an IonPac AS4A-SC column following USEPA 300.0. Aluminum (PQL = $30 \mu\text{g L}^{-1}$) was measured on a Spectro Genesis ICP OES following USEPA 200.7.

2.4. Jar tests.

Jar tests were conducted on each raw water sample at pH 6, 7, and 8 following Pifer and Fairey (2012). In brief, 1-L aliquots were pH adjusted using 1 N HCl or 1 N NaOH, and were coagulated with alum (aluminum sulfate octadecahydrate) at 60 mg L^{-1} on an eight-position magnetic stir plate (Challenge Technology). To maintain the coagulation pH, 1-6 mL of $10.6 \text{ g L}^{-1} \text{ Na}_2\text{CO}_3$ was added simultaneously with alum. After settling, the supernatant was filtered and stored in amber glass bottles in the dark at 4°C .

2.5. Disinfection byproducts.

DBPFP was measured following Pifer and Fairey (2012). In summary, 250 mL aliquots of filtered raw or alum-treated water were chlorinated at $\text{pH } 7.0 \pm 0.2$ with stock sodium hypochlorite ($5,000 \text{ mg L}^{-1}$ as Cl_2). Chlorine doses were chosen such that residuals were between 3.7 and 11.3 mg L^{-1} as Cl_2 after 7 days in the dark at room temperature. After the hold time,

chlorine residual was measured using Hach DPD total chlorine reagent packs and the UV-Vis spectrophotometer. Thirty mL of each chlorinated sample was quenched using ammonium chloride, and DBPs were extracted by liquid-liquid extraction into pentane with 1,1,1-trichloroethane as an internal standard (Wahman 2006). Concentrations of chloroform, bromodichloromethane, dibromochloromethane, bromoform, dichloroacetonitrile, trichloroacetonitrile, and 1,1,1-trichloro-2-propanone were measured by gas chromatography with an electron capture detector following USEPA 551.1. Eleven-point standard curves from 0-200 $\mu\text{g L}^{-1}$ as each DBP were used to quantify DBPs, and blanks and check standards were included after every twelfth injection.

2.6. Asymmetric flow-field flow fractionation.

AF4 fractograms were collected in duplicate following Pifer and Fairey (2012) using a 1,000 Da polyethersulfone membrane and an elution time of 30 minutes. Filtered raw waters were fractionated at pH 6 and pH 8 for comparison with samples coagulated at pH 6 and 8. The fractionation pH was controlled by the eluent, a phosphate-carbonate buffer pH-adjusted with 1 N HCl. The conductivity of the pH 8 eluent was adjusted with 1 M NaCl to match that of the pH 6 eluent ($470 \mu\text{S cm}^{-1}$).

2.7. Fluorescence-PARAFAC analysis.

Fluorescence data was collected and analyzed following Pifer and Fairey (2012). Briefly, fluorescence EEMs were collected using a dual monochromator fluorescence detector (Agilent Technologies, Model G1321A) from each filtered raw and alum coagulated sample at excitation wavelengths of 200-400 nm and emission wavelengths of 270-600 nm with 1 nm step sizes. The EEMs were corrected for Rayleigh and Raman scattering in MATLAB[®] with *Cleanscan* (Zepp et al. 2004). The 44 EEMs were added to a dataset containing 378 EEMs from raw, alum

coagulated, and magnetic ion exchange- (MIEX[®]) treated waters from Beaver Lake in Northwest Arkansas. A PARAFAC model for this dataset was constructed following Stedmon et al. (2008) using the *DOM-Fluor toolbox* (available for download at <http://www.models.life.ku.dk/algorithms>). One outlier was identified using the function *OutlierTest* and was removed. The remaining 421 EEMs were resolved into one noise and five meaningful fluorophore groups (components). The model was validated using *SplitHalfAnalysis* and *SplitHalfValidation*, and the least squares model was chosen using *RandInitAnal*.

3. RESULTS AND DISCUSSION

3.1. Raw water parameters.

Raw water parameters are summarized in Tables 1 and 2. The turbidity ranged from <0.1 NTU-110 NTU, with the lowest turbidity in the groundwater sample (LNE) and the 4 highest turbidities in river samples (YAZ, COH, HMO, and BNY). Conductivity ranged from 42-1,097 $\mu\text{S cm}^{-1}$. UNY had the lowest conductivity, likely due to an undeveloped, forested watershed (Mohawk Valley Water Authority 2011) underlain by granite bedrock, which has been shown to be resistant to weathering (Clow et al. 1996). YAZ and LNV had the highest conductivities, likely due to watershed characteristics (e.g. sedimentary rock (Apodaca et al. 1996)) and human activities (e.g. irrigation (Butler and von Guerard 1996)). The pH of the water samples ranged from 6.9 at UNY to 8.5 at MMN. The remaining 9 samples had pH values between 7.8 and 8.2. The alkalinity ranged from 10-232 mg L^{-1} as CaCO_3 , with the low at UNY and the high at LNE. Similar to conductivity, sulfate ranged from 3 mg L^{-1} at UNY to 277 mg L^{-1} at YAZ. DOC ranged from 0.69-4.07 mg L^{-1} as C, and SUVA_{254} ranged from 3.10-7.39 $\text{L mg}^{-1}\text{-m}^{-1}$. Although DOC was lowest at PPA and highest at MMN, SUVA_{254} was lowest at RNC and highest at COH, which indicated that the quantity and aromatic content of DOM varied across the sampling

locations. Bromide was detectable only in raw waters from LNE, LNV, PPA, and YAZ at concentrations of 100, 60, 60, and 80 $\mu\text{g L}^{-1}$, respectively.

3.2. Size characterization of chromophoric dissolved organic matter.

Figure 1 shows AF4 fractograms of chromophoric DOM (CDOM) with 95% confidence intervals for each raw water at pH 6 and 8 and each coagulated water at pH 6 and 8. Each AF4 fractogram contains a void peak at approximately 2 minutes. The similar void peak heights and times indicated that the AF4-UV₂₅₄ system was sufficiently rinsed between samples and that system performance was consistent throughout the study.

The AF4-UV₂₅₄ sample peak heights for raw water CDOM varied with sample location, with the lowest peak maxima from PPA CDOM and the highest from UNY CDOM. As reported by Pifer and Fairey (2012), raw water samples fractionated at pH 6 had higher AF4-UV₂₅₄ peak maxima than those fractionated at pH 8. Because the mass of DOM present in each raw water sample was the same at pH 6 and pH 8, this result indicated that CDOM characteristics were influenced by pH. CDOM in alum coagulated waters at pH 6 and 8 resulted in lower AF4-UV₂₅₄ peak maxima than the corresponding raw water, indicating CDOM removal by alum coagulation. The reduction in AF4-UV₂₅₄ peak maxima averaged 91% for coagulated pH 6 samples and 34% for coagulated pH 8 samples. This result was similar to those of Pifer and Fairey (2012) and Yang et al. (2010), and indicates coagulation was more effective for CDOM removal at lower pH. However, it is important to note that CDOM removal may not represent total DOM removal, and that coupling additional detectors (e.g. DOC) to the AF4 could allow improved estimation of DOM removal.

In AF4, DOM is fractionated by diffusivity, and elutes from the separation channel from highest to lowest diffusivity, or smallest to largest size. Therefore, the times to AF4-UV₂₅₄ peak

maxima could be used to compare relative CDOM sizes, and are listed in Table S1. The peak maxima for raw water CDOM occurred between 3.88-5.24 minutes at pH 6 and 4.08-5.37 minutes at pH 8. The CDOM remaining in alum treated waters had peak maxima between 3.25-4.15 minutes at pH 6 and 3.61-5.21 minutes at pH 8. Raw water CDOM from COH was larger than the other ten waters when fractionated at pH 6, whereas raw water CDOM from HMO was largest when fractionated at pH 8. The RNC raw water CDOM was smallest at pH 6 and 8, suggesting certain types of CDOM were more sensitive to pH. These results indicated the importance of controlling pH during AF4 size characterizations and comparing samples fractionated at the same pH when evaluating the impact of treatment. Alum coagulation impacted the CDOM size distributions of many samples. Alum-treated samples at pH 6 had consistently smaller CDOM than the corresponding raw water samples, which indicated preferential removal of the larger CDOM fraction. Conversely, alum coagulation at pH 8 did not consistently remove larger CDOM, and, in some cases, shifted the size distributions toward larger CDOM (LNV and MMN samples). Overall, these results indicated that coagulation at pH 6 preferentially removed the larger CDOM fraction and was more effective than coagulation at pH 8.

3.3. Fluorescence-PARAFAC Analysis.

A six-component PARAFAC model was constructed from the dataset consisting of 421 EEMs. Each of the six components represented a fluorophore group, and was classified by comparing the location of the excitation and emission maxima to previously reported fluorophore groups. One component was identified as instrument noise (Pifer et al. 2011), and was excluded from further analysis. The remaining five components (C1-C5) and their identifications are presented in Table 3. The PARAFAC algorithm output contains the maximum fluorescence intensity (F_{MAX}) of each component, which are shown in Figure 2. Although Na_2CO_3 was added

during alum coagulation, some pH drift occurred, and the pH of each treated sample after filtration is shown above each bar. Raw water samples from MMN, HMO, and RNC had the highest F_{MAX} values. These samples also had high DOC and AF4-UV₂₅₄ peak maxima, but moderate-to-low SUVA₂₅₄ values (Table 2). The inconsistency of sample rankings (i.e. highest to lowest) between the various DOM measures highlights the importance of using multiple techniques to acquire detailed DOM characterizations and choosing appropriate metrics for applications such as optimizing DBP control processes.

For all sampling locations, the sum of F_{MAX} from the five components ($F_{MAX,TOT}$) for raw waters was higher than for waters coagulated at pH 6 and 7. Although coagulation at pH 8 was effective for lowering $F_{MAX,TOT}$ at some locations (e.g. HMO, MMN, and RNC), little-to-no removal was observed for LNE, LNV, PPA, RVA, and YAZ samples. The percent contribution of each component's F_{MAX} to a sample's $F_{MAX,TOT}$ and the percent reduction in F_{MAX} for each component from alum coagulation are shown in Table S2. C1 was the dominant PARAFAC component in all raw (46-62% of $F_{MAX,TOT}$) and alum-treated (24-58% of $F_{MAX,TOT}$) waters, and was removed to varying extents by alum coagulation (8-94%). On average, C1 removal increased from 27% to 68% as coagulation pH decreased from 8 to 6, consistent with results reported elsewhere (Pifer and Fairey 2012). C2 comprised 9 to 33% of each sample's $F_{MAX,TOT}$, and was present in the highest levels in HMO, MMN, and RNC samples. C2 was removed by alum coagulation at pH 6 (19-97%), but some samples showed little-to-no removal by alum coagulation pH 7 and 8. C3 was present at low levels (1-33% of $F_{MAX,TOT}$) in the majority of raw and treated samples and was removed to varying extents by alum coagulation (0-58%). C4 was present at low levels (7-20% of $F_{MAX,TOT}$) in raw and treated samples, and was removed by alum coagulation at pH 6 (54-91%) and pH 7 (20-82%) more so than at pH 8 (0-39%). C5 was present

at low levels, with highest F_{MAX} values occurring in RNC and RVA samples. Over all sampling locations, C5 removal varied widely (0-100%). In general, C1 and C4 were removed more effectively than the other components at all pH values, as indicated by increasing percent contributions of C2, C3, and C5 to $F_{MAX,TOT}$ following treatment.

3.4. Disinfection Byproducts.

Three THMs – chloroform, bromodichloromethane, and dibromochloromethane – were detected at quantifiable levels ($> 0.01 \mu\text{M}$) in the chlorinated raw and alum-treated samples. Check standards were within $\pm 16\%$ for chloroform, $\pm 12\%$ for bromodichloromethane, and $\pm 8\%$ for dibromochloromethane. These checks were within EPA 551.1 requirements, i.e., 90% of checks within $\pm 20\%$ and all checks within $\pm 25\%$. The concentrations of each DBP are presented in Figure 3 in micromolar units with the exception of two treated samples (HMO pH 8 and RNC pH 7), which were lost during extraction. As in Figure 2, the final pH of each treated sample is shown above each bar in Figure 3. For convenience, DBPFP is tabulated in Table S3 in units of $\mu\text{g L}^{-1}$ along with percent reductions resulting from alum treatment.

Chloroform was the dominant DBP, with concentrations ranging from 0.58-2.03 μM in raw waters and from 0.33-1.88 μM in alum-treated waters. In general, alum coagulation removed chloroform precursors from raw waters. Exceptions to this were treatment at pH 7 and 8 for YAZ and pH 8 for MMN. For BNY, COH, HMO, LNV, MMN, RNC, and UNY, reduction in chloroform FP increased with decreasing coagulation pH. Bromodichloromethane was present in all raw (0.02-0.28 μM) and treated (0.01-0.31 μM) waters except UNY. No general trends were observed in reduction of bromodichloromethane FP. Dibromochloromethane was present in raw and treated waters from HMO, LNE, LNV, PPA, and YAZ at concentrations between 0.01-0.07 μM . Bromine incorporation factor (BIF) was calculated following Chang et al. (2001), and is

shown in Table 2. BIF was highest for the raw and treated LNE, LNV, PPA, and YAZ samples (0.23-0.45), as expected based on the relatively high bromide concentrations in the raw waters (Section 3.1).

3.5. Correlations between TTHMFP and DOM properties.

Linear models were developed to relate TTHMFP to F_{MAX} and $SUVA_{254}$ at the individual sampling location level, soil order level, and for all samples. Strong linear models were developed for fluorescence-PARAFAC components C1 and C4, but not for C2, C3, or C5. Correlations were identified at the sampling location level between TTHMFP and C1 for all locations except LNE (the sole groundwater sample). Therefore, LNE samples were not included in additional TTHMFP-C1 correlations. Analysis of covariance (ANCOVA) was performed, and TTHMFP-C1 correlations could be described using one slope and one y-intercept for all sampling locations except MMN and UNY ($p < 0.05$). MMN was unique in that it was the only softening plant in the study; however, its water quality parameters were moderate relative to the other locations (Tables 1 and 2). This suggested that the MMN DOM responded differently to alum coagulation than DOM from the other locations. UNY DOM had the lowest conductivity, pH, alkalinity, and sulfate (Table 1), and was most amenable to alum coagulation at pH 6 and 7 (Table 2). Therefore, the unique slope was not unexpected. Soil order level analyses confirmed these results, and indicated that soil characteristics may be important to DBP studies because MMN and LNE were the only Mollisol samples, and UNY was the only Spodosol sample. Three TTHMFP-C1 models were constructed using Dataset 1 (all surface water data except MMN and UNY, $r^2 = 0.91$), MMN ($r^2 = 0.77$), and UNY ($r^2 = 1.00$), and are presented in Figure 4a with grey-shaded 95% prediction intervals. The Dataset 1 model was compared by ANCOVA to a TTHMFP-C1 model ($r^2 = 0.85$) constructed using data from Pifer and Fairey (2012). This

analysis indicated the slopes and intercepts were statistically similar ($p > 0.5$), suggesting C1 could be used to assess TTHMFP in a broad range of sample waters.

A similar analysis was performed for C4 with LNE excluded from the correlations. Although the correlations between TTHMFP and C4 could be described by one slope for all source waters, MMN required a different intercept ($p < 0.01$). Therefore, Figure 4b shows TTHMFP-C4 models for Dataset 2 (all surface water data except MMN, $r^2 = 0.90$) and MMN itself ($r^2 = 0.79$) with grey-shaded 95% prediction intervals. The Dataset 2 model was also compared to TTHMFP-C4 ($r^2 = 0.76$) data from Pifer and Fairey (2012), and the slopes were significantly different ($p < 0.001$). This result indicates that despite the strong correlations between TTHMFP and C4 observed for both datasets, C4 was not a universal predictor of TTHMFP.

These analyses were repeated for $SUVA_{254}$. Unlike C1 and C4, $SUVA_{254}$ for LNE was strongly correlated to TTHMFP ($r^2 = 0.94$), and $SUVA_{254}$ for MMN was uncorrelated to TTHMFP. MMN was excluded from the dataset and ANCOVA was performed. TTHMFP- $SUVA_{254}$ correlations could be described with one slope and one intercept for all sampling locations except MMN, shown as Dataset 3 ($r^2 = 0.15$) in Figure 4c with grey-shaded 95% prediction intervals.

Linear models were also constructed to predict formation of individual THMs using PARAFAC components and $SUVA_{254}$. Linear models for chloroform were similar to TTHMFP models, but bromodichloromethane and dibromochloromethane did not produce meaningful models due to smaller sample sizes and lower ranges of FPs.

These linear models indicated that although $SUVA_{254}$ was an effective TTHMFP surrogate for some sampling locations, it could not be applied to waters from a wide range of

sources, which confirmed the results from studies with fewer DOM sources (Weishaar et al. 2003; Pifer and Fairey 2012). TTHMFP was correlated to C1 for the 10 surface water sources, and a single slope and intercept was applied to 8 of the 10 waters, which indicated that C1 was a significant improvement over SUVA₂₅₄ as a TTHMFP surrogate. Based on the comparisons with data from Pifer and Fairey (2012), C1 was a more robust TTHMFP predictor than C4. The fact that the Mollisol and Spodosol samples were outliers indicates that additional sampling should be conducted in areas with these soil orders. It is possible that effective fluorophore-DBP correlations could be developed for areas containing these soils, particularly Spodosols. Also, further work is needed to determine if fluorescence-PARAFAC components would be reliable DBPFP surrogates for groundwater sources.

4. ASSOCIATED CONTENT

Supporting Information

Contains additional information as noted, including: map of sampling locations, table of times to AF4 peak maxima, table of the percent contributions and removals of each PARAFAC component, and table of the DBPFP and percent reductions with treatment.

5. AUTHOR INFORMATION

Corresponding Author.

*Phone (479) 575-4023; fax (479) 575-7168; email: julianf@uark.edu.

Notes

The authors declare no competing financial interest

ACKNOWLEDGEMENTS

This work was partially funded by grants from the Beaver Water District (Lowell, AR) and the United States Geological Survey (Award #G11AP20066). The authors thank the participating water utilities for their support and assistance with sample collection and shipping.

Table 1 – Raw water quality parameters

Sample Location	Source Water	Dominant Soil Orders*	Turbidity (NTU)	Conductivity ($\mu\text{S cm}^{-1}$)	pH	Alkalinity ($\text{mg L}^{-1}\text{-CaCO}_3$)	Sulfate (mg L^{-1})
BNY	Susquehanna River	Inceptisols	10	167	7.8	57	7
COH	Ohio River	Alfisols	60	287	7.8	60	49
HMO	Mississippi River	Alfisols	15	458	8.3	166	32
LNE	Platte River Aquifer	Mollisols	< 0.1	690	8.2	232	100
LNV	Lake Mead	Aridisols	1	973	8.2	153	209
MMN	Mississippi River	Mollisols	1	544	8.5	221	18
PPA	Monongahela River	Alfisols	4	410	7.8	58	98
RNC	Falls Lake Reservoir	Ultisols	3	150	7.8	35	10
RVA	James River	Ultisols	3	163	7.9	55	13
UNY	Hinckley Reservoir	Spodosols	4	42	6.9	10	3
YAZ	Colorado River	Aridisols	110	1097	8.2	185	277

See Section 2.1 for definitions of the sample location abbreviations.

* <http://soils.usda.gov/technical/classification/orders/>

Table 2 – Raw and treated water parameters

Sample Location	Treatment	DOC (mg L ⁻¹)	DOC Removal (%)	SUVA ₂₅₄ (L mg ⁻¹ m ⁻¹)	BIF
BNY	Raw	0.95	-	5.27	0.02
	Alum, pH 6	0.32	66	4.01	0.03
	Alum, pH 7	0.37	61	4.88	0.02
	Alum, pH 8	0.58	39	4.48	0.02
COH	Raw	1.15	-	7.39	0.06
	Alum, pH 6	0.61	47	2.98	0.11
	Alum, pH 7	0.67	42	3.59	0.09
	Alum, pH 8	0.94	18	4.47	0.08
HMO	Raw	3.51	-	4.25	0.09
	Alum, pH 6	1.19	66	4.29	0.13
	Alum, pH 7	1.62	54	4.32	0.13
	Alum, pH 8	2.60	26	4.15	ND
LNE	Raw	1.23	-	4.39	0.27
	Alum, pH 6	0.64	48	3.46	0.45
	Alum, pH 7	0.94	24	3.40	0.33
	Alum, pH 8	1.53	0	3.14	0.39
LNV	Raw	1.25	-	4.24	0.23
	Alum, pH 6	0.58	54	4.12	0.34
	Alum, pH 7	0.89	29	3.60	0.31
	Alum, pH 8	1.10	12	4.09	0.24
MMN	Raw	4.07	-	3.27	0.06
	Alum, pH 6	1.38	66	3.55	0.03
	Alum, pH 7	1.93	53	3.63	0.03
	Alum, pH 8	3.65	10	3.04	0.06
PPA	Raw	0.69	-	4.90	0.19
	Alum, pH 6	0.46	33	3.30	0.26
	Alum, pH 7	0.42	39	4.01	0.28
	Alum, pH 8	0.54	22	4.09	0.23
RNC	Raw	3.00	-	3.10	0.04
	Alum, pH 6	1.55	48	2.90	0.05
	Alum, pH 7	1.57	48	3.38	ND
	Alum, pH 8	2.02	33	3.51	0.05
RVA	Raw	0.98	-	5.33	0.03
	Alum, pH 6	0.42	57	3.33	0.04
	Alum, pH 7	0.42	57	3.82	0.03
	Alum, pH 8	0.70	29	3.99	0.03

See Section 2.1 for definitions of the sample location abbreviations.

DOC: dissolved organic carbon; SUVA₂₅₄: specific ultraviolet absorbance at 254 nm; BIF: bromine incorporation factor; ND: no data.

Table 2 – Raw and treated water parameters, continued.

Sample Location	Treatment	DOC (mg L ⁻¹)	DOC Removal (%)	SUVA ₂₅₄ (L mg ⁻¹ m ⁻¹)	BIF
UNY	Raw	2.09	-	5.36	0.00
	Alum, pH 6	0.43	79	3.04	0.00
	Alum, pH 7	0.52	75	4.05	0.00
	Alum, pH 8	1.45	31	6.07	0.00
YAZ	Raw	1.44	-	3.54	0.33
	Alum, pH 6	0.99	31	2.52	0.38
	Alum, pH 7	1.19	17	2.77	0.34
	Alum, pH 8	1.31	9	3.05	0.32

See Section 2.1 for definitions of the sample location abbreviations.

DOC: dissolved organic carbon; SUVA₂₅₄: specific ultraviolet absorbance at 254 nm; BIF: bromine incorporation factor; ND: no data.

Table 3 – Maxima location and characteristics of the fluorescence-PARAFAC components

Component	Excitation Maxima (nm)	Emission Maxima (nm)	Identification*
C1	239 (330)	430	Humic-like*
C2	231 (298)	375	Protein-like*
C3	354 (231, <200)	427	Humic-like*
C4	374 (269, 214)	476	Humic-like*
C5	225 (272)	313	Protein-like**

Values in parentheses are secondary and tertiary Excitation Maxima

*Pifer and Fairey (2012)

**Dubnick et al. (2010).

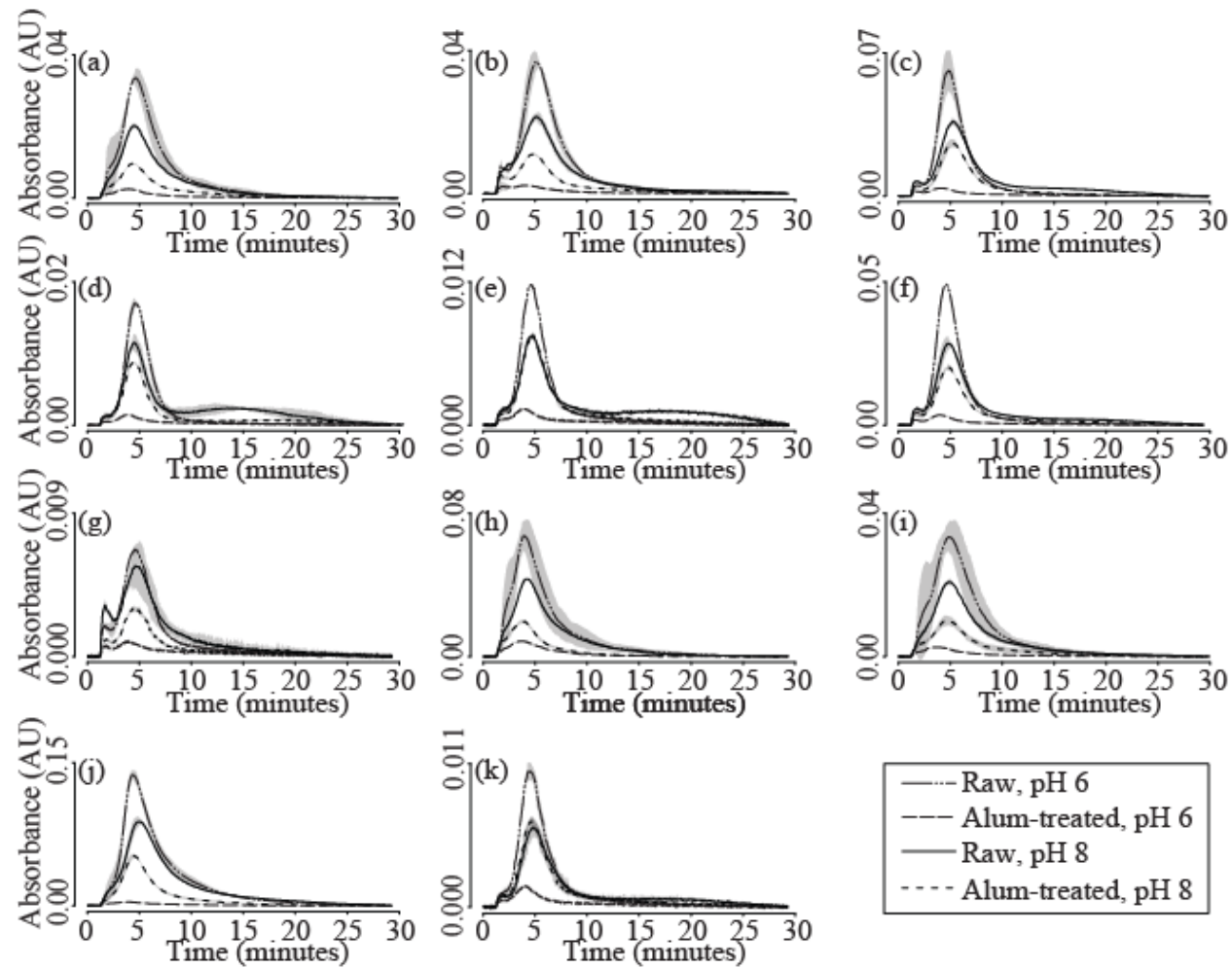


Figure 1 – Average fractograms produced using asymmetric flow field-flow fractionation coupled with UV₂₅₄ absorbance detection on raw and treated samples at pH 6 and 8 for (a) BNY, (b) COH, (c) HMO, (d) LNE, (e) LNV, (f) MMN, (g) PPA, (h) RNC, (i) RVA, (j) UNY, (k) YAZ. See Section 2.1 for definitions of the sample location abbreviations. Shading represents 95% confidence intervals.

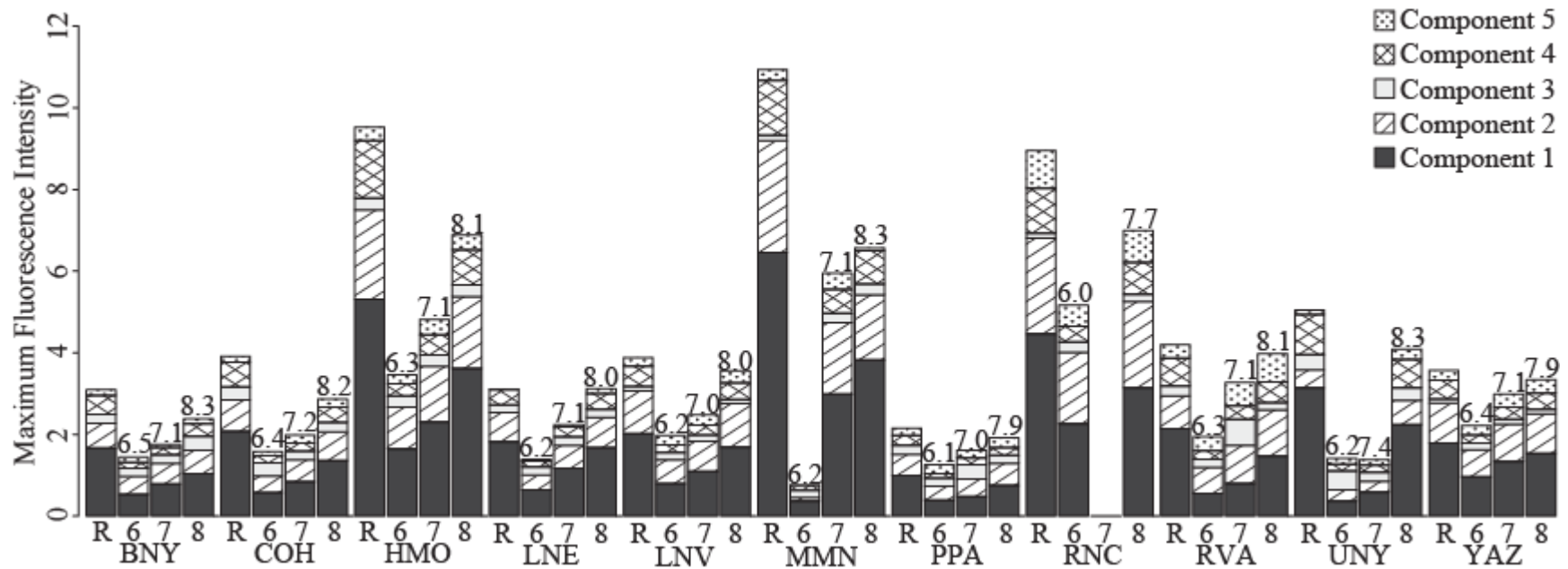


Figure 2 – Maximum fluorescence intensity for PARAFAC components by sampling location and treatment. R refers to a raw water sample, and 6, 7, and 8 refer to the coagulation pH. See Section 2.1 for definitions of the sample location abbreviations. Numbers above the bars refer to the pH measured immediately following coagulation.

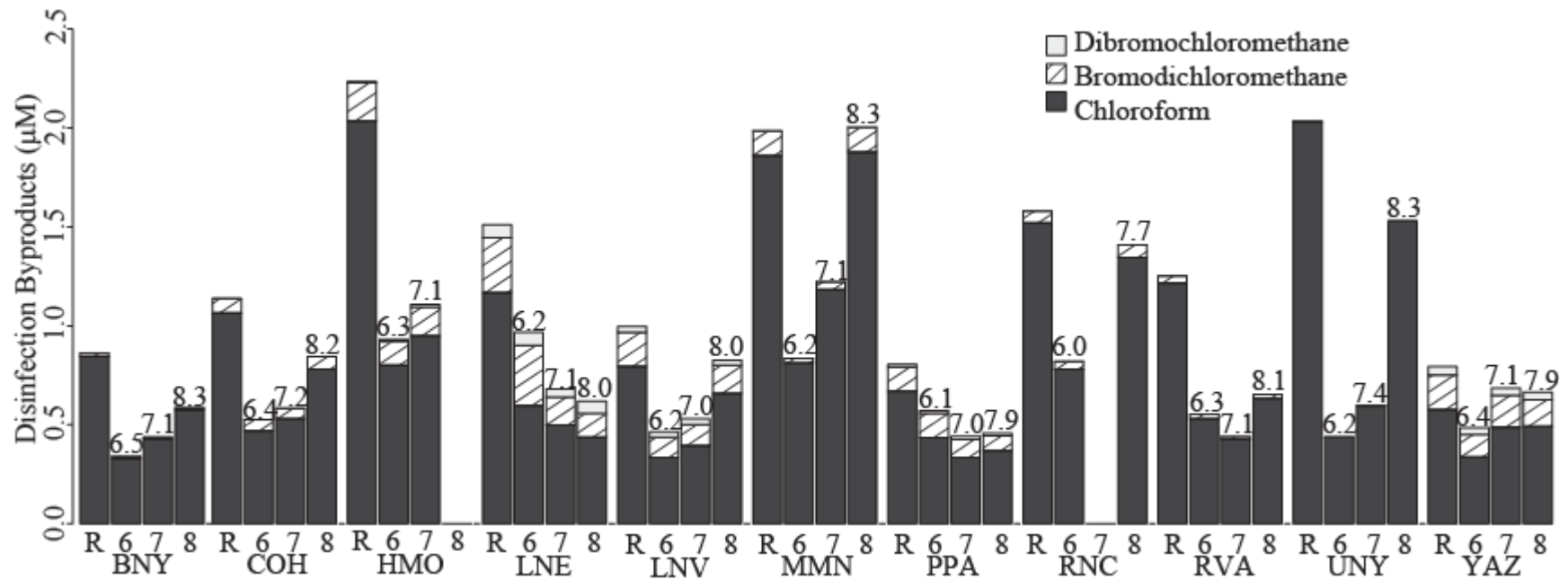


Figure 3 – Disinfection byproducts (DBPs) formed during free chlorine formation potential tests by drinking water treatment plant and treatment. R refers to a raw water sample, and 6, 7, and 8 refer to the coagulation pH. See Section 2.1 for definitions of the sample location abbreviations. Numbers above the bars refer to the pH measured immediately following coagulation.

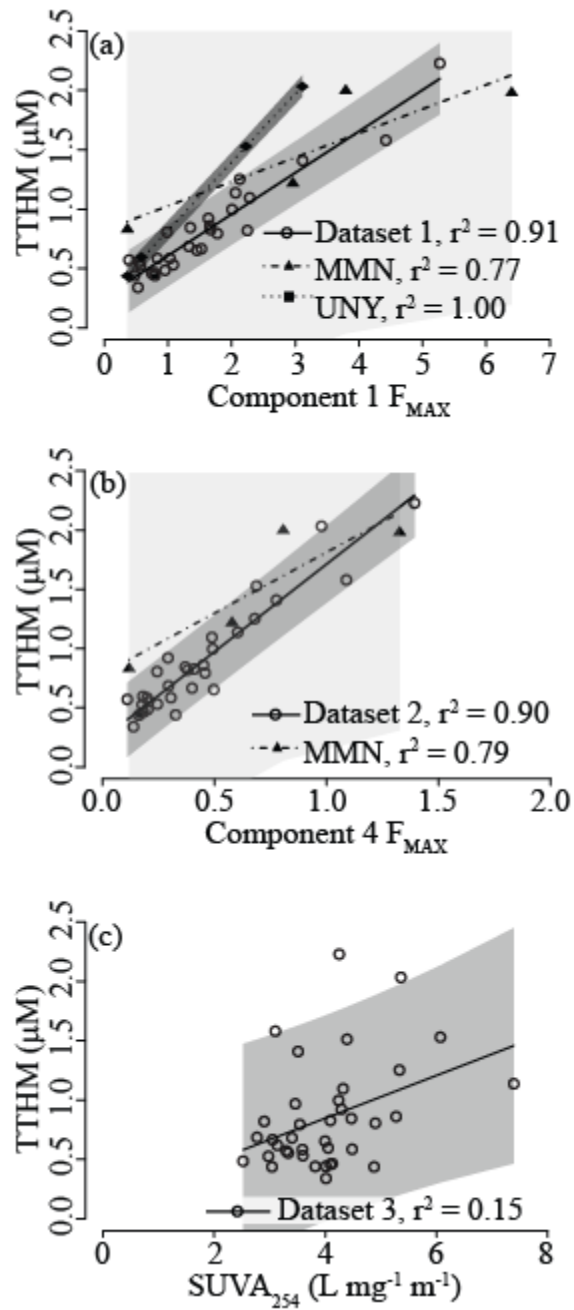


Figure 4 – Correlations between total trihalomethanes (TTHM) formed during the free chlorine disinfection byproduct formation potential tests and (a) F_{MAX} for Component 1, (b) Component 4, and (c) SUVA_{254} . Dataset 1 contains samples from all surface water plants except MMN and UNY. These plants were modeled separately due to statistically significant differences in slope ($p < 0.05$). Dataset 2 contains all surface water samples except those from MMN. Dataset 3 contains all samples except those from MMN. See Section 2.1 for definitions of the sample location abbreviations. Shading represents 95% prediction intervals for the linear models.

6. REFERENCES

- Aiken, G. and Cotsaris, E., 1995. Soil and hydrology - their effect on NOM. *Journal American Water Works Association* 87 (1), 36-45.
- Andersen, C. M. and Bro, R., 2003. Practical aspects of PARAFAC modeling of fluorescence excitation-emission data. *Journal of Chemometrics* 17 (4), 200-215.
- Apodaca, L. E., Stephens, V. C. and Driver, N. E. (1996). What affects water quality in the Upper Colorado River Basin? United States Department of the Interior - United States Geological Survey.
- Ates, N., Kitis, M. and Yetis, U., 2007. Formation of chlorination by-products. in waters with low SUVA-correlations with SUVA and differential UV spectroscopy. *Water Research* 41 (18), 4139-4148.
- Beggs, K. M. H. and Summers, R. S., 2011. Character and Chlorine Reactivity of Dissolved Organic Matter from a Mountain Pine Beetle Impacted Watershed. *Environmental Science & Technology* 45 (13), 5717-5724.
- Bond, T., Goslan, E. H., Parsons, S. A. and Jefferson, B., 2010. Disinfection by-product formation of natural organic matter surrogates and treatment by coagulation, MIEX® and nanofiltration. *Water Research* 44 (5), 1645-1653.
- Butler, D. L. and von Guerard, P. (1996). Salinity in the Colorado River in the Grand Valley, Western Colorado, 1994-95. United States Department of the Interior - United States Geological Survey.
- Cantor, K. P., Lynch, C. F., Hildesheim, M. E., Dosemeci, M., Lubin, J., Alavanja, M. and Craun, G., 1998. Drinking water source and chlorination byproducts I. Risk of bladder cancer. *Epidemiology* 9 (1), 21-28.
- Chang, E. E., Lin, Y. P. and Chiang, P. C., 2001. Effects of bromide on the formation of THMs and HAAs. *Chemosphere* 43 (8), 1029-1034.
- Chow, A. T., Dahlgren, R. A., Qian, Z. and Wong, P. K., 2008. Relationships between specific ultraviolet absorbance and trihalomethane precursors of different carbon sources. *Journal of Water Supply: Research & Technology-AQUA* 57 (7), 471-480.
- Chow, C. W. K., Fabris, R., Leeuwen, J. v., Wang, D. and Drikas, M., 2008. Assessing Natural Organic Matter Treatability Using High Performance Size Exclusion Chromatography. *Environmental Science & Technology* 42 (17), 6683-6689.

- Clow, D. W., Mast, M. A. and Campbell, D. H., 1996. Controls on surface water chemistry in the Upper Merced River Basin, Yosemite National Park, California. *Hydrological Processes* 10, 727-746.
- Eaton, A. D., Franson, M. A. H., American Public Health Association., American Water Works Association. and Water Environment Federation., 2005. Standard methods for the examination of water & wastewater. Washington, DC, American Public Health Association.
- Eswaran, H., Van Den Berg, E. and Reich, P., 1993. Organic Carbon in Soils of the World. *Soil Sci. Soc. Am. J.* 57 (1), 192-194.
- Johnstone, D. W., Sanchez, N. P. and Miller, C. M., 2009. Parallel Factor Analysis of Excitation-Emission Matrices to Assess Drinking Water Disinfection Byproduct Formation During a Peak Formation Period. *Environmental Engineering Science* 26 (10), 1551-1559.
- Kitis, M., Karanfil, T., Wigton, A. and Kilduff, J. E., 2002. Probing reactivity of dissolved organic matter for disinfection by-product formation using XAD-8 resin adsorption and ultrafiltration fractionation. *Water Research* 36 (15), 3834-3848.
- Korshin, G., Chow, C. W. K., Fabris, R. and Drikas, M., 2009. Absorbance spectroscopy-based examination of effects of coagulation on the reactivity of fractions of natural organic matter with varying apparent molecular weights. *Water Research* 43 (6), 1541-1548.
- Miller, M. P. and McKnight, D. M., 2010. Comparison of seasonal changes in fluorescent dissolved organic matter among aquatic lake and stream sites in the Green Lakes Valley. *J. Geophys. Res.* 115, G00F12.
- Mohawk Valley Water Authority (2011). Water Quality Report 2011. Utica.
- Murphy, K. R., Ruiz, G. M., Dunsmuir, W. T. M. and Waite, T. D., 2006. Optimized Parameters for Fluorescence-Based Verification of Ballast Water Exchange by Ships. *Environmental Science & Technology* 40 (7), 2357-2362.
- Natural Resource Conservation Service. "Distribution Maps of Dominant Soil Orders." Retrieved June 5, 2012, from <http://soils.usda.gov/technical/classification/orders/>.
- Nieuwenhuijsen, M. J., Toledano, M. B., Eaton, N. E., Fawell, J. and Elliott, P., 2000. Chlorination disinfection byproducts in water and their association with adverse reproductive outcomes: a review. *Occupational and Environmental Medicine* 57 (2), 73-85.

- Pifer, A. D. and Fairey, J. L., 2012. Improving on SUVA₂₅₄ using fluorescence-PARAFAC analysis and asymmetric flow-field flow fractionation for assessing disinfection byproduct formation and control. *Water Research* 46 (9), 2927-2936.
- Pifer, A. D., Miskin, D. R., Cousins, S. L. and Fairey, J. L., 2011. Coupling asymmetric flow-field flow fractionation and fluorescence parallel factor analysis reveals stratification of dissolved organic matter in a drinking water reservoir. *Journal of Chromatography A* 1218 (27), 4167-4178.
- Stedmon, C. A. and Bro, R., 2008. Characterizing dissolved organic matter fluorescence with parallel factor analysis: a tutorial. *Limnology and Oceanography-Methods* 6, 572-579.
- Stedmon, C. A., Markager, S. and Bro, R., 2003. Tracing dissolved organic matter in aquatic environments using a new approach to fluorescence spectroscopy. *Marine Chemistry* 82 (3-4), 239-254.
- Wahman, D. G. (2006). Cometabolism of trihalomethanes by nitrifying biofilters under drinking water treatment plant conditions. *Civil, Architectural, and Environmental Engineering*. Austin, The University of Texas at Austin. **Ph.D**: 398.
- Weishaar, J. L., Aiken, G. R., Bergamaschi, B. A., Fram, M. S., Fujii, R. and Mopper, K., 2003. Evaluation of Specific Ultraviolet Absorbance as an Indicator of the Chemical Composition and Reactivity of Dissolved Organic Carbon. *Environmental Science & Technology* 37 (20), 4702-4708.
- Yang, Z., Gao, B. and Yue, Q., 2010. Coagulation performance and residual aluminum speciation of Al₂(SO₄)₃ and polyaluminum chloride (PAC) in Yellow River water treatment. *Chemical Engineering Journal* 165 (1), 122-132.
- Zepp, R. G., Sheldon, W. M. and Moran, M. A., 2004. Dissolved organic fluorophores in southeastern US coastal waters: correction method for eliminating Rayleigh and Raman scattering peaks in excitation-emission matrices. *Marine Chemistry* 89 (1-4), 15-36.

APPENDIX 3

Supporting Information for

“Assessing Fluorescence-PARAFAC for Prediction of Disinfection Byproduct Formation

Potential in Drinking Water from Diverse Watersheds”

Summary: There are 6 pages, including 3 tables and 1 figure.

Table S1 – Times to peak maxima for duplicate dissolved organic matter size distributions obtained by asymmetric flow field-flow fractionation.

Sample Location	Time to Peak Maximum (min)			
	Raw, pH 6	Treated, pH 6	Raw, pH 8	Treated, pH 8
BNY	4.47 - 4.73	3.69 - 4.09	4.54 - 4.56	4.29 - 4.52
COH	5.09 - 5.24	3.75 - 4.15	5.13 - 5.20	4.66 - 4.92
HMO	4.84 - 4.85	3.89 - 4.01	5.17 - 5.37	5.11 - 5.21
LNE	4.54 - 4.61	3.64 - 3.79	4.37 - 4.55	4.34 - 4.55
LNV	4.55 - 4.68	3.60 - 4.04	4.41 - 4.66	4.63 - 4.89
MMN	4.54 - 4.65	3.79 - 4.04	4.75 - 4.93	4.82 - 4.97
PPA	4.47 - 4.72	3.67 - 3.93	4.58 - 5.03	4.38 - 4.71
RNC	3.88 - 4.07	3.35 - 3.80	4.08 - 4.26	3.61 - 4.02
RVA	4.75 - 5.04	3.25 - 3.76	4.78 - 4.96	4.47 - 4.93
UNY	4.33 - 4.41	3.75 - 4.02	4.79 - 5.03	4.49 - 4.58
YAZ	4.25 - 4.69	3.78 - 4.12	4.63 - 4.99	4.42 - 4.82
Average \pm 95% Confidence Intervals	4.52 \pm 0.07	3.77 \pm 0.05	4.73 \pm 0.09	4.53 \pm 0.08

See Figure S1 for definitions of sample location abbreviations.

Table S2 – Percent contribution of each fluorescence-PARAFAC component to overall fluorescence intensity and percent reduction in fluorescence intensity of each component with treatment.

Sample Locations	Treatment	C1		C2		C3		C4		C5	
		%C	%R	%C	%R	%C	%R	%C	%R	%C	%R
BNY	Raw	54	-	20	-	7	-	15	-	5	-
	Alum, pH 6	37	68	30	28	14	9	10	69	9	7
	Alum, pH 7	45	53	29	17	12	2	10	63	5	44
	Alum, pH 8	44	38	24	6	15	0	13	32	5	20
COH	Raw	53	-	20	-	8	-	16	-	4	-
	Alum, pH 6	36	72	26	46	20	3	11	71	6	29
	Alum, pH 7	42	59	27	30	11	33	10	67	10	0
	Alum, pH 8	48	34	24	8	8	27	13	39	7	0
HMO	Raw	56	-	23	-	3	-	15	-	4	-
	Alum, pH 6	48	69	30	53	8	8	9	79	6	34
	Alum, pH 7	48	57	28	38	6	3	10	65	8	0
	Alum, pH 8	53	32	26	19	4	4	13	38	5	6
LNE	Raw	59	-	23	-	-	-	12	-	-	-
	Alum, pH 6	46	64	25	50	14	0	10	62	4	-
	Alum, pH 7	52	36	25	21	10	0	11	37	2	-
	Alum, pH 8	54	8	24	0	6	0	12	0	4	-
LNV	Raw	52	-	27	-	3	-	13	-	5	-
	Alum, pH 6	40	61	30	44	9	0	9	63	12	0
	Alum, pH 7	44	46	30	29	6	0	10	50	10	0
	Alum, pH 8	47	17	30	0	3	8	12	17	8	0
MMN	Raw	59	-	25	-	1	-	12	-	2	-
	Alum, pH 6	49	94	12	97	24	0	16	91	0	100
	Alum, pH 7	50	54	29	36	4	0	10	56	7	0
	Alum, pH 8	58	41	24	42	4	0	12	39	1	74
PPA	Raw	46	-	24	-	10	-	11	-	8	-
	Alum, pH 6	31	61	27	34	16	10	9	54	17	0
	Alum, pH 7	30	52	26	18	22	0	11	31	11	0
	Alum, pH 8	39	24	28	0	10	11	10	23	12	0
RNC	Raw	50	-	26	-	1	-	12	-	10	-
	Alum, pH 6	44	49	34	26	5	0	7	65	10	44
	Alum, pH 7	39	23	32	0	1	58	10	20	18	0
	Alum, pH 8	45	30	30	10	3	0	11	29	11	16

C1 – C5 are fluorescence-PARAFAC components 1-5. %C is the percent contribution of a given component to the overall maximum fluorescence intensity (F_{MAX}) of a sample. %R is the percent reduction in F_{MAX} of a given component with treatment. See Figure S1 for definitions of sample location abbreviations.

Table S2, continued – Percent contribution of each fluorescence-PARAFAC component to overall fluorescence intensity and percent reduction in fluorescence intensity of each component with treatment.

Sample Locations	Treatment	C1		C2		C3		C4		C5	
		%C	%R	%C	%R	%C	%R	%C	%R	%C	%R
RVA	Raw	51	-	19	-	6	-	16	-	8	-
	Alum, pH 6	28	74	33	19	10	17	11	70	18	0
	Alum, pH 7	24	63	28	0	20	0	10	52	17	0
	Alum, pH 8	37	32	29	0	4	27	13	27	18	0
UNY	Raw	62	-	9	-	8	-	20	-	2	-
	Alum, pH 6	26	88	20	36	33	0	12	83	10	0
	Alum, pH 7	42	81	19	39	15	44	13	82	10	0
	Alum, pH 8	55	29	14	0	8	18	17	30	6	0
YAZ	Raw	50	-	27	-	3	-	13	-	7	-
	Alum, pH 6	43	46	30	32	7	0	9	56	11	2
	Alum, pH 7	45	25	31	6	4	0	10	36	11	0
	Alum, pH 8	46	14	29	1	3	1	12	13	10	0

C1 – C5 are fluorescence-PARAFAC components 1-5. %C is the percent contribution of a given component to the overall maximum fluorescence intensity (F_{MAX}) of a sample. %R is the percent reduction in F_{MAX} of a given component with treatment. See Figure S1 for definitions of sample location abbreviations.

Table S3 – Disinfection byproduct formation potential (FP) and percent reduction in FP with treatment.

Sample Location	Treatment	Chloroform		Bromodichloromethane		Dibromochloromethane	
		FP ($\mu\text{g L}^{-1}$)	%R	FP ($\mu\text{g L}^{-1}$)	%R	FP ($\mu\text{g L}^{-1}$)	%R
BNY	Raw	101	-	3	-	0	-
	Alum, pH 6	39	61	2	32	0	-
	Alum, pH 7	51	49	1	49	0	-
	Alum, pH 8	69	32	2	40	0	-
COH	Raw	127	-	12	-	0	-
	Alum, pH 6	56	56	9	22	0	-
	Alum, pH 7	63	50	9	26	0	-
	Alum, pH 8	93	27	10	12	0	-
HMO	Raw	243	-	32	-	2	-
	Alum, pH 6	96	611	20	38	2	0
	Alum, pH 7	113	53	24	25	3	0
	Alum, pH 8	ND	-	ND	-	ND	-
LNE	Raw	139	-	45	-	14	-
	Alum, pH 6	71	49	50	0	14	2
	Alum, pH 7	59	57	23	49	8	40
	Alum, pH 8	52	63	20	56	13	10
LNV	Raw	95	-	28	-	6	-
	Alum, pH 6	40	58	17	40	6	5
	Alum, pH 7	47	50	18	38	6	0
	Alum, pH 8	79	17	23	17	6	9
MMN	Raw	222	-	20	-	0	-
	Alum, pH 6	97	56	4	81	0	-
	Alum, pH 7	141	36	6	69	0	-
	Alum, pH 8	224	0	20	0	0	-

%R is the percent reduction in disinfection byproduct formation potential with treatment. ND is no data. See Figure S1 for the definitions of sample location abbreviations.

Table S3, continued – Disinfection byproduct formation potential (FP) and percent reduction in FP with treatment.

Sample Location	Treatment	Chloroform		Bromodichloromethane		Dibromochloromethane	
		FP ($\mu\text{g L}^{-1}$)	%R	FP ($\mu\text{g L}^{-1}$)	%R	FP ($\mu\text{g L}^{-1}$)	%R
PPA	Raw	80	-	20	-	3	-
	Alum, pH 6	52	35	20	0	3	0
	Alum, pH 7	40	50	15	26	3	0
	Alum, pH 8	44	45	12	39	3	0
RNC	Raw	181	-	10	-	0	-
	Alum, pH 6	93	49	6	35	0	-
	Alum, pH 7	ND	-	ND	-	ND	-
	Alum, pH 8	161	11	10	0	0	-
RVA	Raw	145	-	6	-	0	-
	Alum, pH 6	63	56	4	36	0	-
	Alum, pH 7	51	65	3	59	0	-
	Alum, pH 8	75	48	2	42	0	-
UNY	Raw	243	-	0	-	0	-
	Alum, pH 6	52	79	0	-	0	-
	Alum, pH 7	71	71	0	-	0	-
	Alum, pH 8	183	25	0	-	0	-
YAZ	Raw	69	-	29	-	9	0
	Alum, pH 6	40	42	19	35	7	18
	Alum, pH 7	58	15	26	7	8	15
	Alum, pH 8	59	15	22	22	8	10

%R is the percent reduction in disinfection byproduct formation potential with treatment. ND is no data. See Figure S1 for the definitions of sample location abbreviations.



Figure S1 – Sample locations. BNY is the City of Binghamton Water Treatment Plant, COH is the Miller Treatment Plant, HMO is the Hannibal Water Treatment Plant, LNE is the Platte River Water Treatment Plant, LNV is the River Mountains Water Treatment Facility, MMN is the Fridley Softening Plant, PPA is the Hays Mine Water Treatment Plant, RNC is the E.M. Johnson Water Treatment Plant, RVA is the Richmond Water Treatment Plant, UNY is the Hinckley Reservoir Water Treatment Plant, and YAZ is the Main Street Water Treatment Facility.

CHAPTER 6

Conclusion

1. SUMMARY

In this work, dissolved organic matter (DOM) was physically and chemically characterized before and after enhanced coagulation and magnetic ion exchange resin (MIEX[®]) treatments. Two relatively new characterization techniques, asymmetric flow-field flow fractionation (AF4) and fluorescence-parallel factor (PARAFAC) analysis, were used throughout this work. Both techniques required low sample volumes and no pre-concentration or extreme pH perturbations, which made the analysis of laboratory-treated samples representative of actual drinking water treatment conditions. These techniques provided insights into the impacts of treatment on DOM size distributions and chemical composition.

Disinfection byproduct (DBP) formation potential (FP) tests on raw and treated samples were conducted using free chlorine, and DBPFP was correlated to the maximum fluorescence intensity (F_{MAX}) of PARAFAC components. In Chapter 3, strong correlations were discovered between chloroform FP and fluorescence components from a set of raw and alum-coagulated waters from Beaver Lake. This work was expanded in Chapter 4 to include chloroform FP and fluorescence-PARAFAC data from a MIEX[®] study which used the same raw waters from Beaver Lake, and the correlations were affirmed. Lastly, in Chapter 5, raw water samples were collected from drinking water sources across the United States and were treated by alum coagulation followed by chlorination in Chapter 5, and strong linear correlations between DBPFP and fluorescence-PARAFAC components were discovered. The work reported in Chapters 4 and 5 were novel validations of the PARAFAC model and were valuable steps towards an improved DBPFP surrogate for use in drinking water treatment plants (DWTPs).

1.1. Objective 1 – Development of AF4 and fluorescence-PARAFAC methods

In Chapter 2, detailed methods were developed to characterize chromophoric DOM (CDOM) physically using AF4 (with a 300 Da membrane) coupled with ultraviolet absorbance at 254 nm (UV₂₅₄) and chemically using fluorescence-PARAFAC. These methods were validated by application to Beaver Lake water samples collected from three depths (3, 10, and 18 m below the surface) over a period of 8 weeks. The CDOM at 10 m had the highest AF4-UV₂₅₄ peak maxima and highest fluorescence intensities, which indicated that CDOM was stratified by depth in Beaver Lake.

In Chapter 3, AF4 methods were adjusted to accommodate a 1,000 Da membrane, which improved the stability of the instrument and reproducibility of AF4-UV₂₅₄ fractograms. In addition, the impact of eluent composition became apparent. Raw water samples were fractionated in phosphate-carbonate buffer solutions at pH 6 and 8 with conductivities of 470 $\mu\text{S cm}^{-1}$. Peaks from samples fractionated at pH 6 were consistently higher than at pH 8, which indicated that pH control was important for comparisons of fractograms (e.g. raw vs. treated samples). In Chapter 5, AF4-UV₂₅₄ showed differences in relative sizes of CDOM from eleven drinking water sources, further validating the methods.

1.2. Objective 2 – Impact of treatment on DOM properties

In Chapter 3, raw waters from four drinking water treatment plants on Beaver Lake were subjected to alum coagulation at pH 6, 7, and 8. AF4-UV₂₅₄ fractograms showed that alum coagulation at pH 6 consistently removed more CDOM than at pH 8. In addition, alum coagulation at pH 6 preferentially removed larger CDOM, while CDOM removal was more uniform at pH 8. Fluorescence-PARAFAC identified one protein-like and three humic-like

components in Beaver Lake DOM. All four components were more effectively removed at pH 6 than at pH 8, and a humic-like component, C1, was preferentially removed by alum coagulation.

In Chapter 4, MIEX[®]-treated Beaver Lake water samples were compared to the alum treated samples from Chapter 3 to test the applicability of PARAFAC across fundamentally different treatment regimes. Two PARAFAC models were constructed: (1) Model 1, from raw and MIEX-treated samples, and (2) Model 3, from raw, MIEX[®]-treated, and alum-treated samples. These models were compared to Model 2, from raw and alum-treated samples. Similar components were identified for Models 1 and 2, and the larger dataset contributing to Model 3 resulted in resolution of an additional component. MIEX[®] treatment at pH 6, 7, and 8 removed DOM with no pH impacts observable using fluorescence-PARAFAC. DOM removal using MIEX[®] at pH 6, 7, and 8 was similar to that of alum coagulation at pH 6. However, a set of samples from a heavy rainfall event contained relatively high levels of a PARAFAC component, and this component was more effectively removed by alum than by MIEX[®].

In Chapter 5, raw water samples from eleven DWTPs from across the United States were subjected to alum coagulation at pH 6, 7, and 8. AF4-UV₂₅₄ fractionation of raw and treated waters at pH 6 and 8 indicated that more CDOM was removed at pH 6 than at pH 8. Further, alum coagulation at pH 6 preferentially removed larger CDOM for all source waters. Although alum coagulation at pH 8 resulted in preferential removal of large CDOM for some source waters, the CDOM size distributions shifted toward larger CDOM for two source waters. Fluorescence-PARAFAC identified three humic-like components and two protein-like components, and indicated consistent, preferential removal of two of the humic-like components by alum coagulation.

1.3. Objective 3 – DBPFP-PARAFAC correlations for alum-treated waters

In Chapter 3, strong correlations ($r^2 = 0.84$) were developed between a humic-like PARAFAC component (C1) and chloroform FP. These correlations were an improvement on chloroform FP-SUVA₂₅₄ correlations ($r^2 = 0.51$) and chloroform FP-chlorine demand correlations ($r^2 = 0.58$).

1.4. Objective 4 – Validation of DBPFP-PARAFAC correlations for two DOM removal processes

In Chapter 4, correlations between C1 and chloroform FP for Models 1, 2, and 3 were statistically similar and strong (e.g., $r^2 = 0.87$ for Model 3). However, chloroform FP and SUVA₂₅₄ for Model 1 were uncorrelated ($r^2 = 0.00$). These results indicated that C1 was an effective chloroform FP surrogate for alum and MIEX[®] treatments and was a significant improvement over SUVA₂₅₄.

1.5. Objective 5 – Validation of DBPFP-PARAFAC correlations for eleven source waters

In Chapter 5, correlations were developed between total trihalomethane (TTHM) FP and PARAFAC components. Analysis of covariance (ANCOVA) indicated that one linear model ($r^2 = 0.91$) could describe TTHMFP-C1 correlations for eight of eleven source waters. This linear model was statistically similar to the models produced in Chapters 3 and 4. C1 from the lone groundwater source (LNE) was uncorrelated to TTHMFP. Two other water sources (MMN and UNY) produced separate linear models relating C1 and TTHMFP. For SUVA₂₅₄ and TTHMFP, a single linear model ($r^2 = 0.15$) was used for 10 of the 11 source waters. C1 for MMN was uncorrelated to TTHMFP. Interestingly, The LNE and MMN samples both came from watersheds dominated by Mollisols, and the UNY sample was the sole sample from a watershed

dominated by Spodosols. These results indicated that fluorescence-PARAFAC was a more broadly applicable TTHMFP surrogate than $SUVA_{254}$.

SIGNIFICANCE AND FUTURE WORK

The conclusions from this work are valuable additions to the current understanding of DOM characterization, the impacts of treatment on DOM properties and the relationship between DOM properties and DBPFP. The pH effects observed during DOM size characterizations using AF4 indicate the importance of pH to CDOM behavior and must be kept in mind when comparing CDOM size distributions. This highlighted the usefulness of AF4 for understanding CDOM in natural and engineered systems because fractionation can be done over a range of pH values applicable to drinking water treatment. Future studies to better understand the impacts of pH on CDOM properties would be beneficial to characterizations of DOM in natural waters as well as optimization of DOM removal processes.

DBPFP-PARAFAC component correlations were shown to be an improvement over DBPFP- $SUVA_{254}$ correlations for two DOM removal processes and a variety of water sources. Future studies could include investigation of source waters from Mollisol- and Spodosol-dominated watersheds to determine if more broadly applicable DBPFP-PARAFAC component correlations could be developed specifically for watersheds containing those soils.

Currently, fluorescence-PARAFAC is of limited use to DWTPs, but it would likely be useful for optimization of processes in addition to DBP precursor removal. Although it could be used for long-term process optimization studies, pilot studies of online fluorescence detectors and development of PARAFAC models capable of resolving specified components in single samples are needed before this technique could be used in daily DWTP operations.

